

Analysis of Burrup Peninsula Rock Art

October 2018

Project: DWER/3

Analysis of Burrup Peninsula Rock Art

October 2018

Client: Department of Water and Environmental Regulation

Project: DWER/3

Consultants: Dr John Henstridge (AStat)
Anna Hayes (AStat)
Marzieh Mehryar
Graeme Ward

Data Analysis Australia Pty Ltd
97 Broadway
Nedlands, Western Australia 6009
(PO Box 3258 Broadway, Nedlands 6009)
Website: www.daa.com.au
Phone: (08) 9468 2533
Email: daa@daa.com.au
A.C.N. 009 304 956
A.B.N. 68 009 304 956

Executive Summary

The Burrup Peninsula rock art is widely recognised as a unique example of human achievement, with many hundreds of thousands of petroglyphs representing perhaps 40,000 years of art, nature and human history. The development of industries in the vicinity, including the Woodside LPG facility, the Yara Ammonia Manufacturing Plant and the Yara Technical Ammonium Nitrate Production Plant, has raised natural concerns for the rock art preservation. Since 2004, a monitoring program has visited a sample of sites on the Peninsula annually, collecting quantitative measurements on their condition.

Initially (up to 2016) this work was conducted by the CSIRO. In 2017, Yara organised for a similar data collection at the sites in proximity to their plants. To ensure as high a level of consistency as possible, the Yara work used the same instruments as had been used by the CSIRO and followed the same methodology. This report analyses the Yara data in conjunction with the CSIRO data.

The Yara 2017 data collection did not include the control sites (1 and 2) in the northern part of the Peninsula. This omission necessitated a change to the statistical analysis, to fit trend models so that the 2017 Yara data could effectively be compared with what the 2017 control would have been if it had been collected. This change in approach, in conjunction with the additional data, had the potential to increase the statistical power of the analysis.

Data preparation included:

- Ensuring that the processing steps such as the transformation to (L^*, a^*, b^*) colour co-ordinates and the extraction of spectral features matched the procedures used by the CSIRO.
- The removal of obviously erroneous data points.

The statistical analysis used linear mixed models, a methodology that is able to allow for the natural variation introduced by the sampling of sites and of spots within sites to be measured. This approach was discussed in earlier Data Analysis Australia reports and adopted in the most recent CSIRO report. It is important to understand the full structure of this variation to achieve accurate statistical inferences, so it was examined in some detail. It was discovered that:

- There was some evidence that each year the workers had difficulty in returning to precisely the same spots at each site, presumably due to restrictions on marking the engravings themselves. Consequently the year-to-year variation was substantially greater than the within year variation, reducing the benefit of the replicate measurements made each year. Future monitoring plans should reduce the replication at each spot each year (and by so doing reduce the risk of damage) and the effort be redirected towards additional sites.
- The analysis of spectral absorption band data indicated that rock type was potentially a significant issue. The two rock types – gabbro and granophyre – appear to have significant differences when measured by the ASD instrument.

For that reason, rock type was introduced into the analysis despite the limitation that the control sites consisted of only one of each rock type.

The statistical analyses focused on the interaction of three factors – control versus industry sites, engraving versus adjacent background points on the rock, and time. In essence, the question was whether the contrast between the engravings and their background changed over time differently for control and industry sites.

The colour measurements with the KM and ASD instruments suggested colour changes may have taken place over the monitoring period at a different rate for the control and industry sites. However the two instruments do not identify a common structure to this possible change, casting some doubt on its true significance. In addition, the dependence of this finding on apparent changes in recent years at just one site (Site 2) lessens the weight that can be attached to it.

The analysis of the ASD spectral line data also suggests some changes may have taken place. Again, the pattern in this is less than clear and the finding relies heavily upon the two control sites.

This investigation has highlighted the limitations of the existing monitoring design which prevents more definitive findings. However the monitoring program has provided valuable information for an improved design.

Table of Contents

1. Introduction.....	1
1.1 Previous studies	1
1.2 Measuring Reflected Light	3
1.2.1 Measuring Colour	3
1.2.2 Measuring Spectra.....	4
1.3 Linear Mixed Models.....	4
1.4 Study Design and the 2017 Data.....	5
2. Data.....	6
2.1 Konica Minolta Data.....	9
2.1.1 Box Plots of KM Data Values for all sites	9
2.1.2 Box Plots of KM Data Values for Yara and Control Sites Only	11
2.2 ASD Data.....	13
2.2.1 Box Plots of ASD Colour Data for all sites	14
2.2.2 Box Plots of ASD Colour Data for Yara and Control Sites Only	16
2.2.3 Box Plots of ASD Spectral Line Data Values for all sites.....	17
2.2.4 Box Plots of ASD Spectral Line Data Values for Yara and Control Sites Only.....	21
3. Modelling of Colour Data	24
3.1 KM Colour Data	25
3.2 ASD Colour Data	27
4. Modelling of ASD Spectral Line Data.....	28
5. Conclusion	32
Appendix A. ASD Spectral Plots	34
Appendix B. Distribution of L*, a* and b* Values With the KM Instrument	36
B.1 All Sites	36
B.2 Yara and Control Sites Only.....	38
Appendix C. Distribution of L*, a*, b* Values with the ASD Instrument	40
C.1 All Sites, Years 2005 to 2017.....	40
C.2 Yara and Control Sites Only, Years 2005-2017	42
Appendix D. Distribution of Spectral Line Values with the ASD Instrument	44
D.1 All Sites, Years 2005 to 2017.....	44
D.2 Yara and Control Sites Only, Years 2005-2017	47
Appendix E. Comparison between Instruments	50
Appendix F. Conversion of ASD Data using the TSG Program.....	61
Appendix G. Fitted Models, Colour Data	68
G.1 KM Data, All sites.....	68

G.2 ASD Colour Data, all sites.....	70
G.3 ASD Spectral Data, All sites.....	72
Appendix H. Interaction Plots,.....	75
H.1 KM Colour Data	75
H.2 ASD Colour Data	78
H.3 ASD Spectral Data.....	81

1. Introduction

The Burrup Peninsula rock art is widely recognised as a unique example of human achievement, with many hundreds of thousands of petroglyphs representing perhaps 40,000 years of art, nature and human history.¹ The development of industries in the vicinity, including the Woodside LPG facility, the Yara Ammonia Manufacturing Plant and the Yara Technical Ammonium Nitrate Production Plant, has raised natural concerns for the rock art preservation. Since 2004, a monitoring program has visited a sample of sites on the Peninsula, annually collecting quantitative measurements on their condition.

Initially (up to 2016) this work was conducted by the CSIRO. In 2017, Yara organised for a similar data collection at the sites in proximity to their plants. To ensure as high a level of consistency as possible, the Yara work used the same instruments as had been used by the CSIRO and followed the same methodology.

1.1 Previous studies

Data Analysis Australia has conducted reviews of the data in 2016² and 2017³ following concerns about the monitoring process. These reviews highlighted several statistical issues:

- Linear mixed models (or random effect models) were identified as the most appropriate statistical approach, but were not conducted in the CSIRO reports⁴. This was originally suggested by John Black and Simon Diffey⁵.
- The analysis focused on a Before-After Control-Intervention (BACI) principle, assessing how the difference between the control and industry related sites changed over time. The main variable being measured was the difference or contrast between the engraved areas of petroglyphs and their background. Hence this can be considered a three way interaction – time, sites and whether the engraving or background is measured.

¹ The petroglyphs are difficult to age but it has been suggested that they could survive for up to 60,000 years (Brad Pillans, L. Keith Fifield, Erosion rates and weathering history of rock surfaces associated with Aboriginal rock art engravings (petroglyphs) on Burrup Peninsula, Western Australia, from cosmogenic nuclide measurements, *Quaternary Science Reviews* **69**, 98-106).

² Data Analysis Australia, Henstridge et al, 2016, Review of Statistical Aspects of Burrup Peninsula Rock Art Monitoring, (Reference DER/1).

³ Data Analysis Australia, Henstridge et al, 2017, Review of CSIRO Report on Burrup Peninsula Rock Art Monitoring, (Reference DER/2).

⁴ Each of the CSIRO reports covers the data over a period from 2004 and is generally published in the year following the latest data. The most recent report was from 2017, with data up to and including 2016.

⁵ Black, J and Diffey, S., 2016, Reanalysis of the Colour and Mineralogy Changes from 2004 to 2014 on Burrup Peninsula Rock Art Sites, unpublished.

- The design focused on replicated measurements (often 20 or more) at a limited number of points at a limited number of sites. Almost surely it would have been more effective to have less replication but many more sites. This would have reduced concerns about damage to specific sites and would have given the opportunity to better understand the effect of different rock types.
- The analyses of the (L^* , a^* , b^*) data indicated that the original spectrophotometer instrument (the BYK brand) was not reliable. We understood that there were problems with the instrument itself and also suggestions that the data was not well managed through the process of cross-calibrating to a newer Konica Minolta (KM) spectrophotometer. We recommended that the BYK data be ignored in any assessment unless a better understanding of how it was used leads to renewed confidence in its data. This has the unfortunate effect of limiting the spectrophotometer measurements to starting in 2009, when the KM instrument was introduced.
- The Analytical Spectral Devices (ASD) spectrometer was used throughout the study period. While its principal advantage is its recording of near infrared (NIR) reflectance spectra, it also recorded in the visible spectrum, and could therefore give colour estimates.
- Substantial apparent variation was discovered in the reproducibility of measurements made at particular points⁶ with the ASD instrument. This suggested that there may have been variation in the procedures used from year to year. There are at least two possible approaches to how replicated measurements can be taken at each point:
 - One approach is to return to and record at a single point each year, using photographs of the points on each petroglyph as a guide. In this case the replicated measurements represent independent attempts to record at the “correct” point. An extreme form of this approach is to leave the instrument in place on the rock surface between replicate measurements.
 - A second approach is that the repeated measurements are an opportunity to broaden the area being measured around each point. In this case the measurements attempt to cover a small area around each central point, to avoid issues that arise if the *exact* same point location was not measured from year to year.

⁶ At each site, measurements were taken at a number of *spots*. The numbering or labelling of the spots was only meaningful within each site – the first spot of one site was not linked to the first spot at another site.

Each spot was, somewhat confusingly, made up of two measurement *points*, one which was on the engraving at that site and one that was close by but not on the engraving, that is, on the background. (The CSIRO Report did not use the terminology of a point, but we do so here to reduce ambiguity.) These points were defined when the monitoring at each site was first done and ideally the measurements should attempt to measure at exactly the same points every year, no simple task since it is not appropriate to mark the rocks in any way.

Each of these approaches has some validity and the choice should be based upon small scale spatial variation typically encountered in the petroglyphs. The CSIRO reports indicate that the former approach was used but there are some suggestions that a change to the second approach was adopted in later years⁷. The data itself suggests a more complex set of changes.

- The CSIRO reports referenced other factors that may affect the data, most notably the two major rock types found on the selected sites – gabbro and granophyre. The design of the monitoring with a small number of sites limited the inclusion of such factors in the analysis.

1.2 Measuring Reflected Light

All the measurements considered in this report are of light reflected off the petroglyph surface. This is interpreted in two ways:

- The colour of the reflected light; and
- The spectrum of the reflected light (or infrared).

In both cases there are a number of issues in just how the measurement is made, relating to the angle of the illumination and the angle of the reflected light. It is beyond the scope of this report to explore these in detail but the complexity of this, particularly when the surface is not smooth, is such that to be of any value in measuring change it is essential that the methods used are absolutely consistent – ideally the same instrument calibrated in the same way and used in the same manner.

1.2.1 Measuring Colour

Colour measurement is intrinsically related to how the human eye perceives light. The three types of cone – the colour sensing cells in the human retina – lead to the natural step of measuring light in three dimensions. Just what these three dimensions are is a matter of choice, depending upon context and convention. For example, in photography it is common to measure the intensity in “red”, “green” and “blue”, leading to the RGB system.

In many contexts it is appropriate to separate out the overall intensity as one dimension and to have the other two dimensions independent of this overall intensity. This report uses one such system, (L^*, a^*, b^*) , where L^* represents the overall intensity and a^* and b^* represent colour. This is a non-linear transformation of the basic intensities developed to match human perception – that is, a difference in (L^*, a^*, b^*) of a certain size in any part of the colour space will have a similar likelihood of being perceived as “different”.

In the case of reflected light from a surface, it is also necessary to consider the light illuminating the surface. Standard illuminants have been defined. The CSIRO appear to have standardised on the D65 illuminant, corresponding to daylight.

⁷ Ian McLeod, formerly of the WA Museum, personal communication.

1.2.2 Measuring Spectra

Measuring the spectrum means considering a single wavelength of light at a time. This avoids many of the compromises involved in low dimensional measures of colour and in the case of reflectance it avoids the issue of which illuminant was used. The problem is that the spectrum must be considered at many wavelengths. Spectroscopy usually focuses on wavelengths associated with particular chemical elements or compounds.

The CSIRO work focused on several spectral absorption bands (or lines) in the near infrared:

- The depth of the spectral absorption band at 900 nm (D900), associated with iron oxides;
- The minimum wavelength associated with the spectral band at 900 nm (W900);
- The depth of the chlorite absorption band at 2250 nm;
- The depth of the kaolinite absorption band at 2206 nm; and
- The depth of the gibbsite absorption bands at 2267 nm (secondary minerals resulting from the weathering of the primary minerals).

In each case the absorption was measured by comparing the reflectance at the wavelength of the band against a value interpolated from the adjacent wavelength in the spectrum.

The CSIRO work used the proprietary program The Spectral Geologist (TSG)⁸ to process the spectra to derive “parameters” and colour values for data from the ASD instrument. In this study we have, for consistency, used the same software with the same configuration. Whilst we have no reason to believe that TSG is not performing this task well, it remains a “black box” in terms of its precise algorithms.

1.3 Linear Mixed Models

At this point it is necessary to introduce some notation for representing models used in the report. If we have factors that we might term A and B which we are trying to use to explain the variation in a measurement y (say the reflectance), we could have a number of possible models that by convention we write as $y \sim \text{expression}$. The possible models are:

$y \sim 1$	y does not depend upon either A or B ;
$y \sim A$	y depends only on A ;
$y \sim B$	y depends only on B ;
$y \sim A + B$	y depends only on both A and B but they act independently of each other; and

⁸ <https://research.csiro.au/thespectralgeologist/>

$$y \sim A * B$$

y depends only on both A and B and each of A and B affects the way that y depends upon the other. This model can also be written as $y \sim A + B + A.B$ where the $A.B$ term makes the inclusion of the interaction between A and B explicit.

This notation generalises to more factors in the obvious manner and allows for complex model choices.

There are at least three factors or variables of immediate concern:

- *engraving* – the difference between an engraving and its background which is what makes the engravings visible – that is, the contrast of the engraving with its background. This is referred to as the *type* variable in the analysis;
- *control* – the difference between the northern control sites and the southern sites close to industry development. This is referred to as the *CI* (Control-Industry) variable in the analysis; and
- *time* – recognising that measurements may change over time, thought of as either the year or the trend over the years. In the analysis, this is referred to as the *YearF* variable when considering the year itself, and as a *quadratic trend* when considering the trend over years.

The measurement (y) could be any of the L^*, a^*, b^* components measured with any instrument, or any of the spectral absorption bands measured on the ASD. In practice the model will also have additional terms, some of which are treated as random, to provide the most appropriate analysis.

The more relevant term in the model is the three-factor interaction *engraving.control.time* that measures the degree to which change in the contrast over time is different between the control and potentially affected areas.

1.4 Study Design and the 2017 Data

While the original monitoring design was not ideal, it did follow basic principles of experimental design in that in each year both industry affected sites and the control sites were measured, until 2016. This ensured that any year specific measurement factors could be corrected for, essentially by assuming that the control sites should remain unchanged. The analysis method required the control data for this purpose.

In 2017, only the Yara related industry sites were measured, with no control sites.⁹ This necessitates changes to the analysis method to utilise the 2017 data. This required making the assumption that the year specific effects would take the form of a trend, allowing the trend estimated for the industry sites using data including 2017 to be compared against the trend estimated for the control sites using data up to

⁹ We understand that Yara were only required to measure the sites in the vicinity of their plant and there may have been access issues for the control sites.

2016. In adopting this assumption, Data Analysis Australia examined the data to ensure that it was reasonable.

In the analysis presented in this report, we were cognisant of the importance of the Yara plants and the changes that have taken place over the period of the monitoring. For that reason it was considered appropriate to use a quadratic trend model, to allow not only for changes, but also for possible increasing or decreasing *rates* of change.

Upon closer examination, the 2004 ASD data was considered systematically different from the data from 2005 onwards. It is not uncommon for the first year of data collection to be different in a context such as this, with refinements and lessons learned being implemented for the second year, so this should not be considered as a criticism. With the previous year's analyses considering each year separately, rather than as a trend, the statistical models could handle this appropriately. With the shift to a trend model, it is inappropriate to retain such data, and all 2004 data has been removed from this year's analysis.

This trend based approach to analysis is particularly effective as the length of the monitoring period increases – the statistical power with respect to estimating trends increases substantially with each addition year of data.

2. Data

2017 data from two instruments were provided to Data Analysis Australia, the Konica Minolta (KM), and Analytical Spectral Devices (ASD), for each replicate for each point. BYK data was not received nor used in any analysis.

The received data corresponded to recordings from November 2017 across sites 5, 6, 7, 21, 22, and 23 as described in the CSIRO report¹⁰.

Data Analysis Australia appended the 2017 data to the data prepared by CSIRO up to and including 2016, which had been made available to Data Analysis Australia when conducting our earlier reviews. Note that the data made available to Data Analysis Australia up to and including 2016 was for each *replicate* of each point for the L*, a* and b* values (for both the KM and ASD data), but was only at an *average* level for each point for the other spectral line data. Data Analysis Australia appended the data at these same levels.

An illustration of the nature of the ASD spectra is provided in Appendix A, including the spectrum of the one errant spectrum removed from the dataset.

¹⁰CSIRO (2017), Burrup Peninsula Aboriginal Petroglyphs: Colour Change & Spectral Mineralogy 2004-2016.

Figure 1 and Figure 2 below show the locations of the petroglyph monitoring sites around the Yara Plant and the location of these sites relative to the control sites, respectively. Inside each site, there were 4 spots inspected, with each spot consisting of an ‘engraving’ and ‘background’ pair of points. Approximately 20 placements occurred for each combination of site, spot, and type.

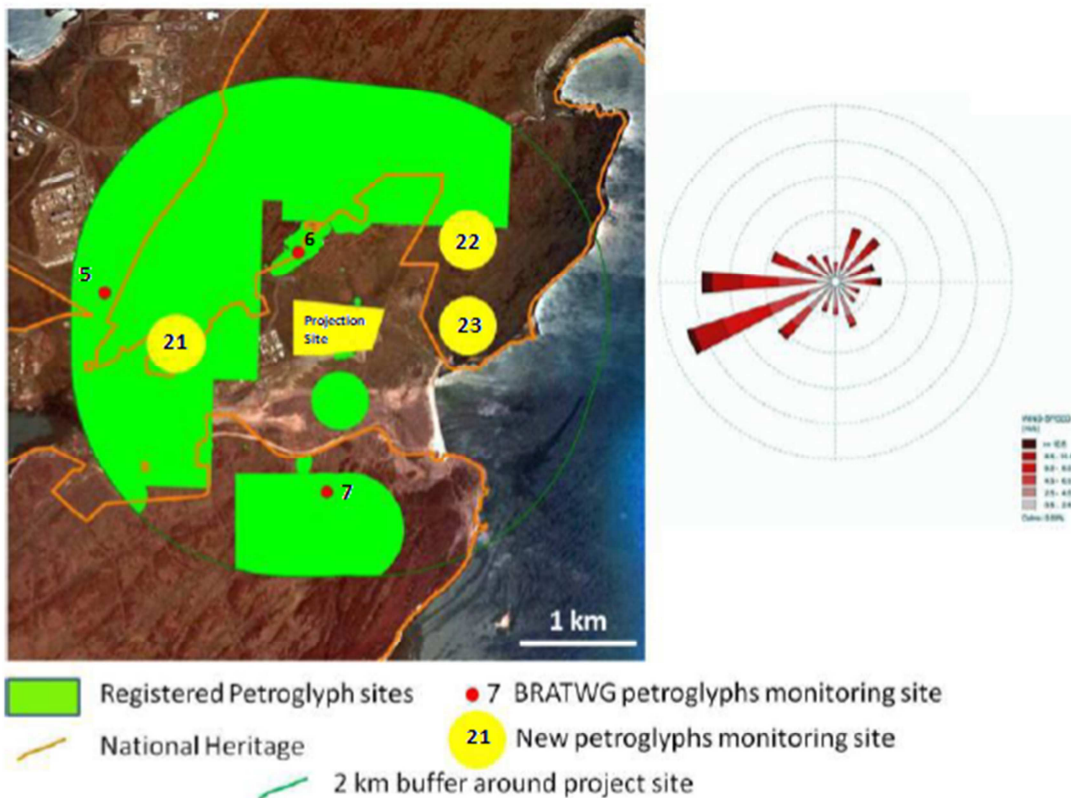


Figure 1. Petroglyph sites around Yara Plant. (Image sourced from CSIRO Report 2017).

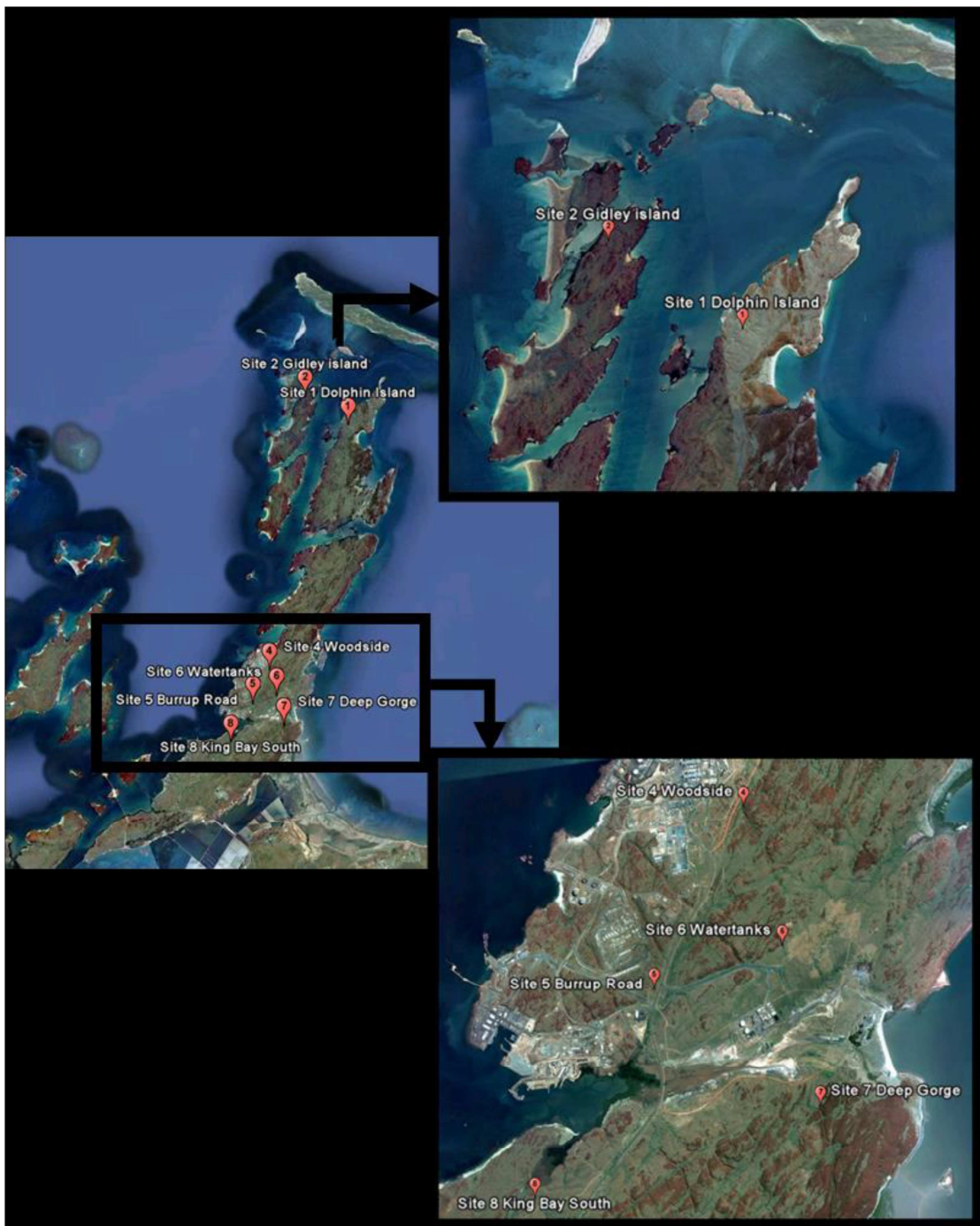


Figure 2. Location of 'industry' sites (southern) in relation to the Control sites (northern). Note that this map does not include the new Yara monitoring sites, but they are in the same vicinity as the other industry sites. (Image sourced from CSIRO Report 2017).

2.1 Konica Minolta Data

The KM spectrophotometer data supplied to Data Analysis Australia totalled 1,029 observations across the six sites. Each data point provided a value for the L*, a*, and b* measurements along with a unique identifier for the site, spot, type, and sample number. Six of the data records had text identifiers specifying that they should be ignored in the analysis, and hence they were excluded. Of the remaining 1023 observations, nine identifiers were blank; however, based on the structure of the file and other QA checks, these could be assigned identifiers based on the records surrounding the blank observations. Hence, they were retained in the analysis.

The 2017 data was added to historical data using the KM instrument, resulting in a final data set of 11,323 observations from 2009-2017.

2.1.1 Box Plots of KM Data Values for all sites

The following set of figures (Figure 3 to Figure 5) show boxplots¹¹ of the L*, a* and b* KM data values respectively, for all sites included in the monitoring. The different colours in the boxplots represent the CI variable (Control or Industry) and the type variable (background or engraving). This allows for visual identification of trends or discrepancies for each combination of these over time¹².

The width of each box plot represents the amount of data available for each combination of year, CI variable and type – the wider the box, the more data there was, and as can be seen, there is no control data for 2017.

¹¹ Box plots are commonly used in statistics to display the spread and symmetry of a data set. The box represents the middle half of the data, extending from the lower quartile (25% of data points are below this value) to the upper quartile (25% of data points are above this value). The horizontal line within the box indicates the median (middle value).

Two vertical lines, called whiskers, extend above and below the box, typically to the smallest and largest values in the data. More extreme values, either higher or lower, are plotted individually beyond the whiskers. For the plots in this report, the extreme values are defined as any value that is more than 1.5 times the interquartile range (the distance between the lower quartile and upper quartile) away from the box. The width of the box is proportional to the number of observations represented.

¹² Boxplots for each variable individually are provided in Appendix B.

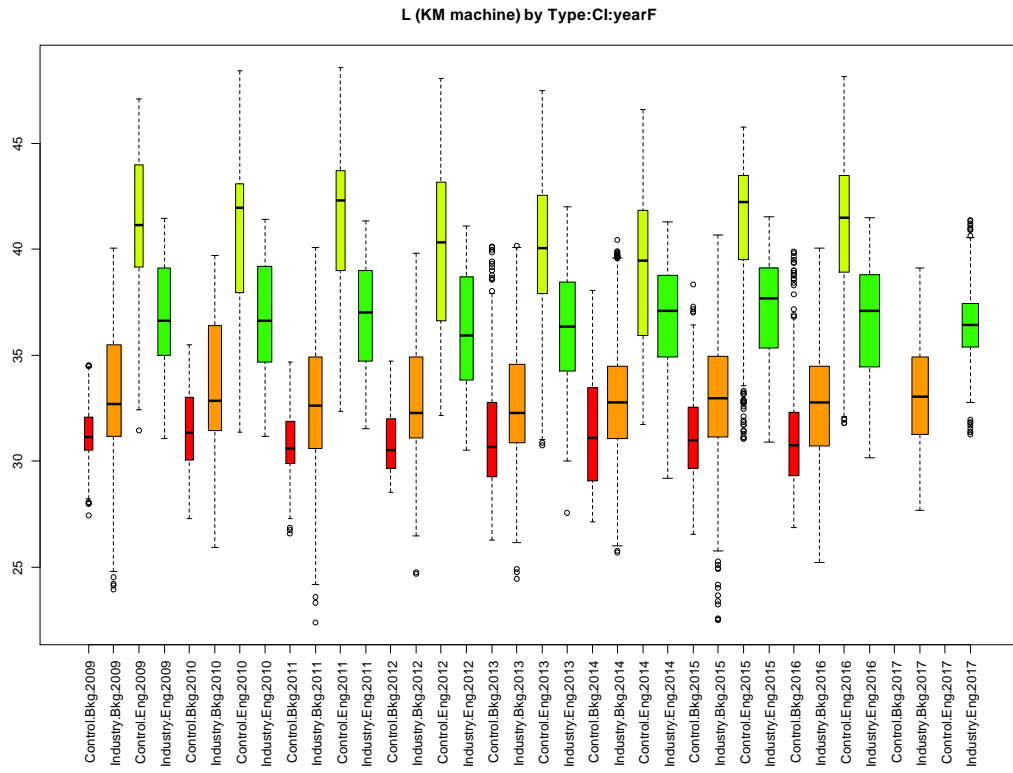


Figure 3. Box plot for the KM L* by Type:Cl:yearF for all sites.

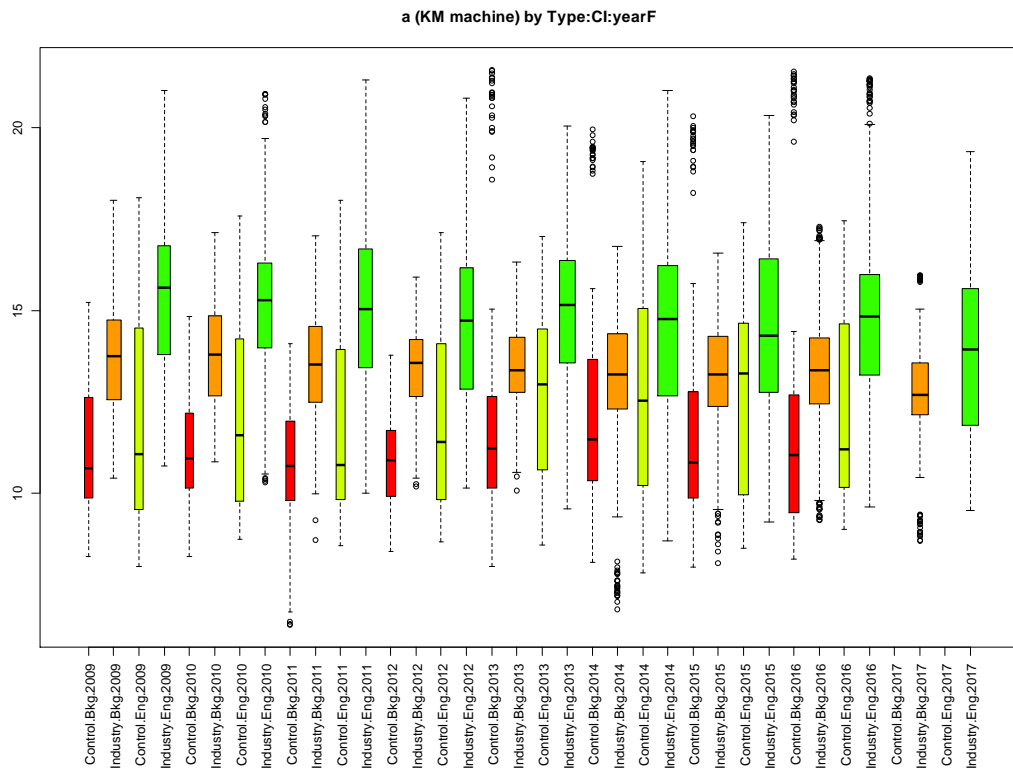


Figure 4. Box plot for the KM a* by Type:Cl:yearF for all sites.

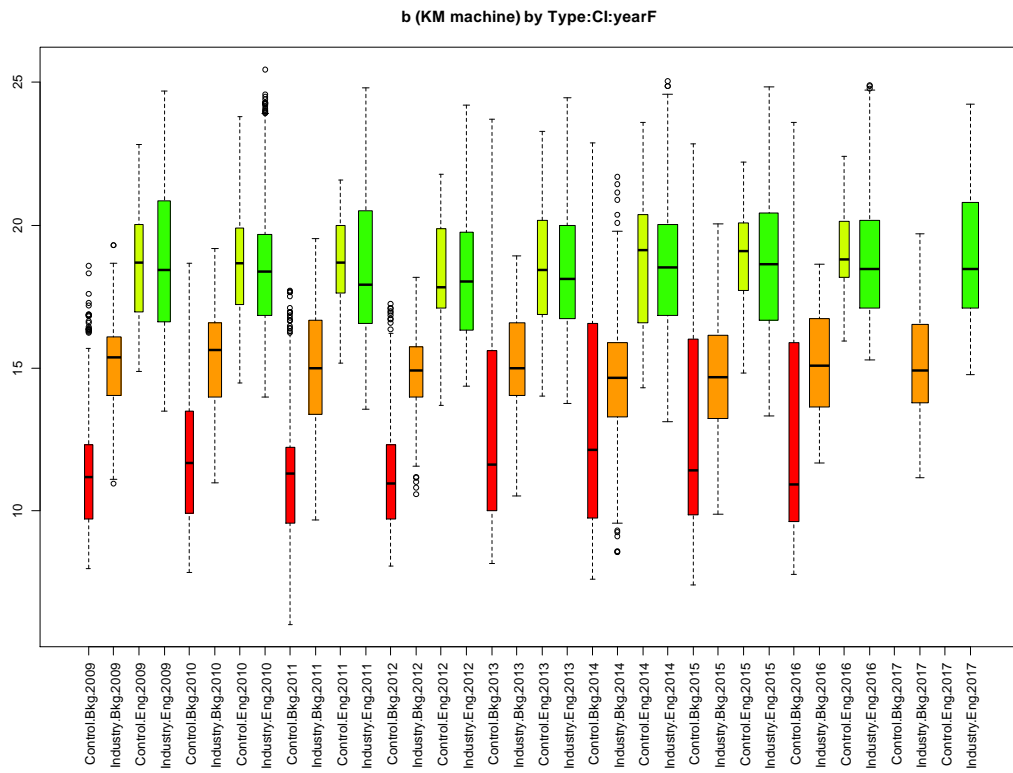


Figure 5. Box plot for the KM b^* by Type:CI:yearF for all sites.

2.1.2 Box Plots of KM Data Values for Yara and Control Sites Only

The following figures (Figure 6 to Figure 8) are analogous to those in the previous section, but are restricted to the Yara and Control sites only.

L (KM machine) by Type:CI:yearF

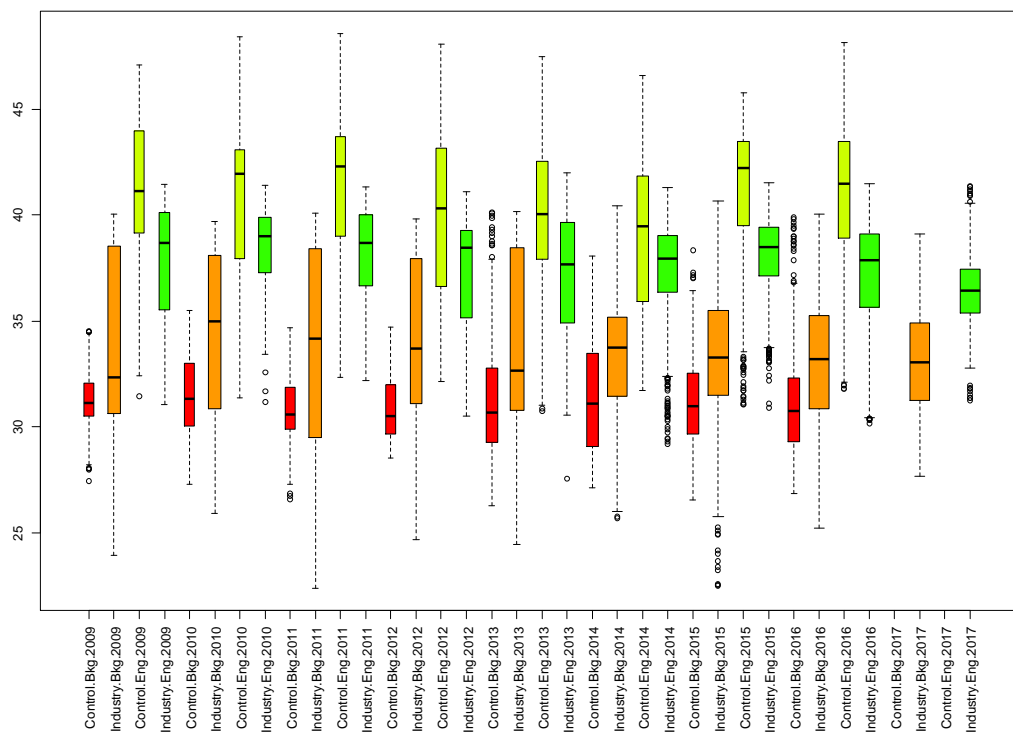


Figure 6. Box plot for the KM L* by Type:CI:yearF for Yara sites and control sites.

a (KM machine) by Type:CI:yearF

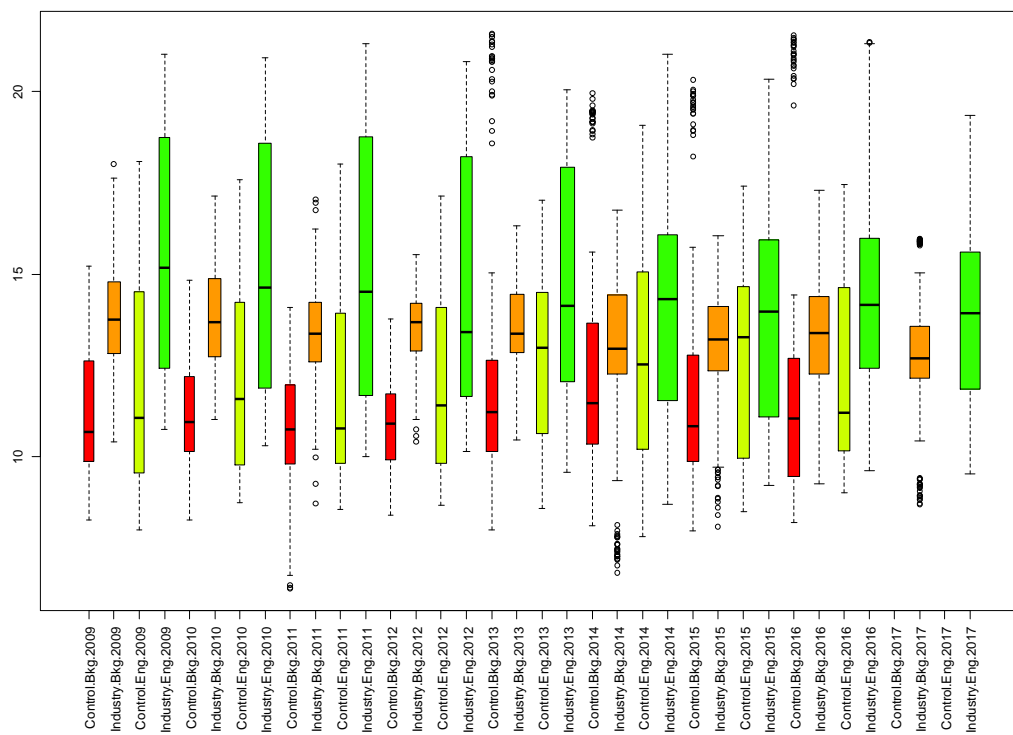


Figure 7. Box plot for the KM a* by Type:CI:yearF for Yara sites and control sites.

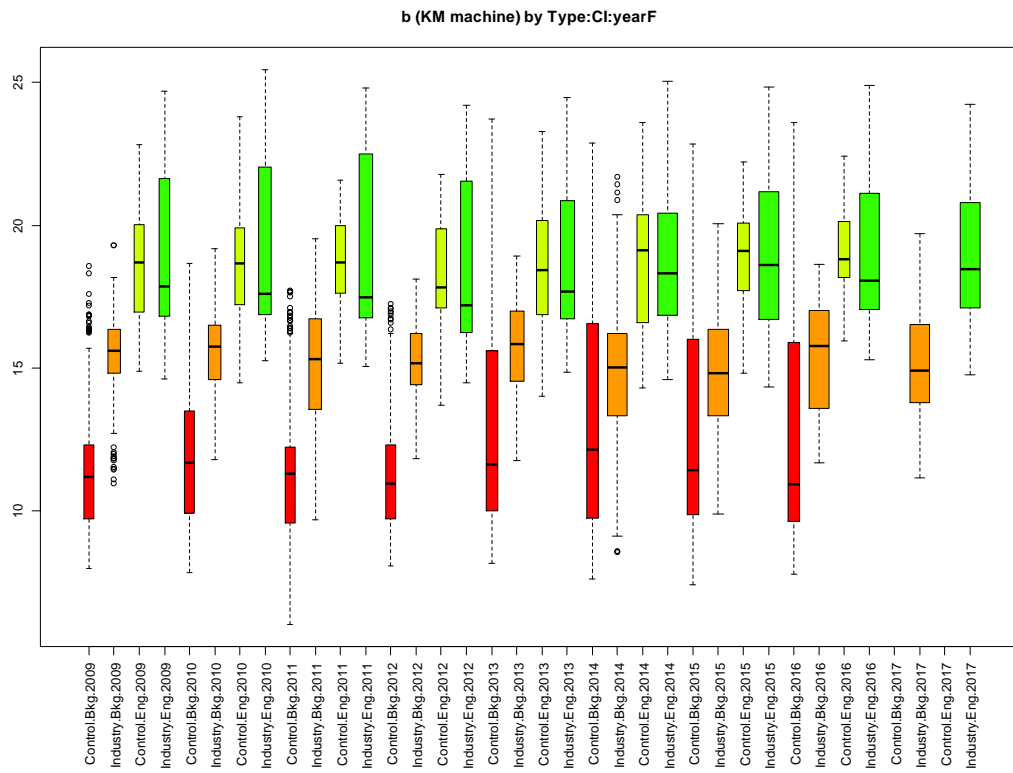


Figure 8. Box plot for the KM b^* by Type:CI:yearF for Yara sites and control sites.

2.2 ASD Data

The format of the ASD data provided was that of reflectance spectra for 1,149 observations in 2017 following the removal of practice and testing placements. The discrepancy between the number of KM and ASD observations was due to approximately two or three more placements on each combination of site/spot/type for the ASD instrument.

The conversion of ASD reflectance data to (L^*, a^*, b^*) and the extraction of the spectral line parameters was performed using The Spectral Geologist (TSG) program, Version 8.0. Assistance was provided by Erick Ramanaidou of the CSIRO in ensuring that the settings in TSG were the same as used for previous years of data. In all cases the methods were tested on 2016 reflectance data to ensure the values matched those previously supplied by the CSIRO. These details are given in Appendix F.

As referenced at the commencement of Section 2, the 2017 ASD (L^*, a^*, b^*) data processed by Data Analysis Australia was appended to the CSIRO provided data for previous years for analysis at a *replicate* level for each point, and the spectral line data at the *average* level for each point.

Data Analysis Australia extracted the 2017 spectral line information by applying the TSG program to each spectrum and then averaging. The results were then appended to similarly calculated data from previous years.

It is appropriate to make some comments on the use of the TSG program:

- It is a proprietary program with the details of algorithms not available for scrutiny. While we have no reason to believe they are faulty, if at some stage

there was concern it would be necessary to re-implement the algorithms in a different system.

- Like all software, TSG undergoes version changes. When using it in the future it would be necessary to ensure that changes have not been made to critical algorithms.
- TSG does not appear to have a scripting language and has a number of settings that must be interactively chosen by the user. This increases the difficulty in obtaining consistent results.

Overall, the continued use of the TSG program must be questioned.

2.2.1 Box Plots of ASD Colour Data for all sites

The following set of figures (Figure 9 to Figure 11) show boxplots of the L*, a* and b* ASD data values respectively, for all sites included in the monitoring¹³. As with the KM data boxplots presented in Section 2.1.1, the different colours in the boxplots represent the CI variable (Control or Industry) and the type variable (background or engraving). This allows for visual identification of trends or discrepancies for each combination of these over time¹⁴.

The width of each box plot represents the amount of data available for each combination of year, CI variable and type – the wider the box, the more data there was, and as can be seen, there is no control data for 2017.

¹³ Note that 2004 data is included in these plots, despite being excluded from all analyses and from all similar plots that don't display each year separately. Its inclusion in this particular set of plots is considered appropriate as it (a) demonstrates the differences between the 2004 data and all subsequent data, hence justifying its exclusion from the analysis, and (b) does not impact on any other data in the plot, because this year's data is being displayed separately.

¹⁴ Boxplots for each variable individually are provided in Appendix C0.

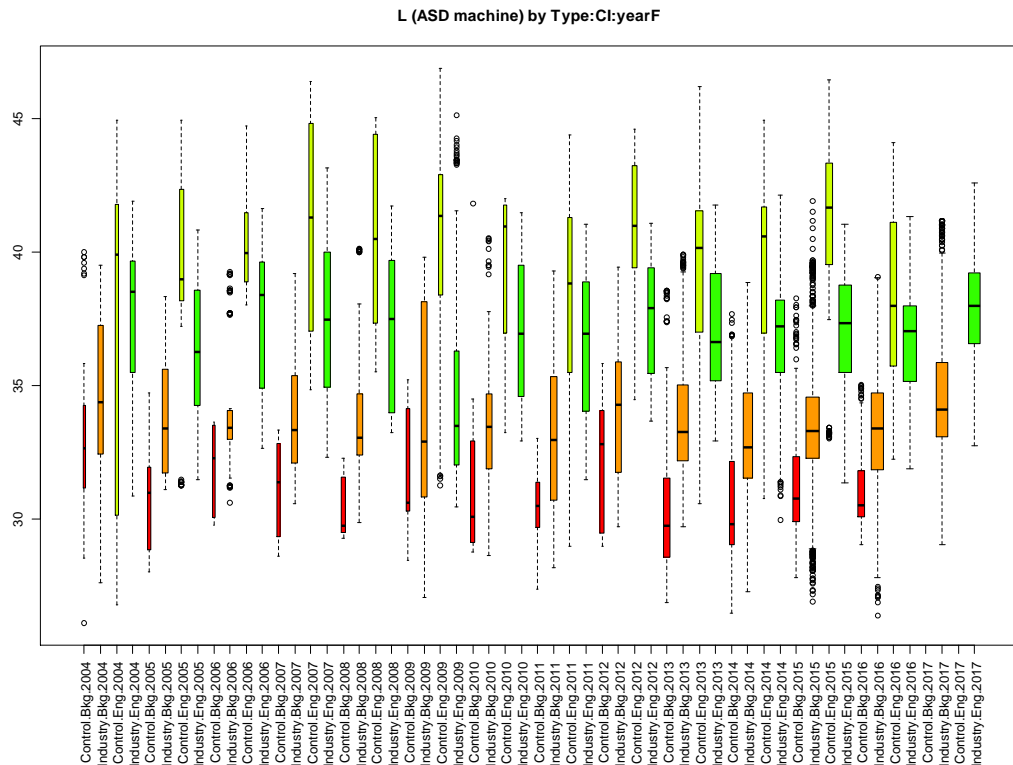


Figure 9. Box plot for the ASD L* by Type:CI:yearF for all sites.

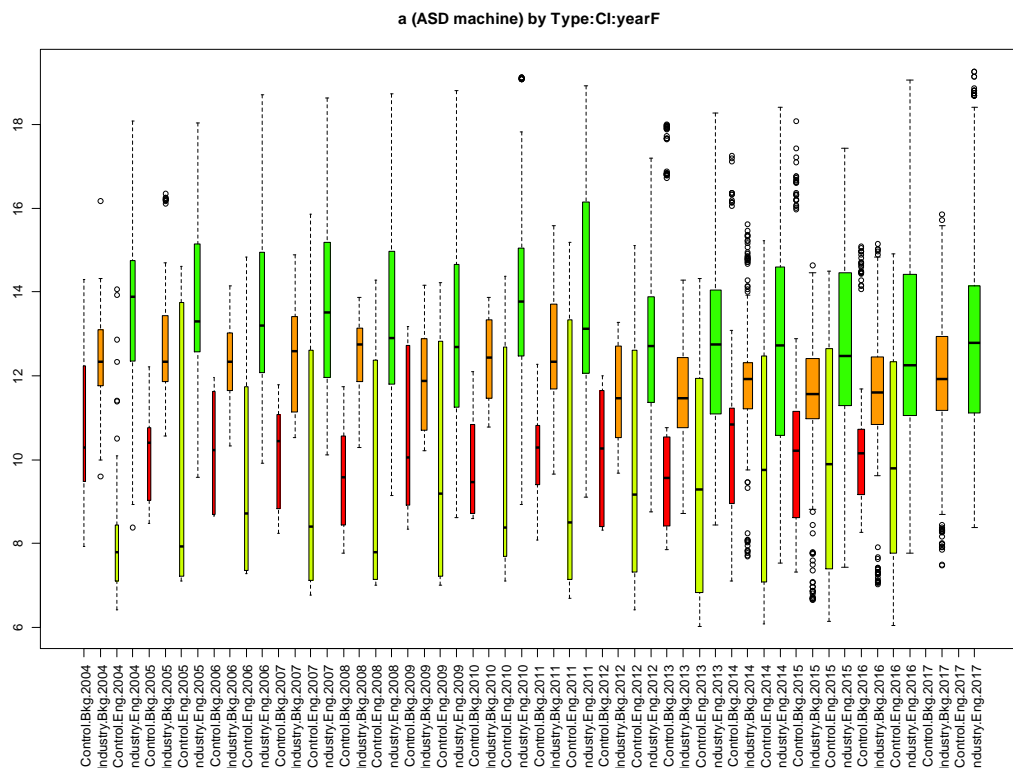


Figure 10. Box plot for the ASD a* by Type:CI:yearF for all sites.

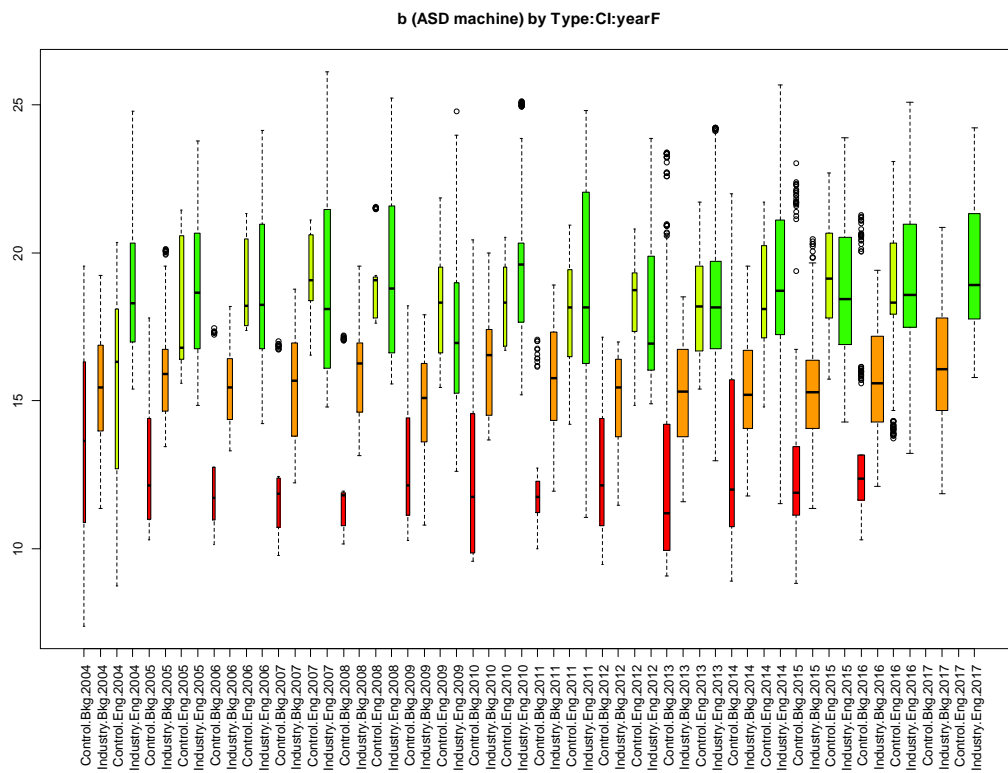


Figure 11. Box plot for the ASD b^* by Type:CI:yearF for all sites.

2.2.2 Box Plots of ASD Colour Data for Yara and Control Sites Only

The following figures (Figure 12 to Figure 14) are analogous to those in the previous section, but are restricted to the Yara and Control sites only.

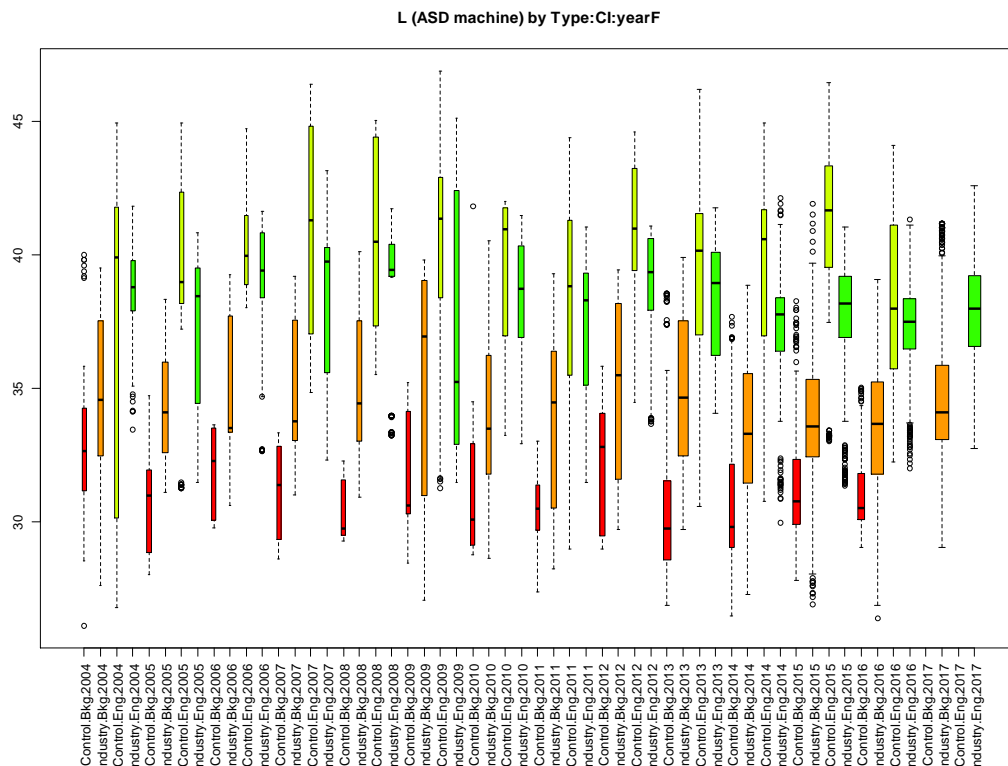


Figure 12. Box plot for the ASD L^* by Type:CI:yearF for Yara sites and control sites.

a (ASD machine) by Type:CI:yearF

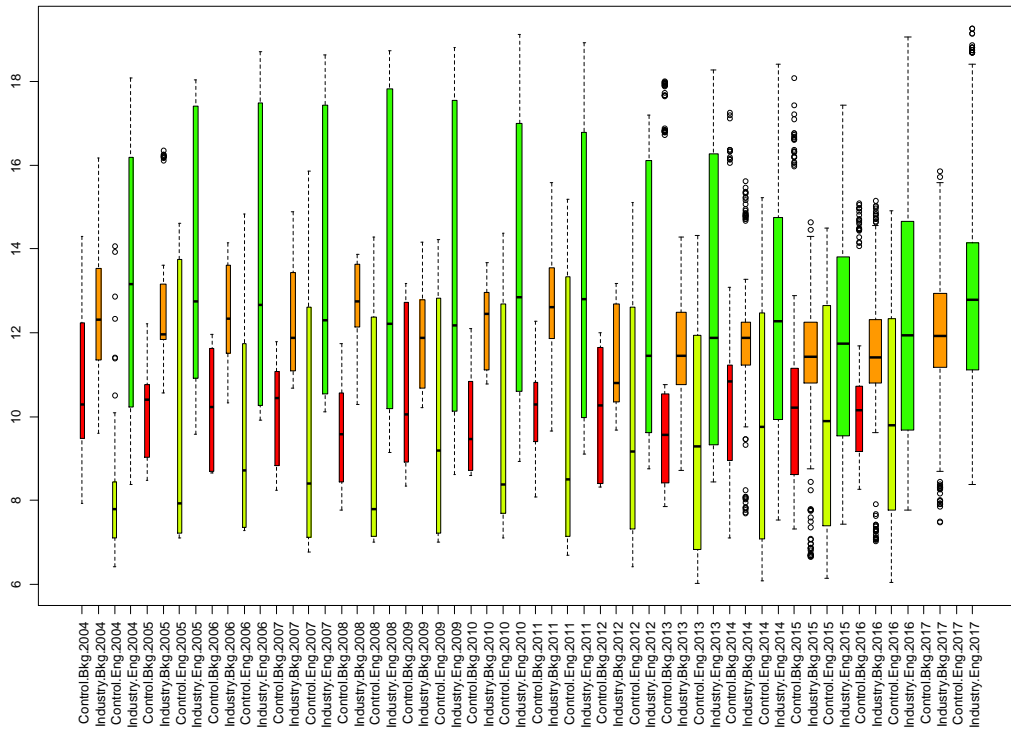


Figure 13. Box plot for the ASD a* by Type:CI:yearF for Yara sites and control sites.

b (ASD machine) by Type:CI:yearF

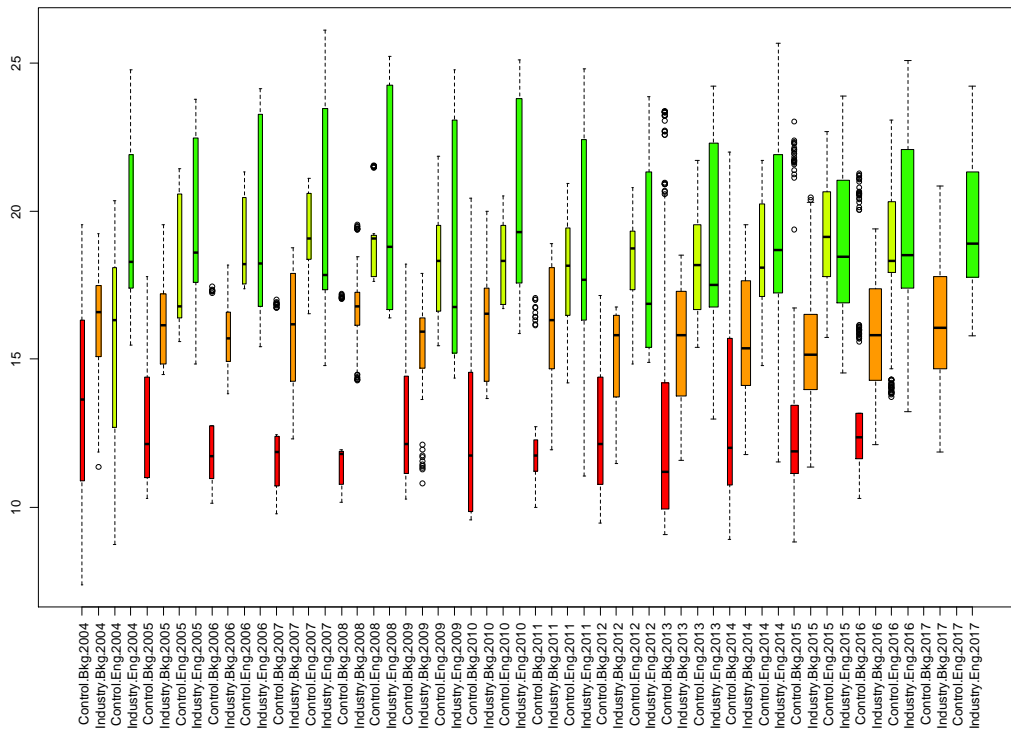


Figure 14. Box plot for the ASD b* by Type:CI:yearF for Yara sites and control sites.

2.2.3 Box Plots of ASD Spectral Line Data Values for all sites

The following set of figures (Figure 15 to Figure 19) show boxplots of the average ASD spectral line data values, for all sites included in the monitoring. The different

colours in the boxplots represent the CI variable (Control or Industry) and the type variable (background or engraving). This allows for visual identification of trends or discrepancies for each combination of these over time.

The width of each box plot represents the amount of data available for each combination of year, CI variable and type – the wider the box, the more data there was, and as can be seen, there is no control data for 2017.

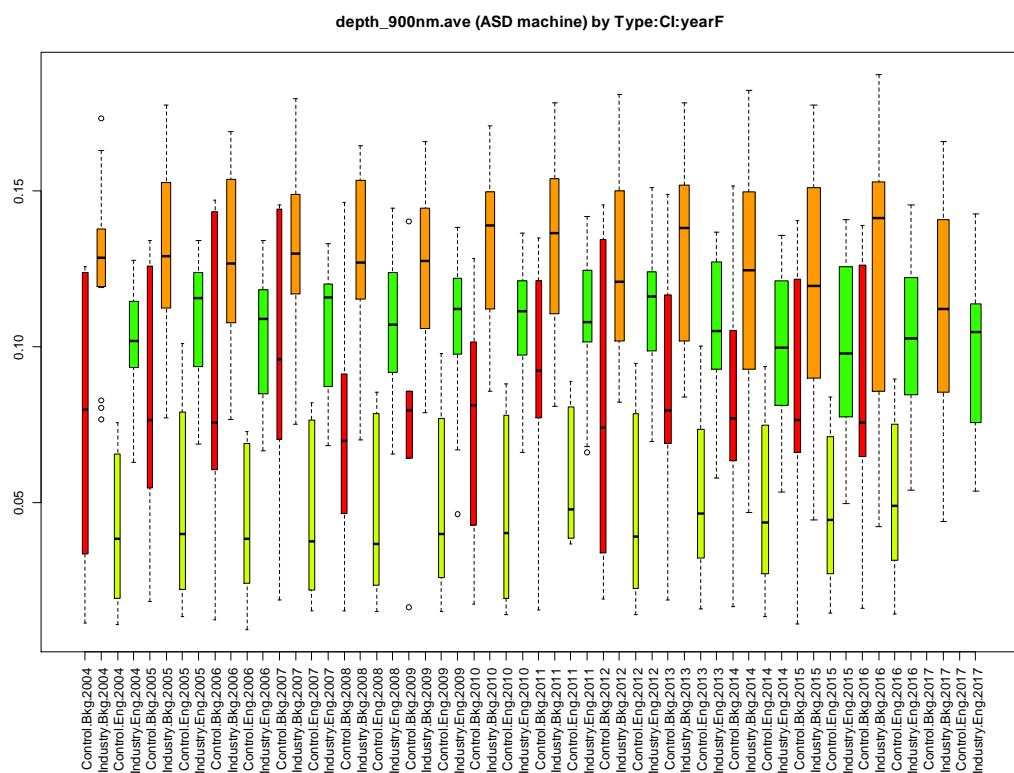


Figure 15. Box plot for the depth at 900 nm by Type:CI:yearF for all sites.

min_wavelength_900nm.ave (ASD machine) by Type:CI:yearF

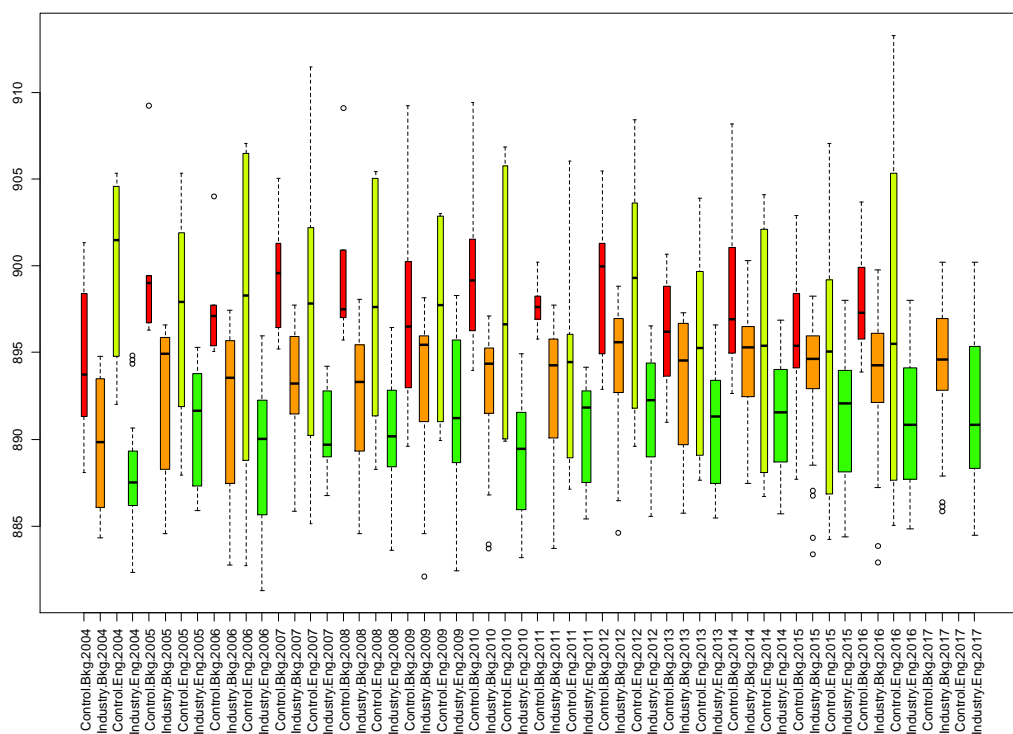


Figure 16. Box plot for the minimum of wave length by Type:CI:yearF for all sites.

depth_chlorite.ave (ASD machine) by Type:CI:yearF

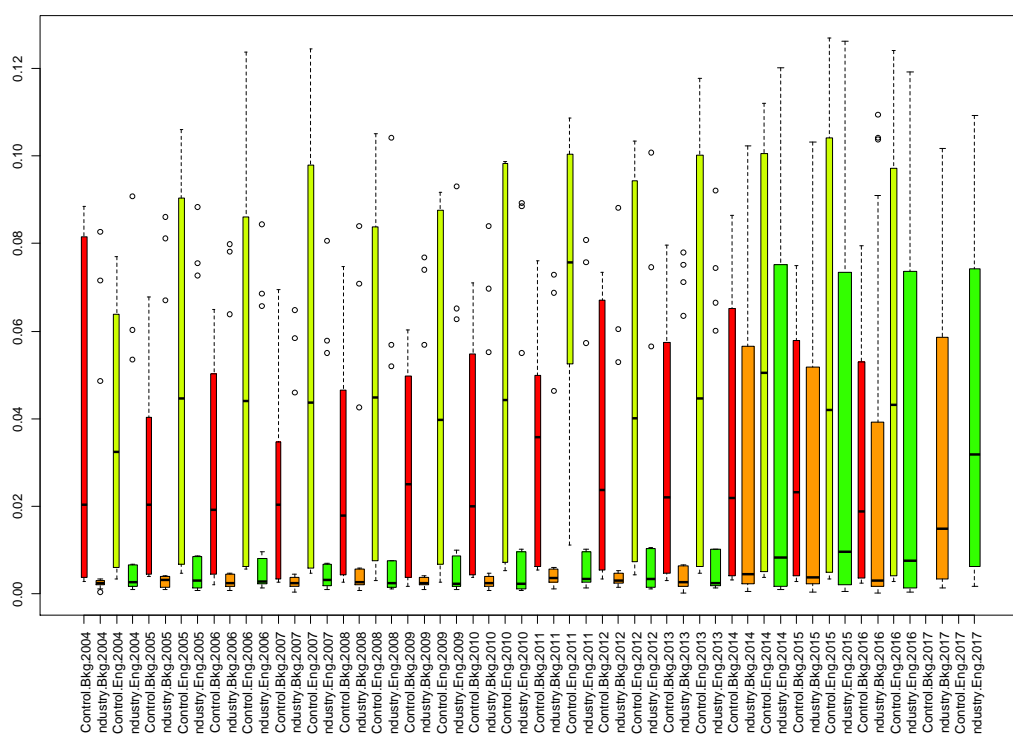


Figure 17. Box plot for the depth of chlorite by Type:CI:yearF for all sites.

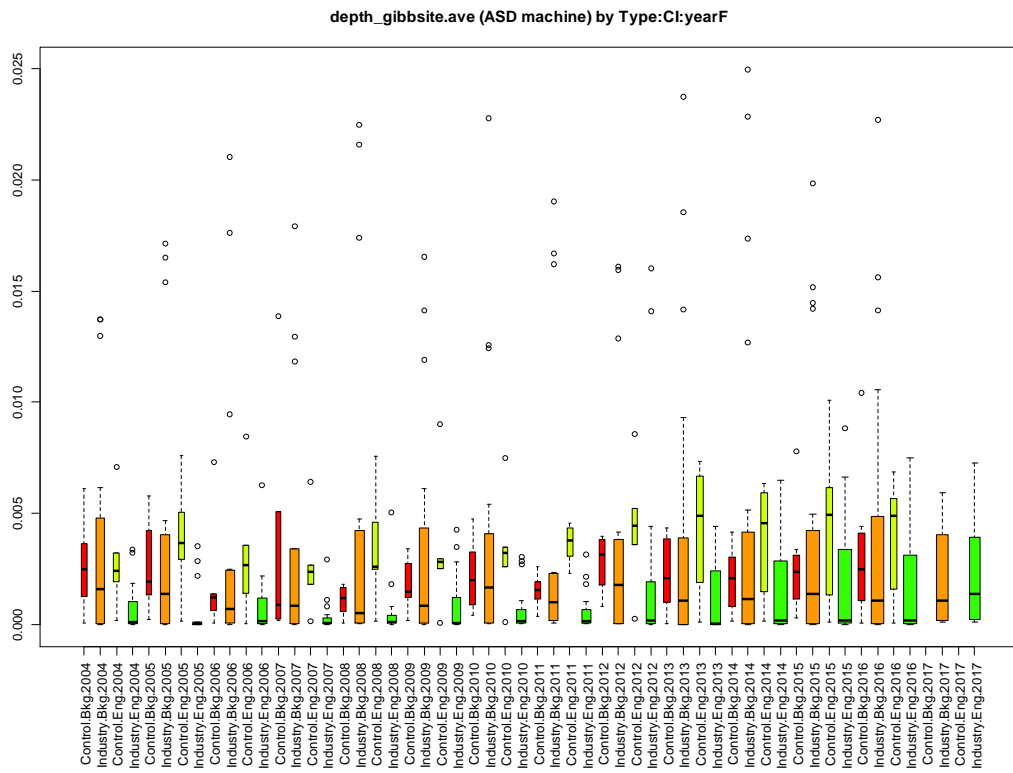


Figure 18. Box plot for the depth of gibbsite by Type:CI:yearF for all sites.

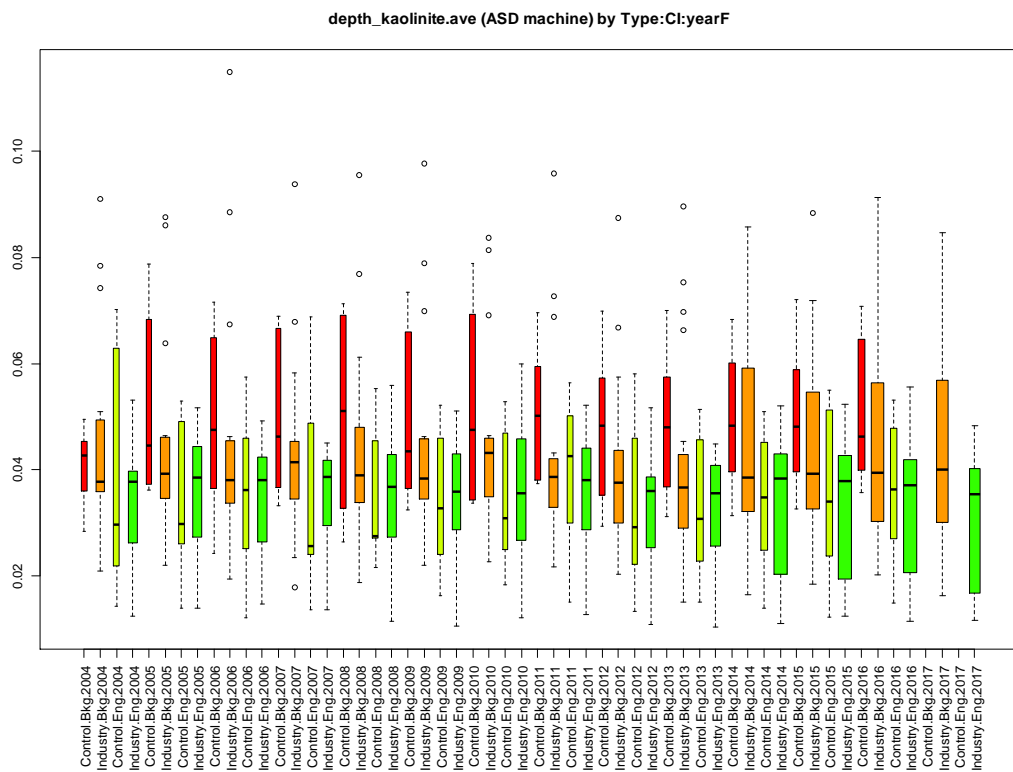


Figure 19. Box plot for the depth of kaolinite by Type:CI:yearF for all sites.

2.2.4 Box Plots of ASD Spectral Line Data Values for Yara and Control Sites Only

The following figures (Figure 20 to Figure 24) are analogous to those in the previous section, but are restricted to the Yara and Control sites only.

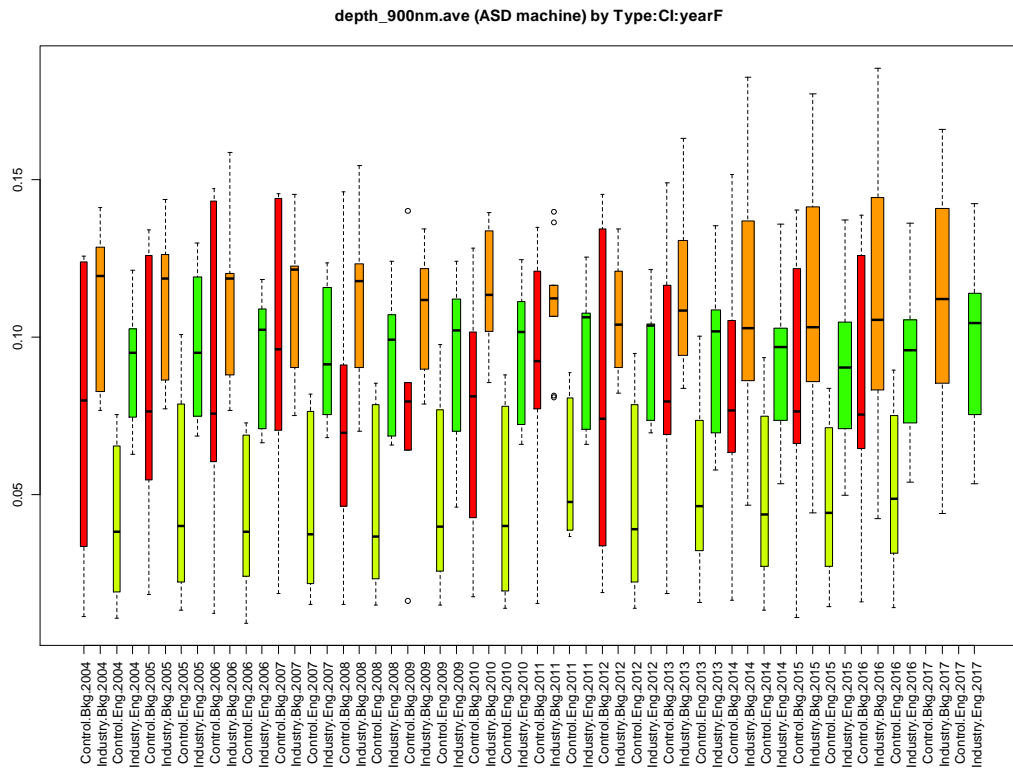


Figure 20. Box plot for the depth at 900 nm by Type:CI:yearF for Yara sites and control sites.

min_wavelength_900nm.ave (ASD machine) by Type:CI:yearF

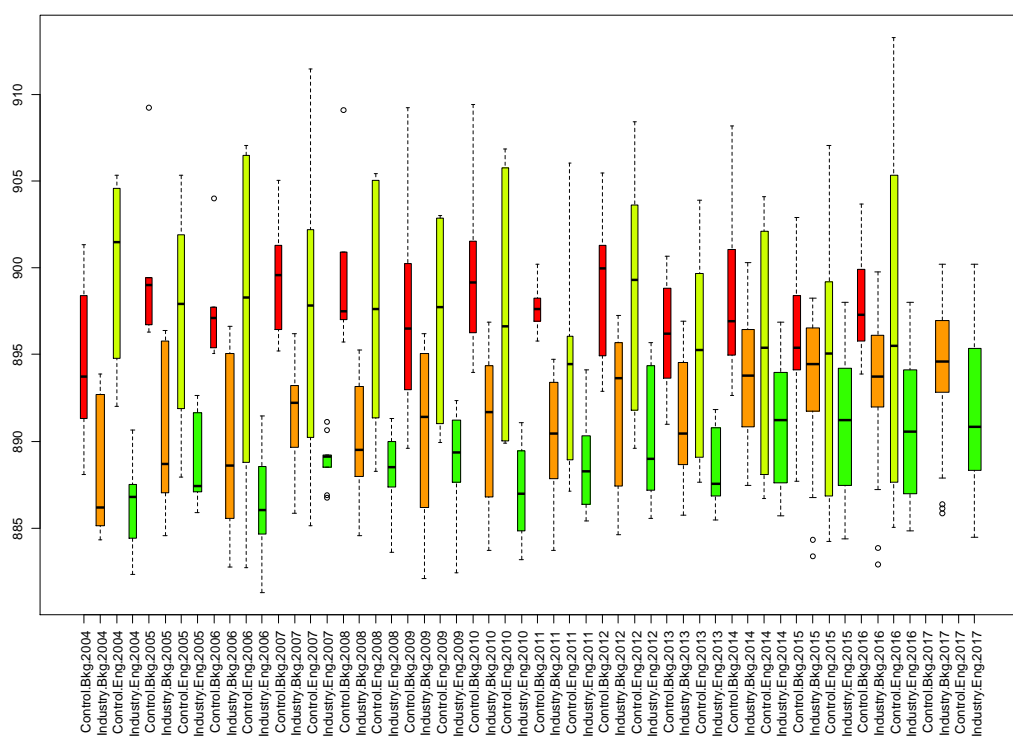


Figure 21. Box plot for the minimum wave length by Type:CI:yearF for Yara sites and control sites.

depth_chlorite.ave (ASD machine) by Type:CI:yearF

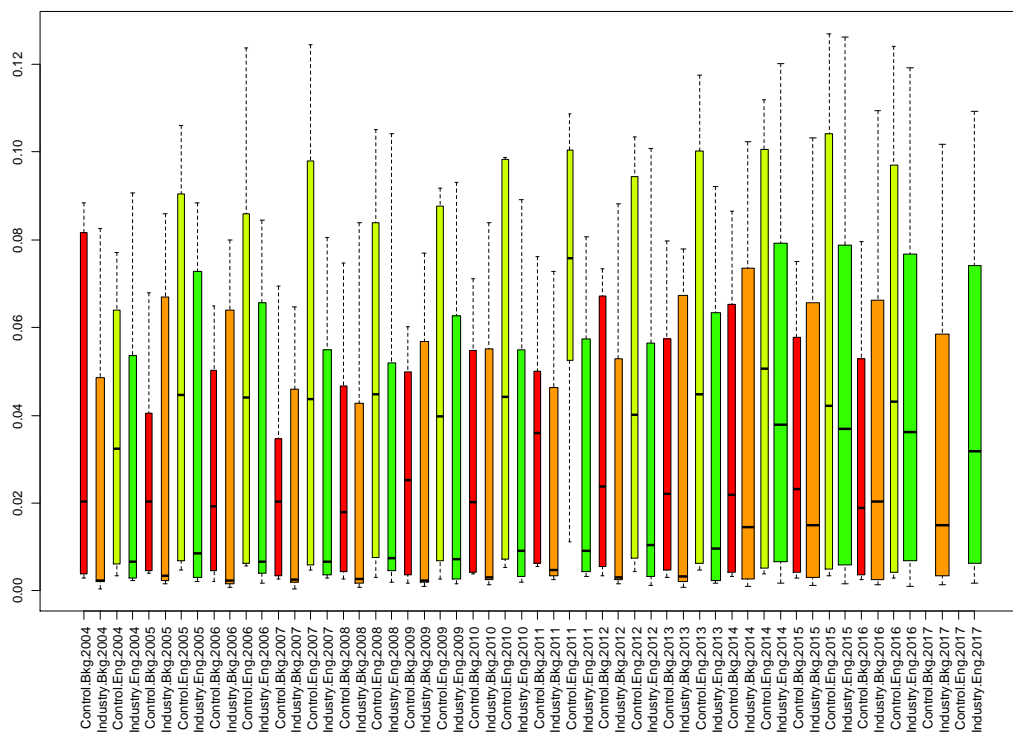


Figure 22. Box plot for the depth of chlorite by Type:CI:yearF for Yara sites and control sites.

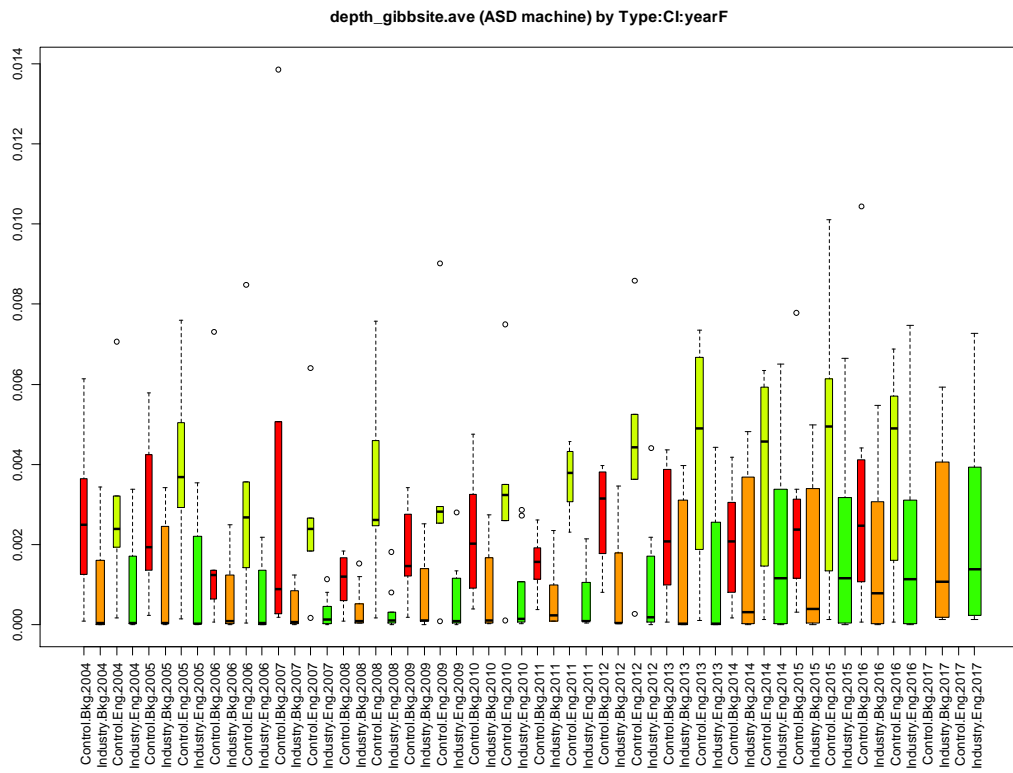


Figure 23. Box plot for the depth of gibbsite by Type:CI:yearF for Yara sites and control sites.

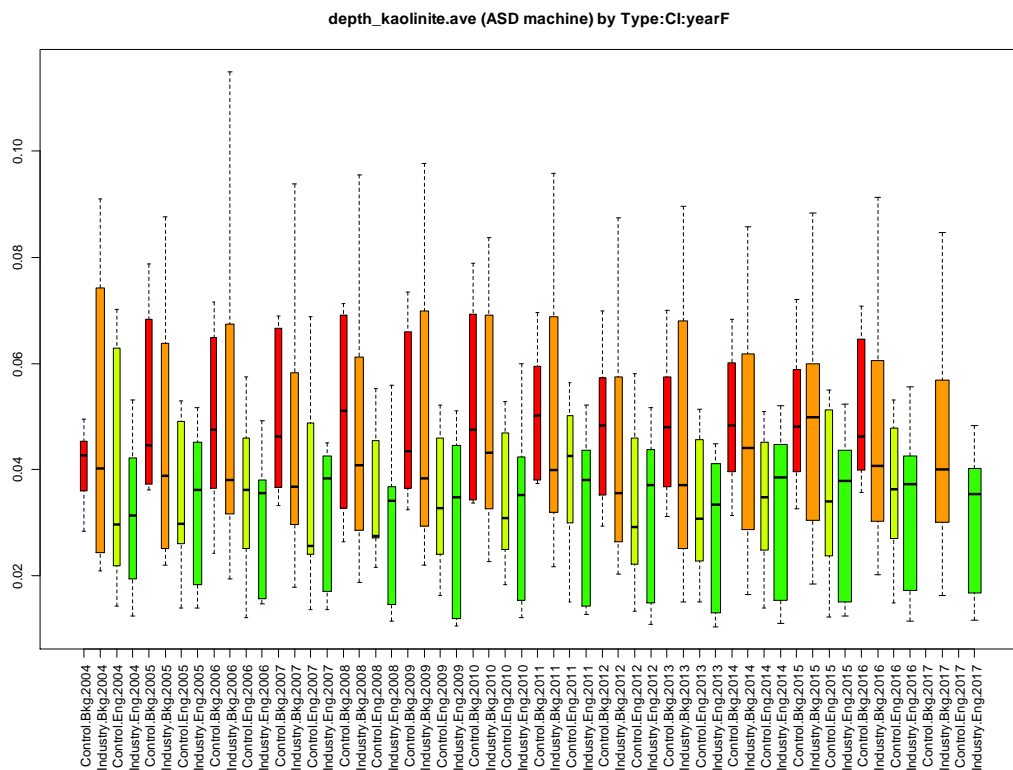


Figure 24. Box plot for the depth of kaolinite by Type:CI:yearF for Yara sites and control sites.

3. Modelling of Colour Data

Data Analysis Australia carried out a number of analyses for variables L^* , a^* and b^* . Since the data for control sites (sites 1 and 2) were not available in 2017, a trend model was used to determine whether the trend remains unchanged over the years.

Linear mixed effects models were fitted, including random effects to take into account variation between sites, between spots on a site and between times for each spot. In the investigation of what would be the most appropriate models, several observations were made:

- We had anticipated that the random effects component – essentially the structure of measurement errors – would have a “spots within sites” aspect and a year-to-year component represented by the model formula $sites/spots+years$. This reflected that sites were chosen at random but thereafter kept constant, and within each site, spots were also chosen at random and then kept constant, but that there was no correspondence between spots at different sites. The year component was thought necessary to allow for subtle changes in methodology and observation conditions.
- It became apparent that the random component had an additional aspect, the variation from year to year at each spot, leading to the model formula $sites/spots/years+years$. This strongly suggests that in each year the fieldworkers had difficulty in identifying the precise points on the rock surface to be measured. That is, each year, the workers attempted to identify a “correct” point and aimed their repeated measurements at that point, but the point varied from year to year. This effect was substantially greater than any systematic variation from year to year, suggesting that the fieldworkers were consistently implementing a flawed methodology – it seems virtually impossible to ensure the precise point is being “found” every year.
- The analysis method we used could readily adapt to this observation, but it does have implications for future planning.
- In parallel to this modelling we also examined the NIR spectral line data. This data made it apparent that rock type – Gidley gabbro (sites 1, 7, 22, and 23) versus Gidley granophyre (2, 4, 5, 6, 8, and 21)¹⁵ – could be more significant than previously thought. Hence this was introduced as a factor in the models, despite our reservations on the small number of sites for each rock type.
- It was also thought appropriate to include analyses that were restricted to the sites around the Yara plant and were measured in 2017. This restored a semblance of statistical balance (the control sites were still missing in 2017) and gave the possibility of giving findings more relevant to Yara.
- Given the number of variables, the key step was to consider overall significance of the interaction $control:type:time$. A simple likelihood ratio test was used to compare a full model that includes this three way interaction (and interactions

¹⁵ CSIRO (2014). *Burrup Peninsula Aboriginal Petroglyphs: Colour Change & Spectral Mineralogy 2004-2014*.

that include it) with a reduced model that does not. It is a standard statistics result that twice the logarithm of the ratio of the likelihoods for these two models will have a chi squared distribution with degrees of freedom corresponding to the differences in the models. A likelihood ratio greater than a critical value derived from the chi squared distribution is indicative of statistical significance. (The significance of rock type made this step slightly more complex, with the need to consider both this three way interaction and the four way interaction that also included rock type.)

- The analysis was performed in the statistical program R¹⁶, using the function `lmer`. The maximum likelihood approach was used so that models could be validly compared using the likelihood ratio statistic. The calculated values of this statistic were compared against the chi-squared distribution which is known to be asymptotically appropriate.

These observations largely applied to the analysis of the spectral line data as well. The key difference was that the spectral line data were based on *average* spectra at each point rather than the individual replicated spectral measurements.

Summary plots of the colour data for the KM and ASD instruments are presented in Appendix E.

3.1 KM Colour Data

The results of the test of statistical significance are given in Table 1 and Table 2 below, considering models without and with rock type as a factor respectively¹⁷. Note however that the overall effect of rock type is statistically significant and hence the primary reference should be Table 2, with Table 1 being provided for comparison with previous reports.

From Table 2, it can be seen that the changes in the colour measures a^* and b^* appear to be statistically significant, with L^* being close to statistically significant, with little difference between whether the analysis uses the full data or just the Yara specific data.

Table 1. Chi square statistics for the test on whether there is a significant three way interaction *control:type:time* with the KM data. These correspond to the models *without* rock type included. The critical value (at the 5% level) for the test is 5.99 based upon 2 degrees of freedom.

	Chi square	
	Full Data	Yara Sites
L^*	0.38	0.76
a^*	0.31	0.16
b^*	3.23	0.67

¹⁶ R Core Team (2018). *R: A language and environment for statistical computing*. R Foundation for Statistical Computing, Vienna, Austria. URL <https://www.R-project.org/>.

¹⁷ The relevant model details are provided in Appendix G.1.

Table 2. Chi square statistics for the test on whether there is a significant three way interaction *control:type:time* with the KM data. These correspond to the models *with* rock type included. The critical value (at the 5% level) for the test is 9.49 based upon 4 degrees of freedom.

	Chi square	
	Full Data	Yara Sites
L^*	8.15	8.58
a^*	17.50	17.95
b^*	16.61	16.12

Using a^* and the full dataset as a demonstrative example, this apparently significant interaction is better illustrated in Figure 25, a diagram termed an interaction plot. Similarly shaped lines on such a plot indicate that there is no interaction. Here the predicted values for a^* are given for the various combinations of engraving versus background, control versus industry and gabbro versus granophyre. (A full set of interaction plots is provided in Appendix H.)

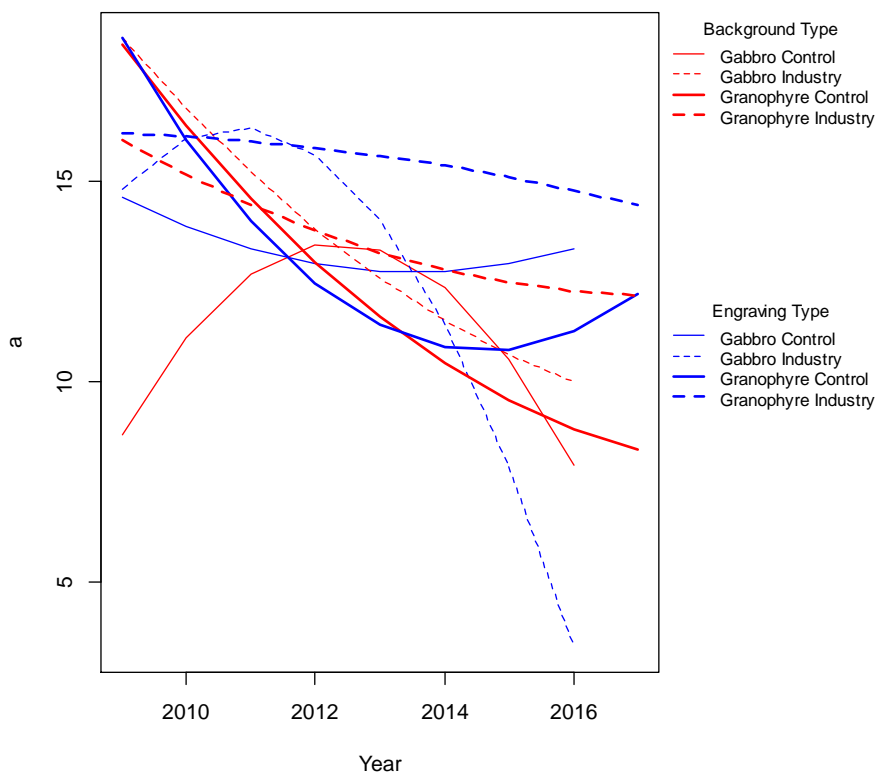


Figure 25. Interaction plot for full KM data, a^* . The engraving effects are in blue, the background in red. The control effects are continuous, the industry dashed. The granophyre effects are heavy lines, the gabbro light.

The picture presented by this plot is complex, indicating that interpretation is not straightforward. There appear to be several different trends. An investigation of the data behind this suggested that the greatest contribution to the interaction is from the granophyre control (Site 2, the heavy continuous lines). It is unfortunate that this site is the only granophyre control site and there is also only one gabbro control site, a limitation of the monitoring design dating back to 2004. Hence care should be taken in assuming that the statistical significance has practical significance.

3.2 ASD Colour Data

The analysis of the ASD data followed closely that of the KM data. In this regard there was a significant difference between the analysis presented here and that done in Data Analysis Australia's 2016 and 2017 reports¹⁸, namely in the consideration of variation in the residual randomness between years. Our 2017 analysis had identified that there were statistically significant differences in the level of randomness, suggesting changes in procedures. The analysis presented in our 2017 report took this into account. In the current project this complexity was dropped when it was observed that it made almost no effect on the analyses (estimated coefficients and significance of effects) while increasing the computational time by a factor of about 100. The faster computation allowed us to explore a greater range of models and hence feel more confident about the overall results.

The results of the test of statistical significance are given in Table 3 and Table 4 below, considering models without and with rock type as a factor respectively¹⁹. The overall effect of rock type is statistically significant and hence the primary reference should be Table 4, with Table 3 being provided for comparison with previous reports. In the case of the models without consideration of rock type, the tests fail to reach a level of statistical significance. In the case of the models with rock type included, the results for a^* and b^* appear to be strongly significant and those for L^* to be close to statistically significant, a result similar to that observed with the KM data.

Table 3. Chi square statistics for the test on whether there is a significant three way interaction *control:type:time* with the ASD data. These correspond to the models *without* rock type included. The critical value (at the 5% level) for the test is 5.99 based upon 2 degrees of freedom.

	Chi square	
	Full Data	Yara Sites
L^*	0.38	0.76
a^*	0.311	0.16
b^*	3.22	0.67

Table 4. Chi square statistics for the test on whether there is a significant three way interaction *control:type:time* with the ASD data. These correspond to the models *with* rock type included. The critical value (at the 5% level) for the test is 9.49 based upon 4 degrees of freedom.

	Chi square	
	Full Data	Yara Sites
L^*	8.15	8.58
a^*	17.50	17.96
b^*	16.61	16.12

¹⁸ Reports referenced in Section 1.1.

¹⁹ The relevant model details are provided in Appendix G.2.

Again the structure of this interaction can be investigated through an interaction plot, such as given in Figure 26 for a^* and the full data. (The full set of interaction plots is again provided in Appendix H.)

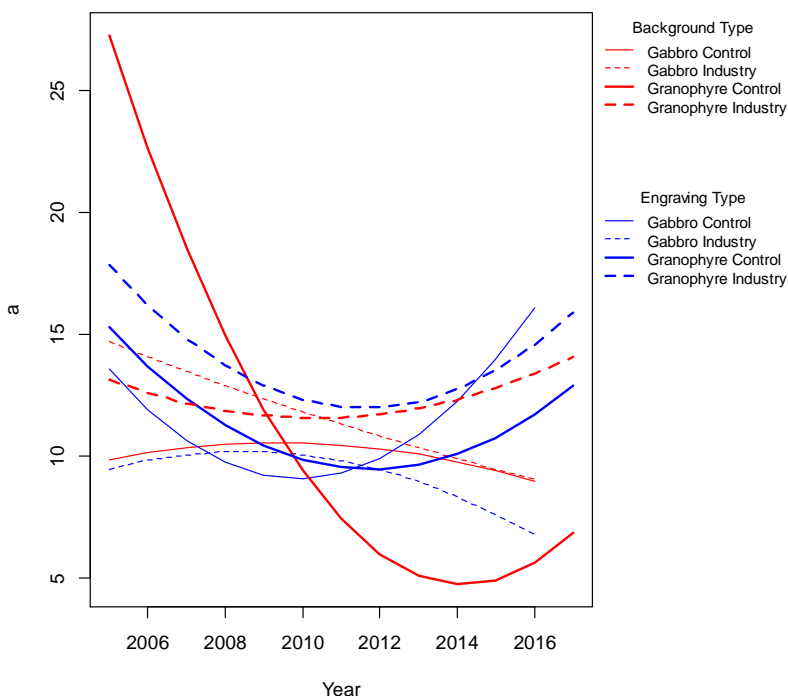


Figure 26. Interaction plot for full ASD data, a^* . The engraving effects are in blue, the background in red. The control effects are continuous, the industry dashed. The granophyre effects are heavy lines, the gabbro light.

Again it appears that this result is strongly affected by possibly aberrant data from Site 2, although the pattern is not particularly similar to that based on the equivalent KM data. This requires further investigation but is beyond the scope of this report as it possibly requires consideration of the differences between the two instruments.²⁰

4. Modelling of ASD Spectral Line Data

The initial analysis of the spectral line data was exploratory, particularly since past studies had not investigated it in detail. The five spectral line parameters (as specified in Section 1.2.2) were:

- The depth of the spectral absorption band at 900 nm (D900), associated with iron oxides;
- The minimum wavelength associated with the spectral band at 900 nm (W900);
- The depth of the chlorite absorption band at 2250 nm;
- The depth of the kaolinite absorption band at 2206 nm; and

²⁰ Differences that we are aware of include the diameters of the measurement area and the illumination system. In addition, the KM instrument calculates the (L^*, a^*, b^*) values using proprietary algorithms that are not necessarily the same as those used in the TSG software.

- The depth of the gibbsite absorption bands at 2267 nm (secondary minerals resulting from the weathering of the primary minerals).

The data was based on the average spectrum at each point in each year. Whilst this averaging process means that the measurement to measurement variation is lost, it seems appropriate given that the algorithms for extracting out spectral bands are non-linear and potentially sensitive to random effects. The 2016 data as provided also had average L*, a* and b* values, and a similar calculation was applied by Data Analysis Australia to the 2017 data. These L*, a* and b* variables were incorporated in the spectral line data *exploratory* analysis discussed below, although the more detailed replicate level L*, a* and b* values were used for the formal ASD colour data analysis in Section 3.2. Comparable formal statistical modelling of the five other parameters from the spectral line data are provided at the end of this Section. Two outliers were removed from the gibbsite depth analysis.

It became immediately apparent from the “pairs plots”²¹ below (Figure 27 and Figure 28) that the distributions of this data had a number of features²²:

- The importance of rock type is immediately evident, being most clear in the scatter plot of chlorite against gibbsite.
- It is also suggestive of the chlorite band showing minimal variation amongst the granophyre measurements.
- The relationships appear to be strongly non-linear, although to some extent this may be due to the different rock types acting as distinct populations.

Note that the differences between rock types (gabbro and granophyre) and measurement types (engraving and background) are displayed as different colours in these plots, to aid with the interpretation.

²¹ Pairs plots are a set (or matrix) of scatterplots that illustrate the relationship between each pair of variables in a dataset. Each plot in the upper-right portion of the matrix shows the relationship between two variables by plotting each data point from the first variable against each data point from the second variable. This allows for any association of the two variables to be seen. The red lines overlaying the scatterplots are loess curves – smoothed regression curves, smoothed by fitting to a localised area of the data, to assist with visualising trends in the data. (The precise details of these red lines are not important for this report.) The linear correlation of each pair of variables is shown in the lower-left portion of the matrix.

²² Additional graphs for each variable individually are provided in Appendix D.

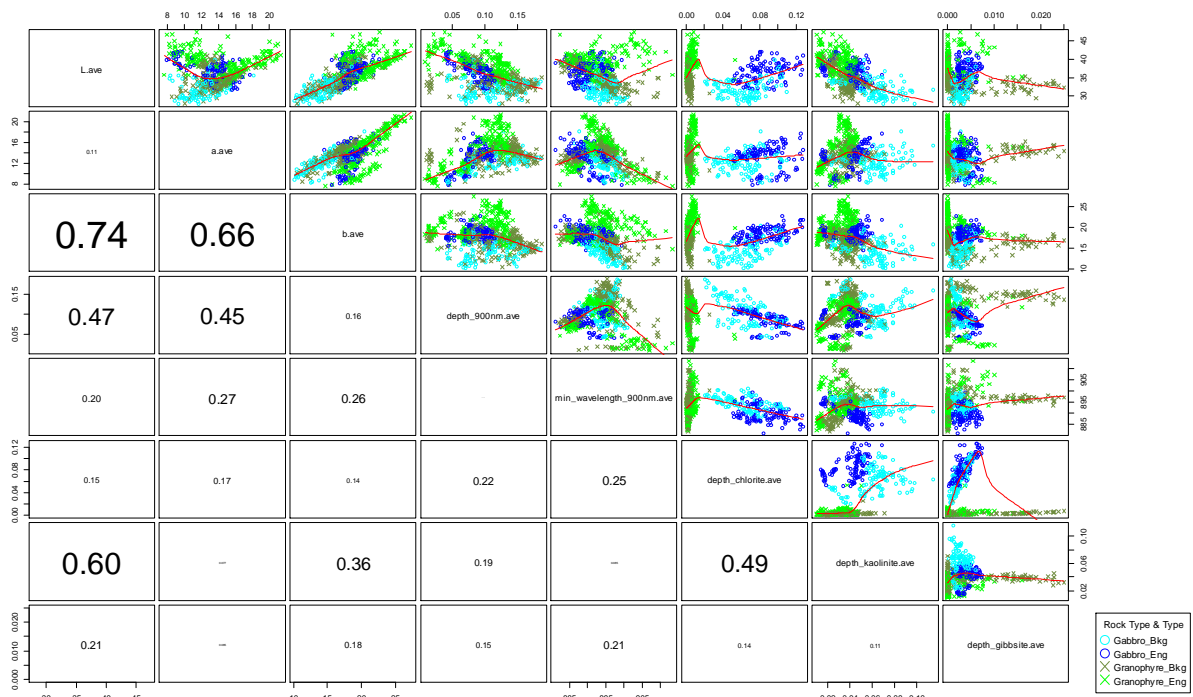


Figure 27. Pairs plot for all sites showing two-way relationships and linear correlations for spectral lines and L^* , a^* , b^* . Note that these L^* , a^* and b^* values are using average spectral data, and hence are not the same data used for the colour analysis in Section 3.2.

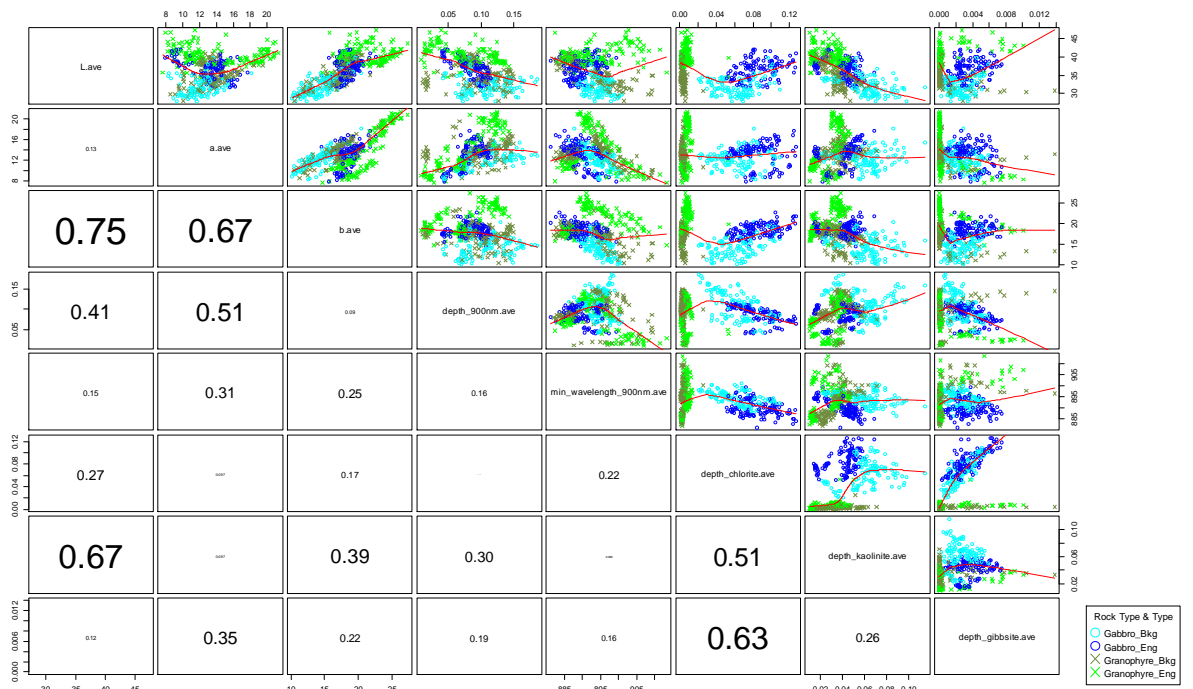


Figure 28. Pairs plot for Yara and control sites showing two-way relationships and linear correlations for spectral lines and L^* , a^* , b^* . Note that these L^* , a^* and b^* values are using average spectral data, and hence are not the same data used for the colour analysis in Section 3.2.

In formally analysing this data, various transformations were considered to ensure that the distributions of the data might reasonably meet the assumptions of the statistical methods. After investigation, two variables were modified:

- For the Gibbsite depth, the logarithm was taken; and
- The chlorite data was restricted to the gabbro sites.

The results of the tests of statistical significance are given in Table 5 below²³. For 900nm depth, kaolinite depth, and chlorite depth, a significant four-way interaction was found, which says that there is statistical evidence that the impact of Industry and Control sites over time is different between background and engraving for the two rock types. For 900nm minimum wavelength and gibbsite depth, there was not a significant four-way interaction.

Table 5. Chi square statistics for the test on whether there is a significant four way interaction *control:type:rocktype:time* with the ASD spectral line data. The critical value (at the 5% level) for the test is 9.49 based upon 4 degrees of freedom, except for the chlorite depth where it is 5.99 on 2 degrees of freedom.

	Chi square	
	Full Data	Yara Sites
900nm Depth	15.00	15.11
900nm Minimum Wavelength	7.86	6.37
Kaolinite Depth	14.38	11.98
Chlorite Depth (only gabbro)	6.50	6.50
Gibbsite Depth (logged)	2.69	4.51

Several of these are statistically significant. The interaction plots are given in Appendix H.3 and should be regarded with the same degree of caution recommended for the colour analyses in Sections 3.1 and 3.2. However several statistical comments can be made:

- The statistically significant interaction for the 900nm band depth is strongly affected by the industry gabbro sites.
- The variations in the depth of the kaolinite band, while statistically significant, are strongly affected by the granophyre control site (Site 2). This site has already been identified by the colour measurements as being potentially anomalous.
- The depth of the chlorite band at industry sites appears to be increasing over time, bringing it closer to the depth observed at the control site. (Note that this applies only to the gabbro sites.)

Data Analysis Australia is not able to comment upon the possible geological significance of these apparent changes.

²³ The relevant model details are provided in Appendix G.3.

5. Conclusion

Data Analysis Australia assembled a dataset that combined the 2017 data collected by Yara with the earlier years' data collected by the CSIRO. To ensure consistency, the 2017 data was processed using the same software – the CSIRO's The Spectral Geologist – before being merged. To assist future work, the settings used with this program are included in an Appendix of this report.

The analysis of the 2017 data collected by Yara raised a number of statistical issues, both in the handling of the data to ensure consistency with past data practices and in the analysis itself. Perhaps the greatest difference was the absence of data for the control sites in 2017.

This made it necessary to use a different approach in the modelling, namely the consideration of trends. While there is a degree of choice in just how trends are considered, after consideration of piecewise linear approaches the decision was made to use a quadratic trend. This allowed the full use of the information in the 2017 data, as well as giving some information on when changes may have been taking place through examination of the interaction plots.

The use of trend models meant that the 2004 ASD data had to be excluded due to inconsistency with following years. This also suggests that 2005 should be considered the "base year" in any future work.

In interpreting the results, it must be remembered that "the absence of evidence is not evidence of absence". If the monitoring does not show statistically significant change then it is appropriate to say that either "the data is consistent with no change" or that "if a change has occurred, it is below the level detectable by the monitoring program".

Key findings are that:

- The reservations Data Analysis Australia expressed in earlier reports about the design of the monitoring have been confirmed. This includes the number of sites monitored, particularly control sites, being inadequate, the difficulty in reliably measuring at the same spots year after year and effort wasted with too many replicate measurements.
 - Having only two control sites was highlighted as a problem in the analysis this year when it became apparent that rock type was statistically important – this means that for each rock type there is only a single control site. This will always throw doubt on the results.
 - There are strong statistical indications that the task of accurately identifying a "spot" (actually a pair of points, one in the engraving and one in the nearby background) to be measured is impossible to do consistently from year to year. Either the method of precisely locating the measurement points needs to be substantially improved or the size of each point being measured needs to be increased so that the effect of misplacement of the instrument is reduced. It is possible that this has implications for the choice of instrument.

- The high number of replicates measured at each spot is largely wasted effort since the repeat measures each year essentially repeat that year's errors. Given that there is concern about the possible damage being done by the measurement process, it seems appropriate to reduce the number of replicates from around 20 to (say) 5.
- Whilst the design of the monitoring is far from ideal, the absence of control site measurements in 2017 is unfortunate, and goes against both the intention of the original design and normal statistical best practice.
- The analysis of the ASD spectral line data highlighted the possible impact of rock type (gabbro versus granophyre) on all measurements. This year our analysis included rock type, initially in exploratory modelling, and this indicated that it has an effect on colour measurements as well. Previous analyses have not considered this.
- Both the KM and ASD instruments suggested colour changes may have taken place over the monitoring period at a different rate for the control and industry sites. However the two instruments do not identify a common structure to this possible change, casting some doubt on its true significance.
 - The lack of sufficient control sites also weakens the weight that can be given to this result.
 - The colour changes recorded by the ASD instrument appear to be significantly affected by the last few years' measurements at Site 2 – unfortunately this is a control site so the effect on the analysis is disproportionate. Further analysis is required to better understand this.
 - The ASD instrument appears more strongly affected by the rock type (gabbro versus granophyre) compared with the KM instrument. It is not possible for the data or statistics to confirm why this is so, but the most likely cause is different illumination and different geometry of the light receptor.
- The near infrared (NIR) spectral line data suggests some statistically significant changes. The analysis of this is particularly strongly affected by the rock type – indeed the NIR data makes the differences between rock types glaringly apparent, suggesting that this factor should have been incorporated into the monitoring from early on. Whilst it might be expected that different rock types give rise to significantly different spectral data, it is not so obvious that *changes* in the spectral data over time are similarly affected. Our analysis has demonstrated that this is the case.

Overall, this analysis extends the previous analyses through the additional data and through a trend based approach to modelling. The analysis suggests that some changes may have occurred, but this finding remains inconclusive.

Further analysis might shed some light on this. In this regard it is worth considering what additional data may be available to explain the observations, such as the possible age of the individual petroglyphs, their orientation etc. However any such analysis is likely to remain limited by the monitoring design.

Appendix A. ASD Spectral Plots

Four arbitrarily selected spectra are presented in Figure 29 to Figure 32 below, for illustrative purposes, as displayed by the TSG program. The first three figures show typical patterns for the measured points (both background and engraving). In contrast, Figure 32 clearly illustrates an erroneous reading, and this point was excluded from the analysis as an outlier.

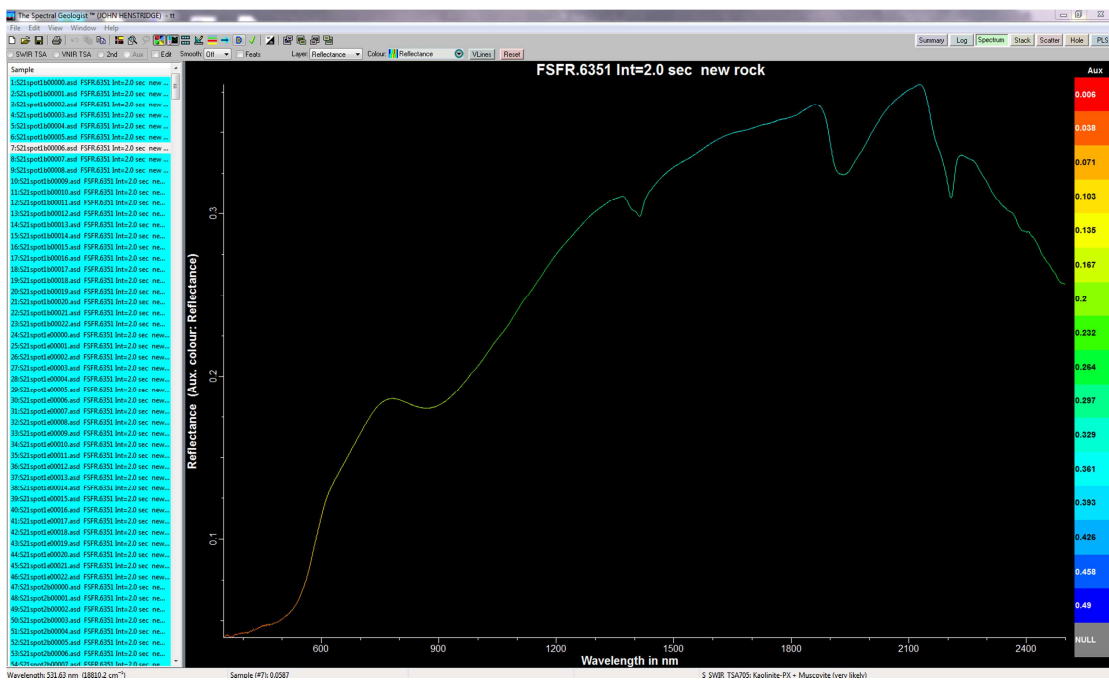


Figure 29. Spectral line for random selected point at site21, spot 6, point 6, and type background.

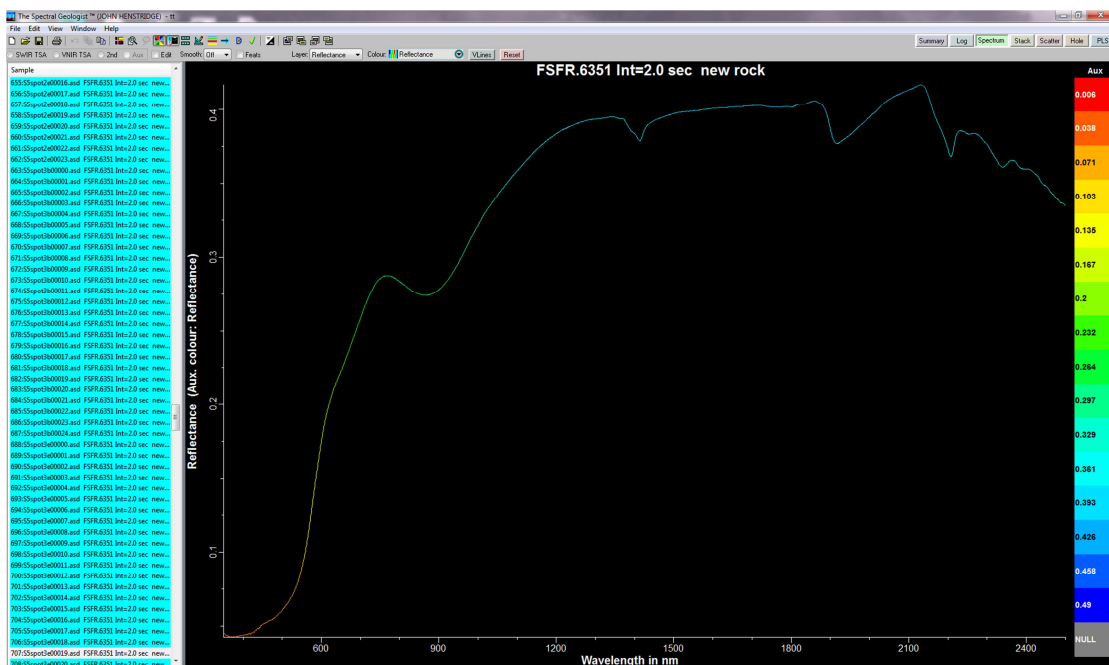


Figure 30. Spectral line for random selected point at site5, spot 3, point 19, and type engraving.

DATA ANALYSIS AUSTRALIA PTY LTD

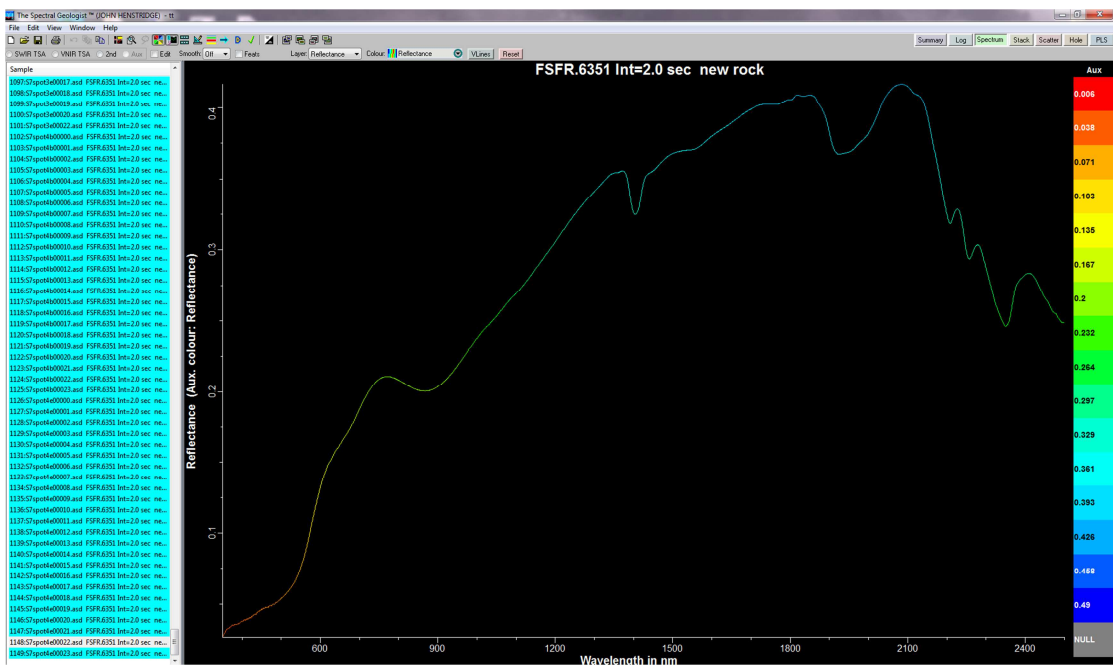


Figure 31. Spectral line for random selected point at site 7, spot 1, point 22, and type engraving.

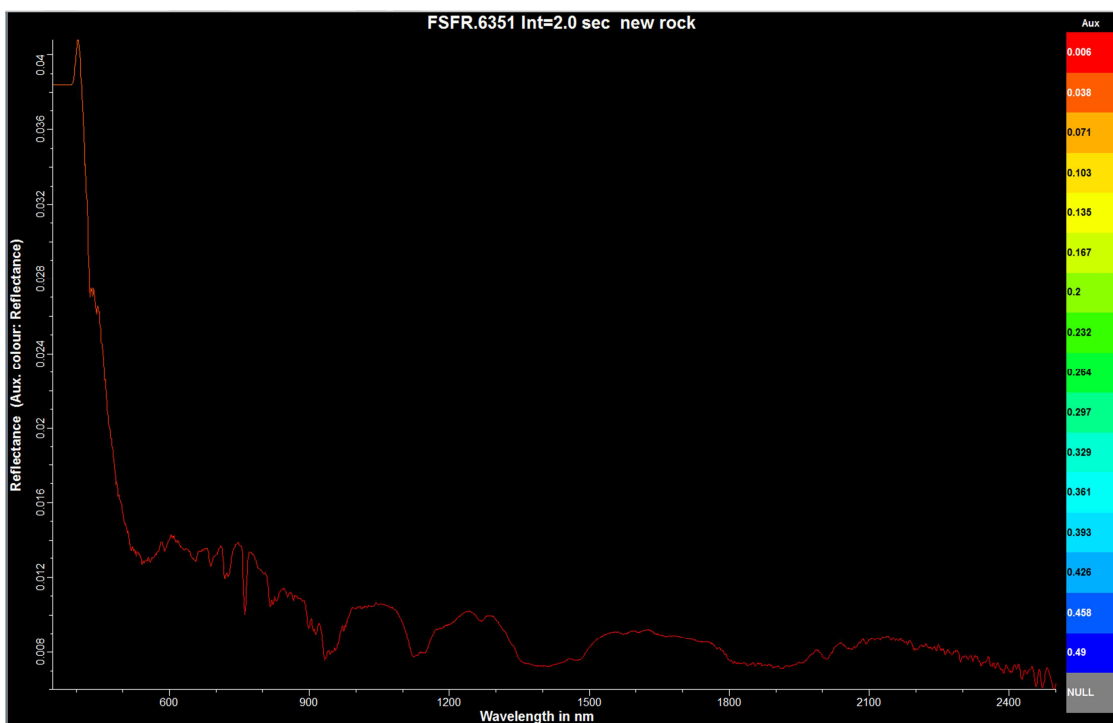


Figure 32. Spectral line for outlier point at site 5, spot 3, and type background.

Appendix B. Distribution of L*, a* and b* Values With the KM Instrument

The boxplots in this Appendix show the distribution of L*, a* and b* values from the KM instrument for all sites and then for Yara and Control sites only. These boxplots show the values for each of type, Control-Industry, Site and Year separately, rather than as the three way plots shown in the main report. As a result, care must be taken when interpreting these boxplots, as apparent differences in one variable (e.g. time) may be caused by a difference in another variable (e.g. that control site data is not available for 2017, but is included for all other years).

B.1 All Sites

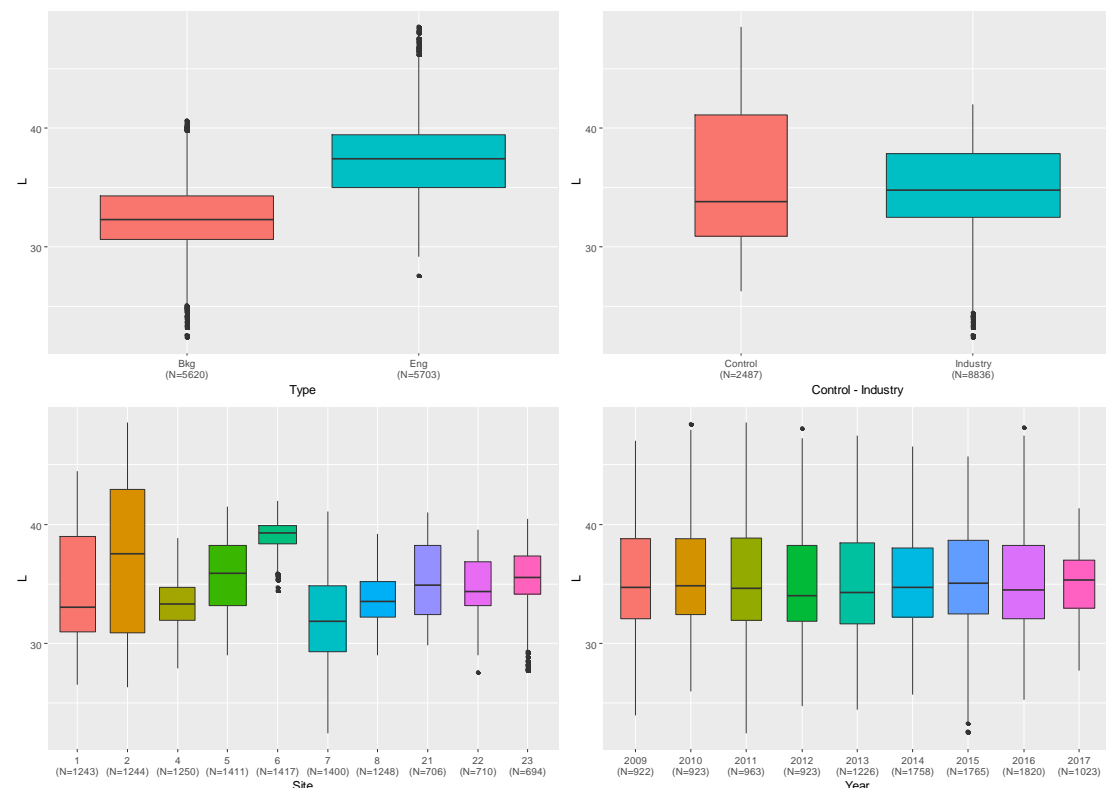


Figure 33. Distribution of L* observations made with the KM instrument, all sites.

DATA ANALYSIS AUSTRALIA PTY LTD

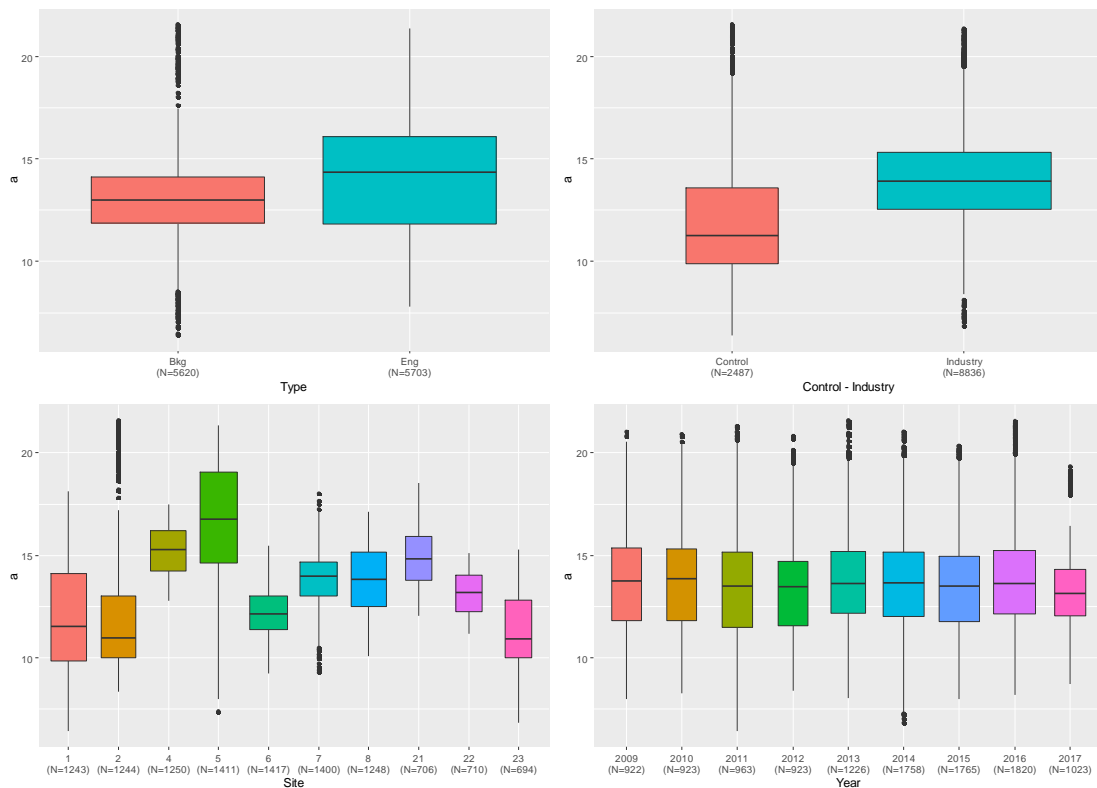


Figure 34. Distribution of a^* observations made with the KM instrument, all sites.

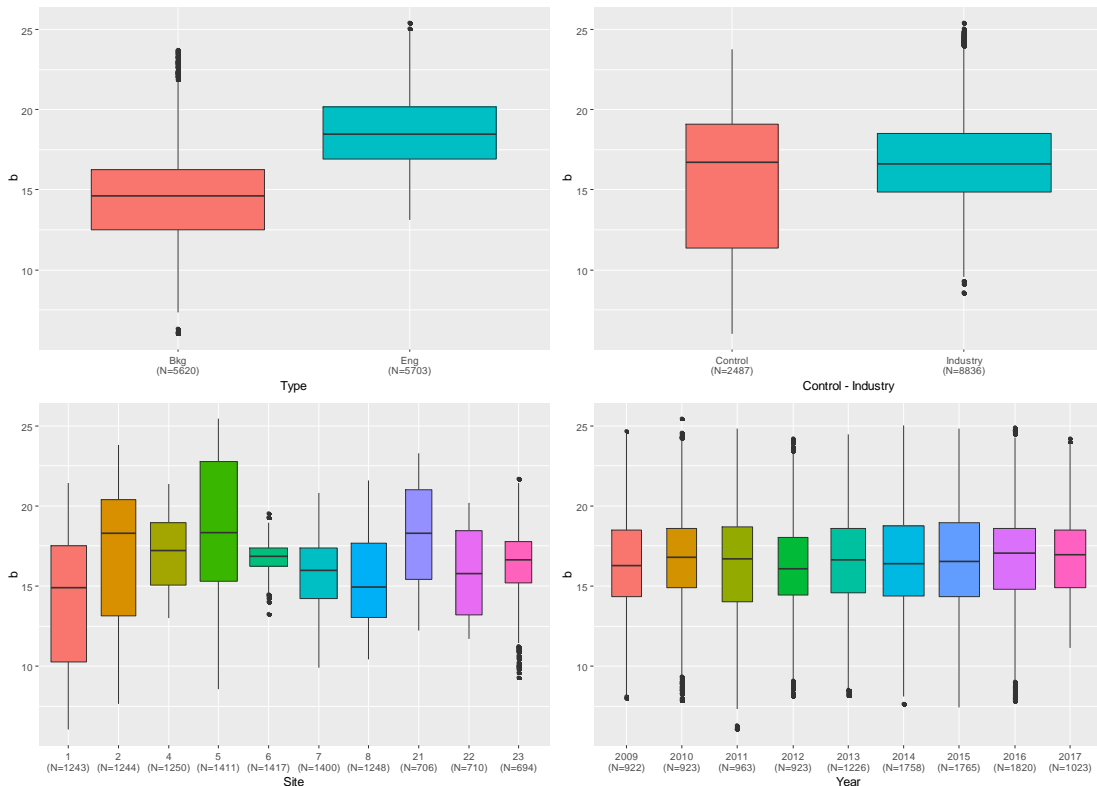


Figure 35. Distribution of b^* observations made with the KM instrument, all sites.

B.2 Yara and Control Sites Only

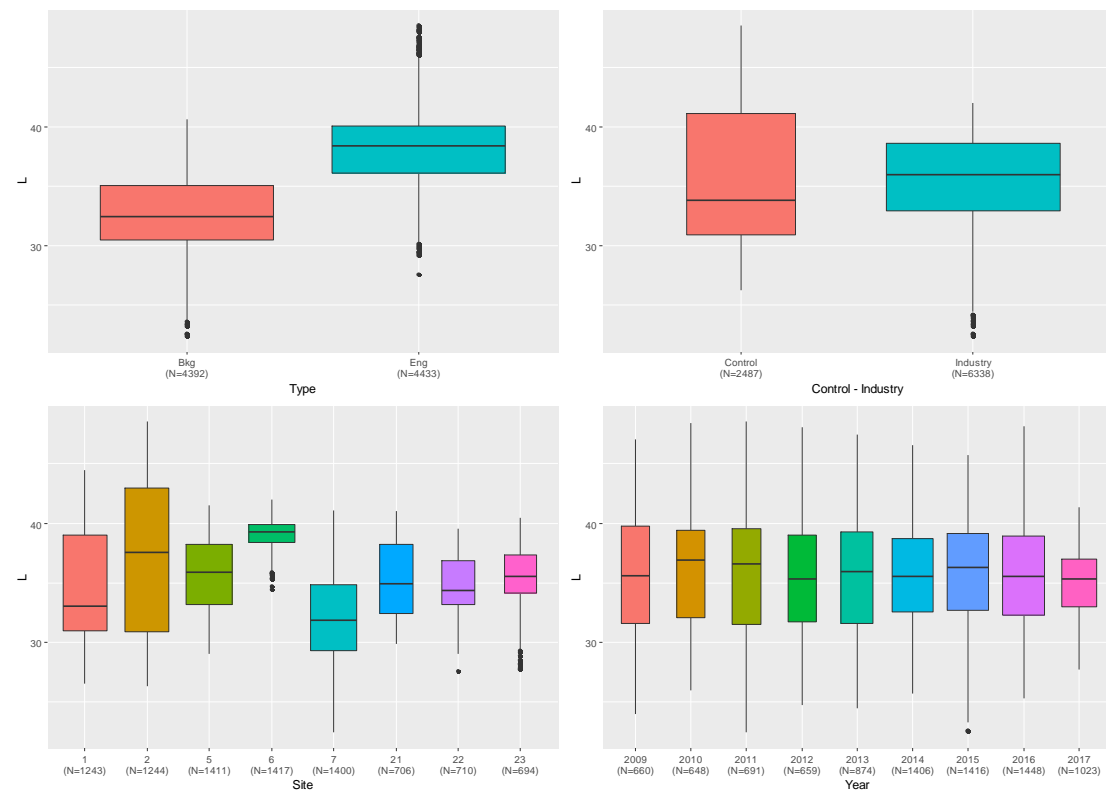


Figure 36. Distribution of L* observations made with the KM instrument, Yara and Control sites only.

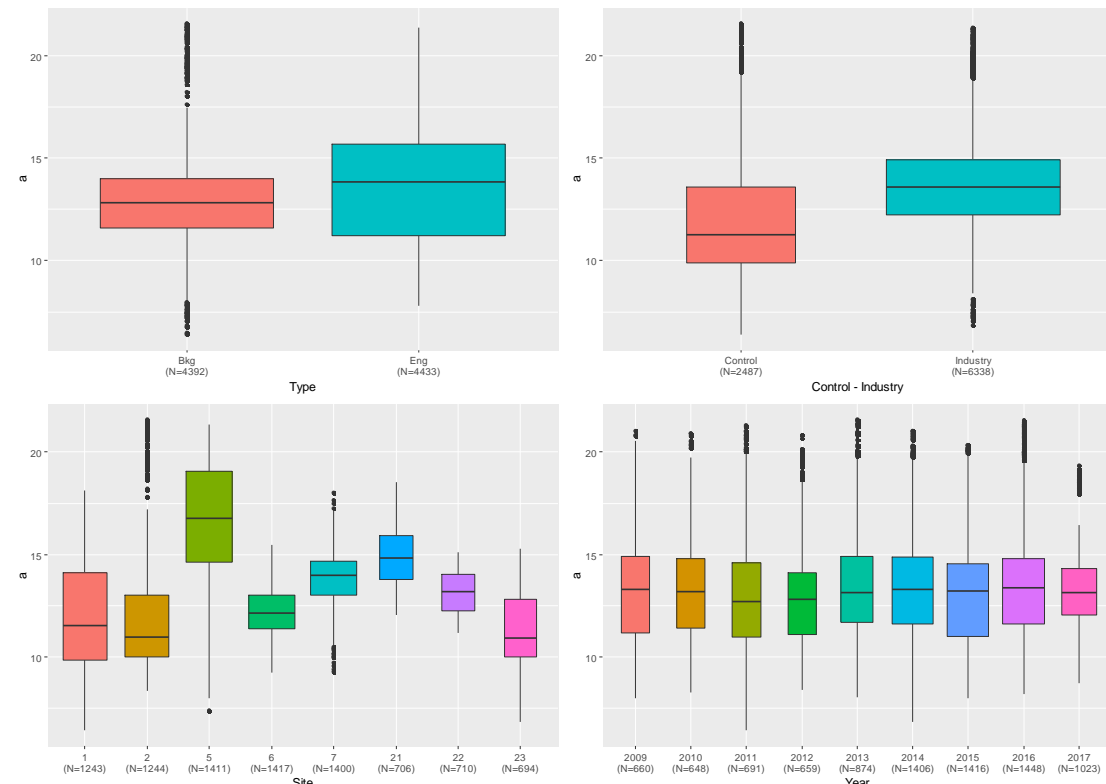


Figure 37. Distribution of a* observations made with the KM instrument, Yara and Control sites only.

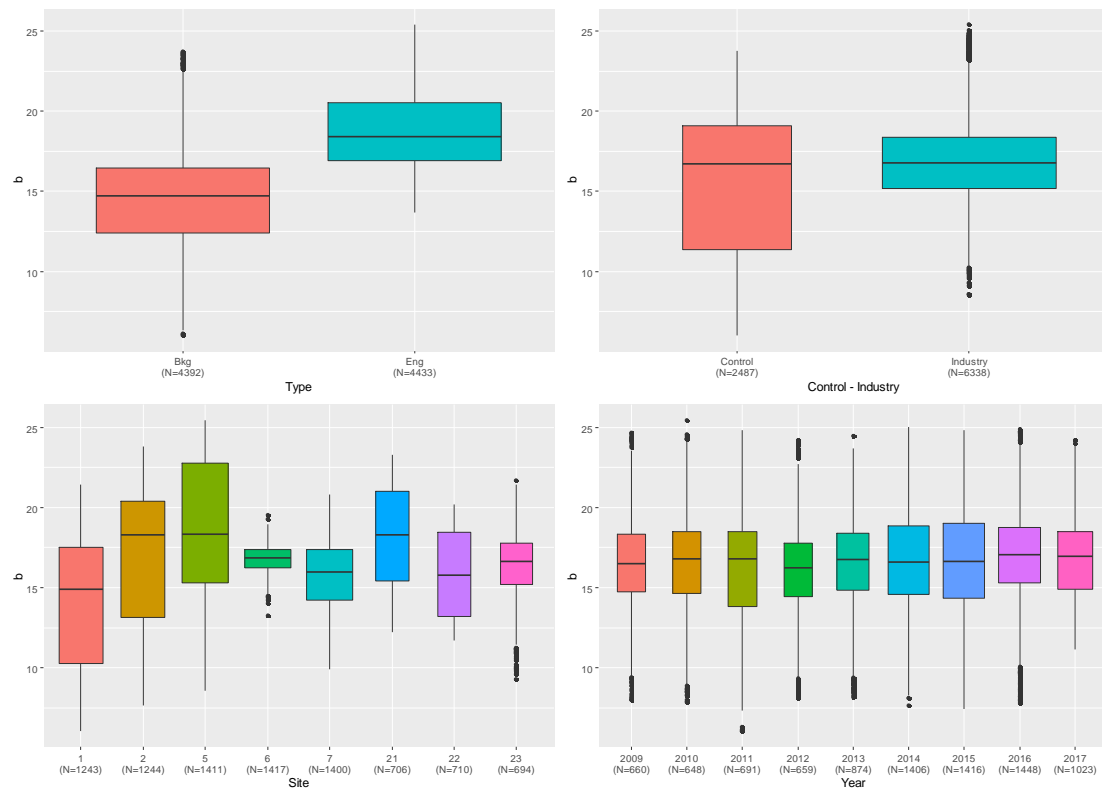


Figure 38. Distribution of b^* observations made with the KM instrument, Yara and Control sites only.

Appendix C. Distribution of L*, a*, b* Values with the ASD Instrument

The boxplots in this Appendix show the distribution of L*, a* and b* values from the ASD instrument for all sites and then for Yara and Control sites only. These boxplots show the values for each of type, Control-Industry, Site and Year separately, rather than as the three way plots shown in the main report. As a result, care must be taken when interpreting these boxplots, as apparent differences in one variable (e.g. time) may be caused by a difference in another variable (e.g. that control site data is not available for 2017, but is included for all other years).

These boxplots exclude the 2004 data as it was excluded from the analysis for reasons outlined in Section 1.4.

C.1 All Sites, Years 2005 to 2017

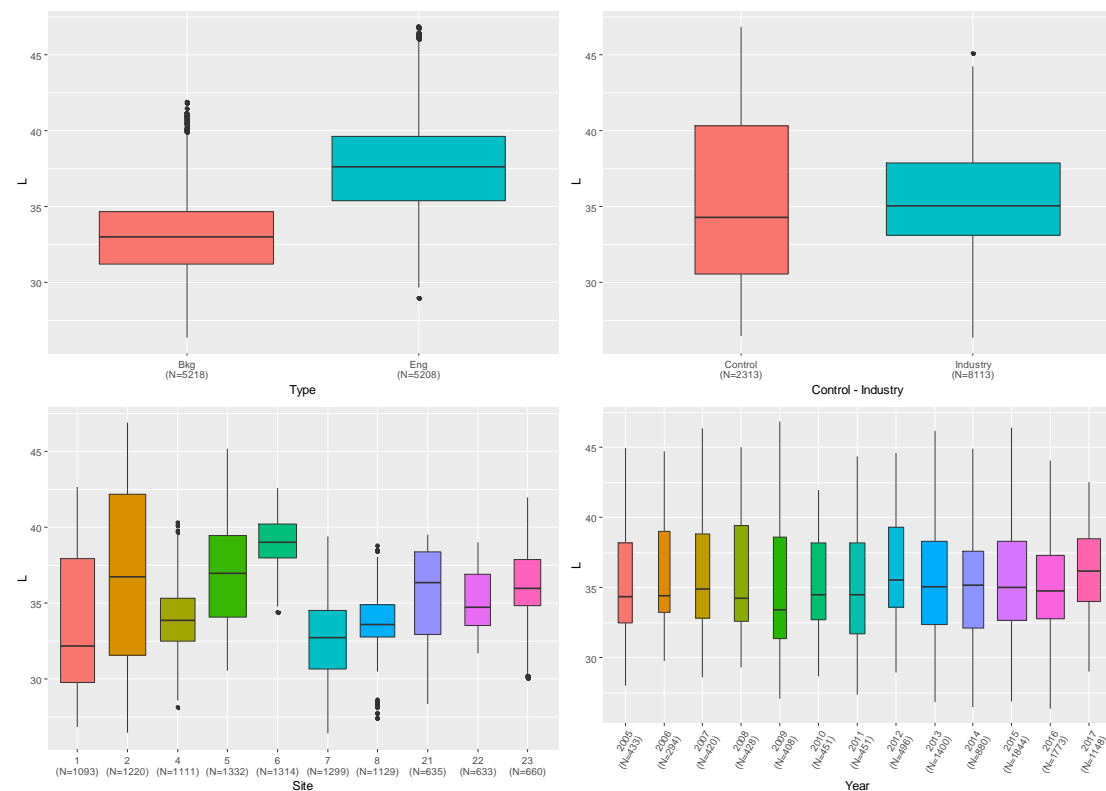


Figure 39. Distribution of L* observations made with the ASD instrument, all sites.

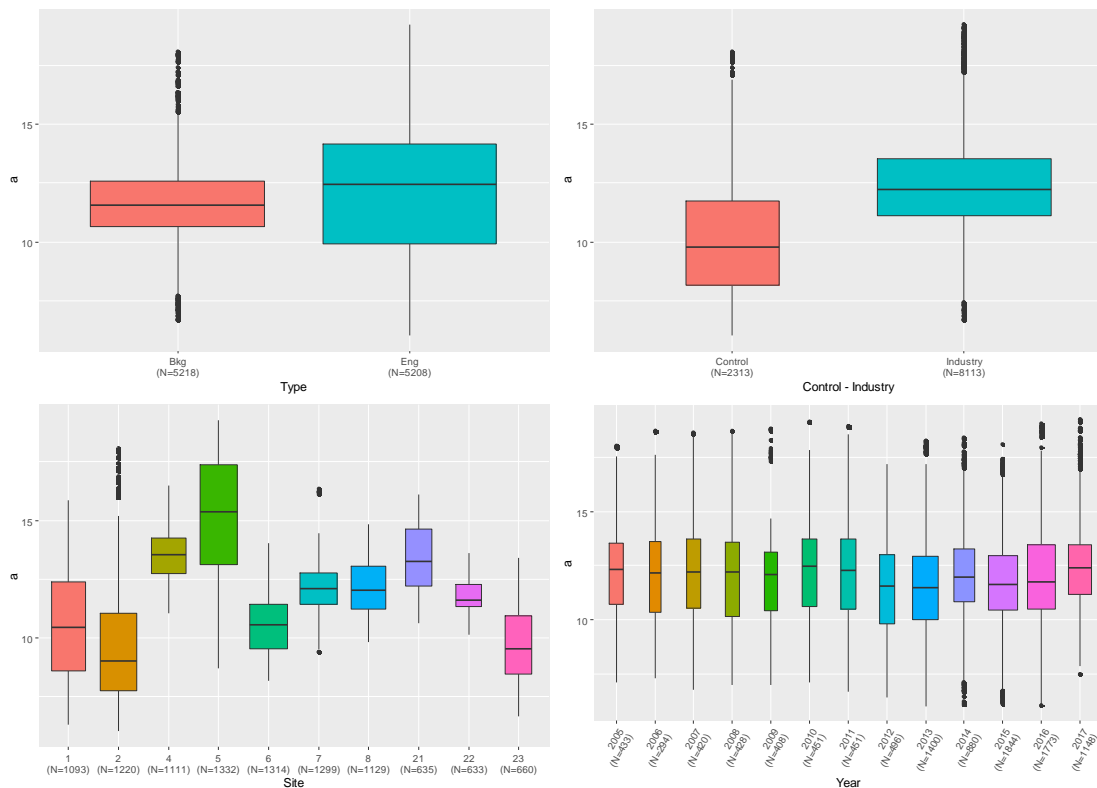


Figure 40. Distribution of a^* observations made with the ASD instrument, all sites.

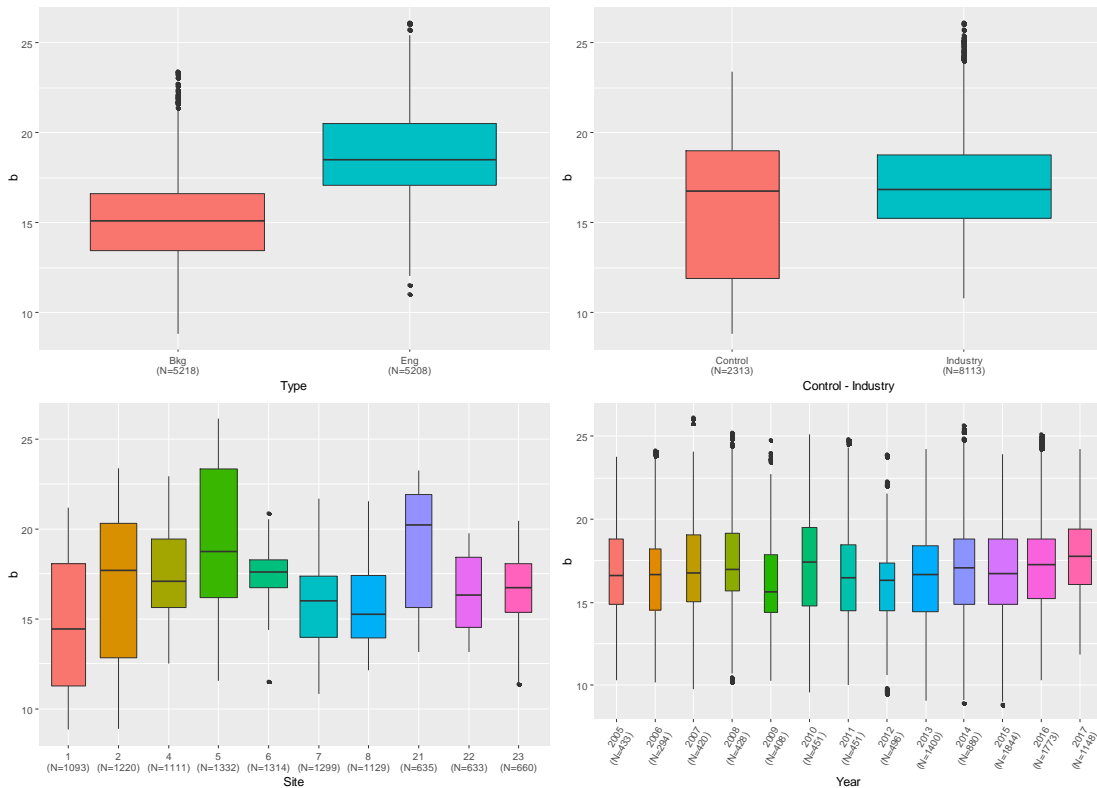


Figure 41. Distribution of b^* observations made with the ASD instrument, all sites.

C.2 Yara and Control Sites Only, Years 2005-2017

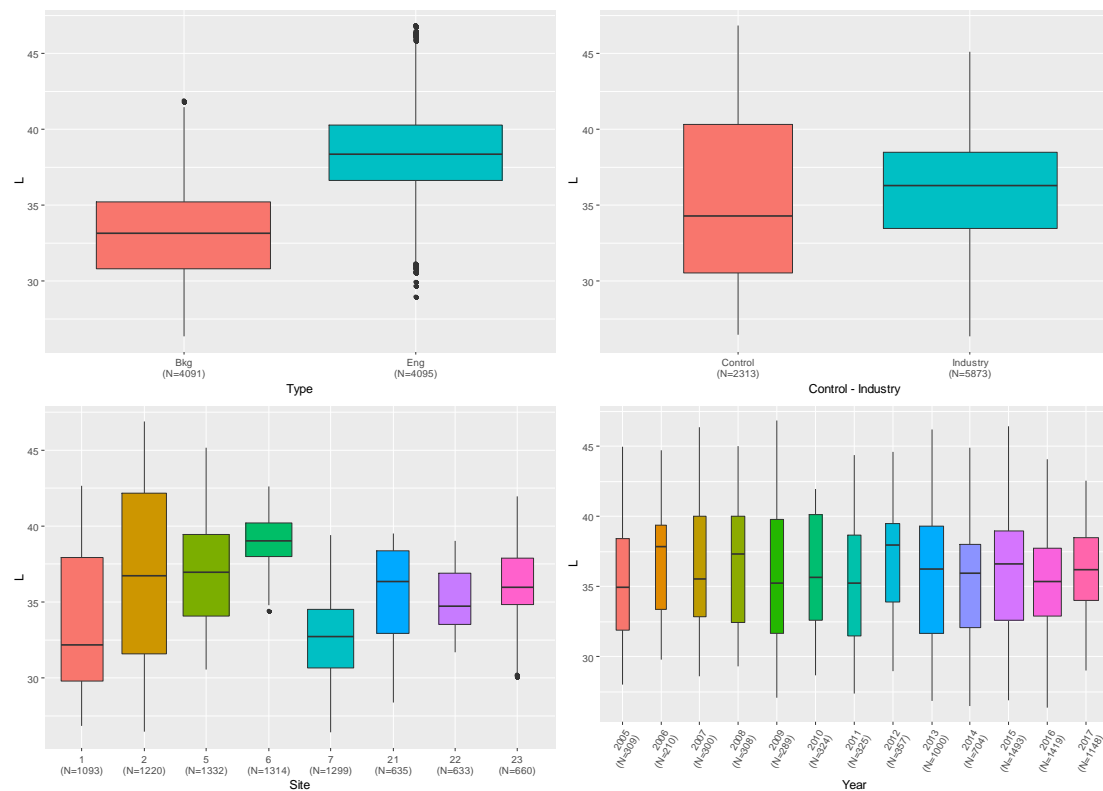


Figure 42. Distribution of L^* observations made with the ASD instrument, Yara and Control sites only.

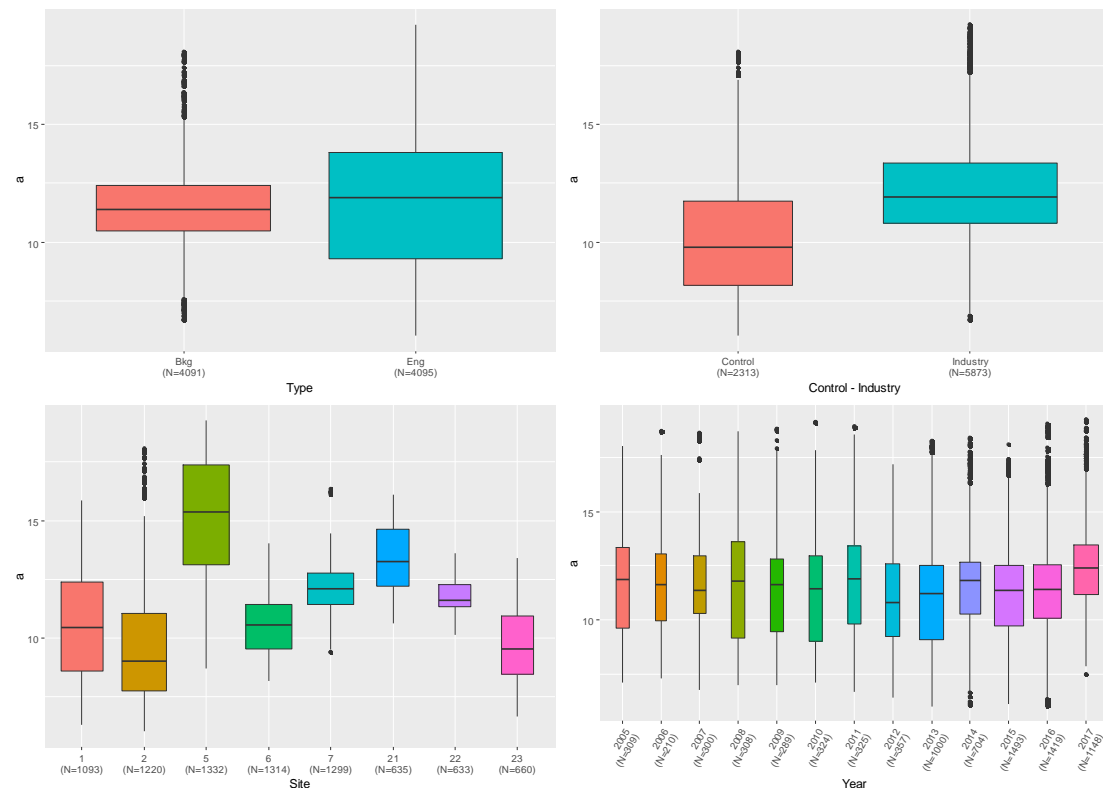


Figure 43. Distribution of a^* observations made with the ASD instrument, Yara and Control sites only.

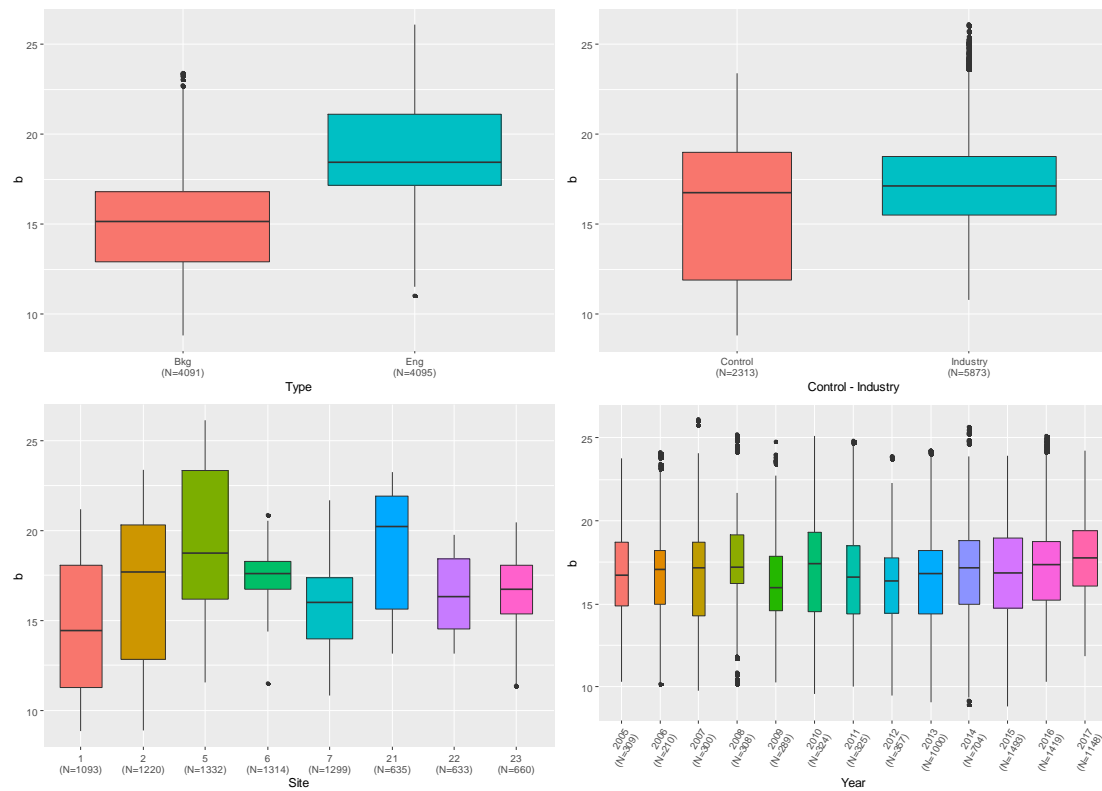


Figure 44. Distribution of b^* observations made with the ASD instrument, Yara and Control sites only.

Appendix D. Distribution of Spectral Line Values with the ASD Instrument

The boxplots in this Appendix show the distribution of the spectral line values from the ASD instrument for all sites and then for Yara and Control sites only. These boxplots show the values for each of type, Control-Industry, Site and Year separately, rather than as the three way plots shown in the main report. As a result, care must be taken when interpreting these boxplots, as apparent differences in one variable (e.g. time) may be caused by a difference in another variable (e.g. that control site data is not available for 2017, but is included for all other years).

D.1 All Sites, Years 2005 to 2017

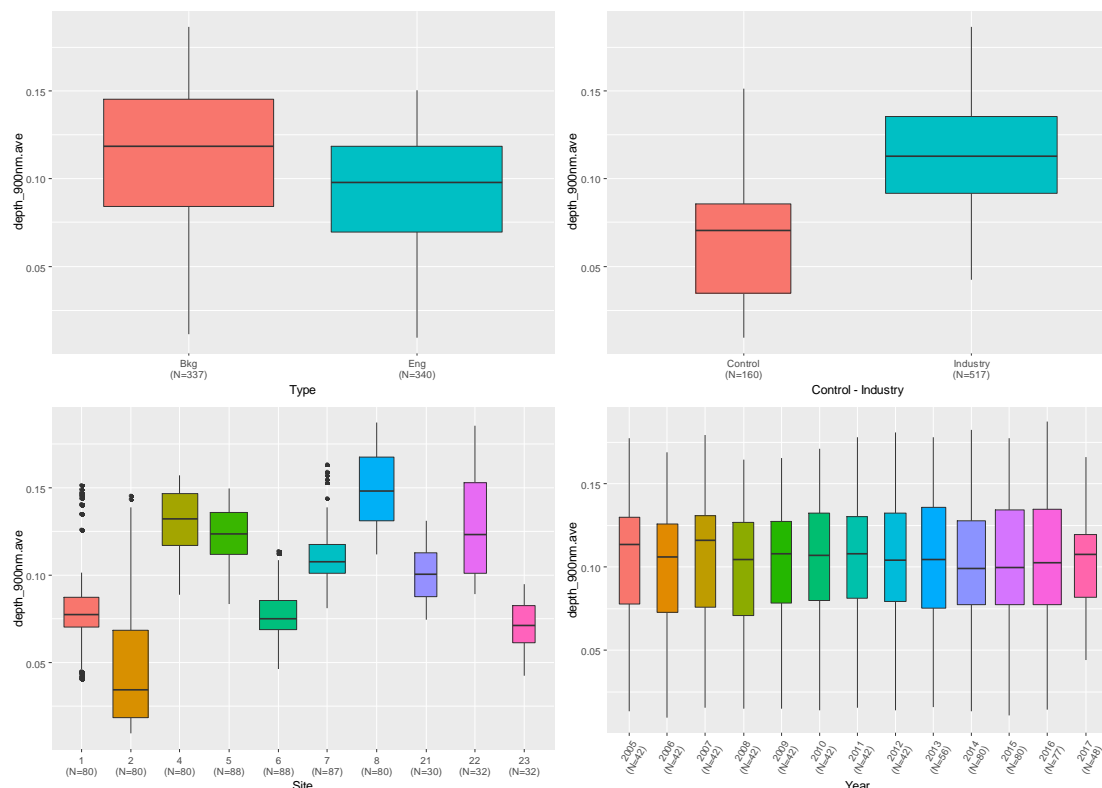


Figure 45. Distribution of depth at 900 nm made with the ASD instrument, all sites.

DATA ANALYSIS AUSTRALIA PTY LTD

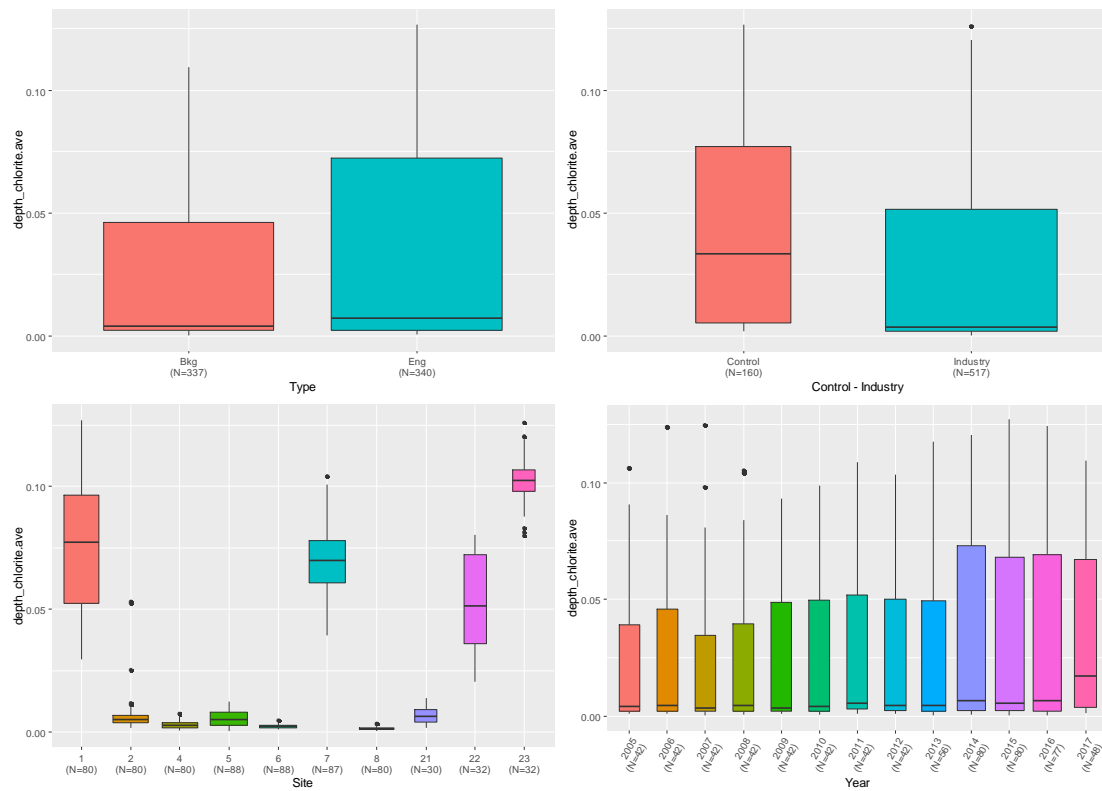


Figure 46. Distribution of depth of chlorite made with the ASD instrument, all sites.

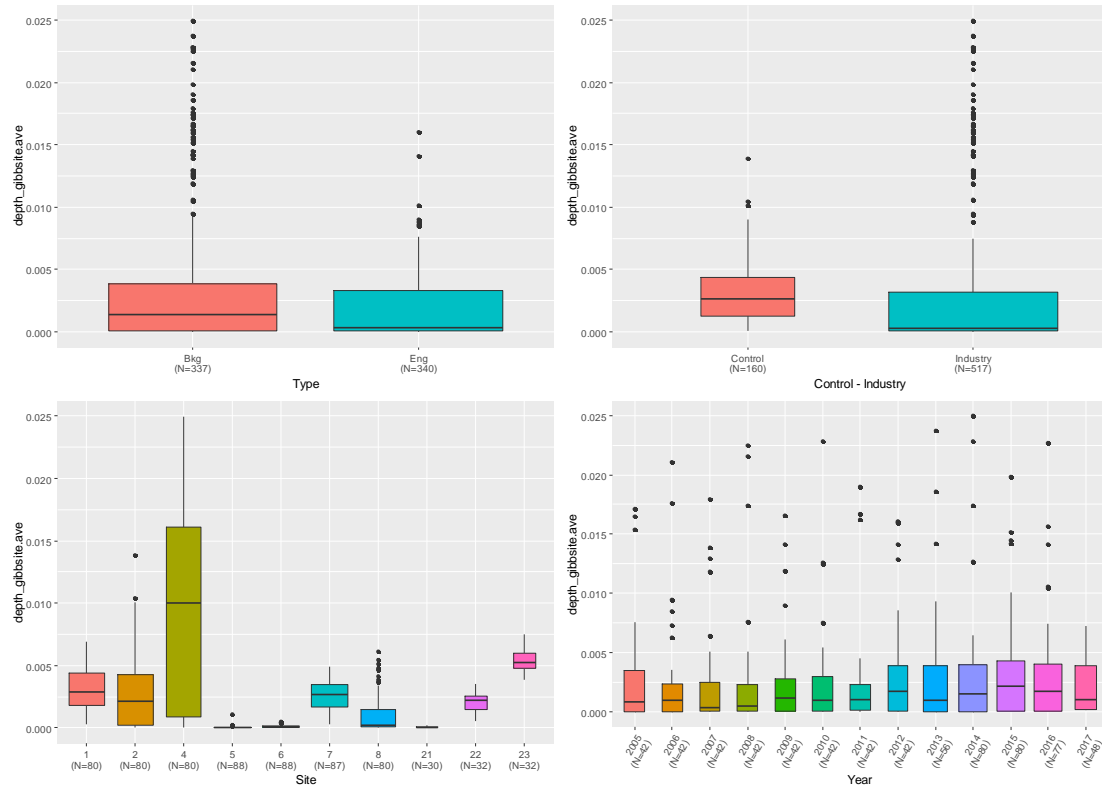


Figure 47. Distribution of depth of gibbsite made with the ASD instrument, all sites.

DATA ANALYSIS AUSTRALIA PTY LTD

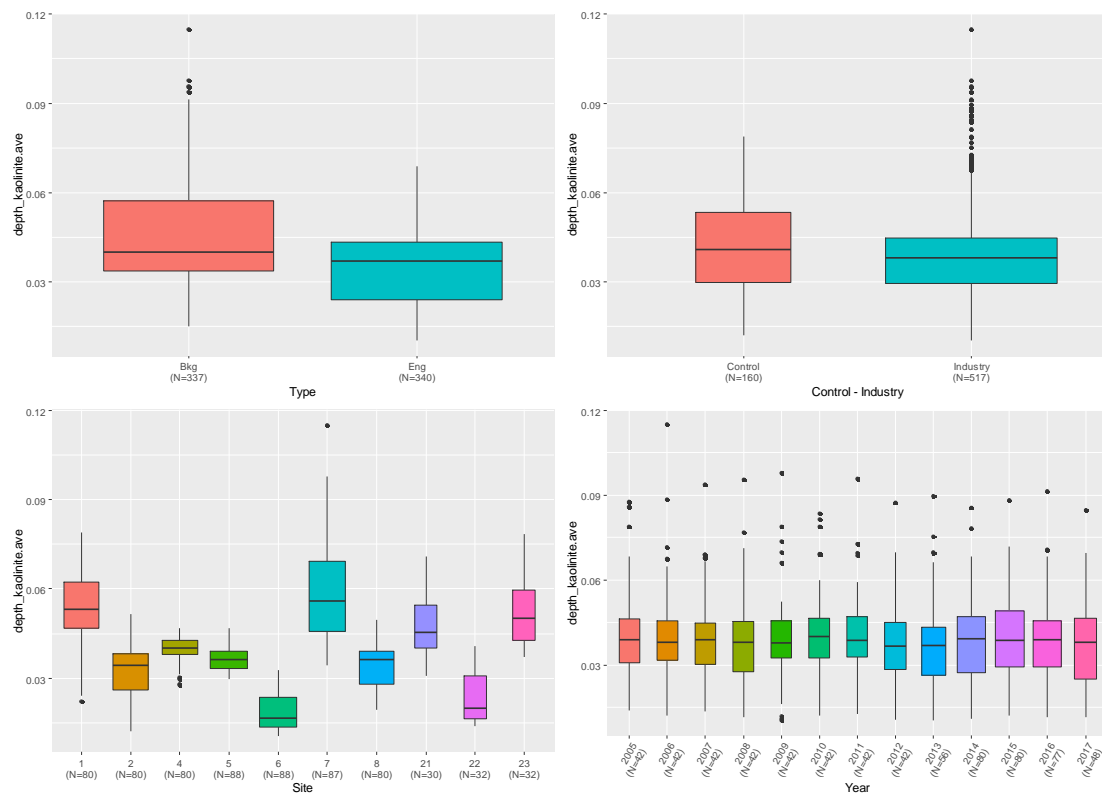


Figure 48. Distribution of depth of kaolinite made with the ASD instrument, all sites.

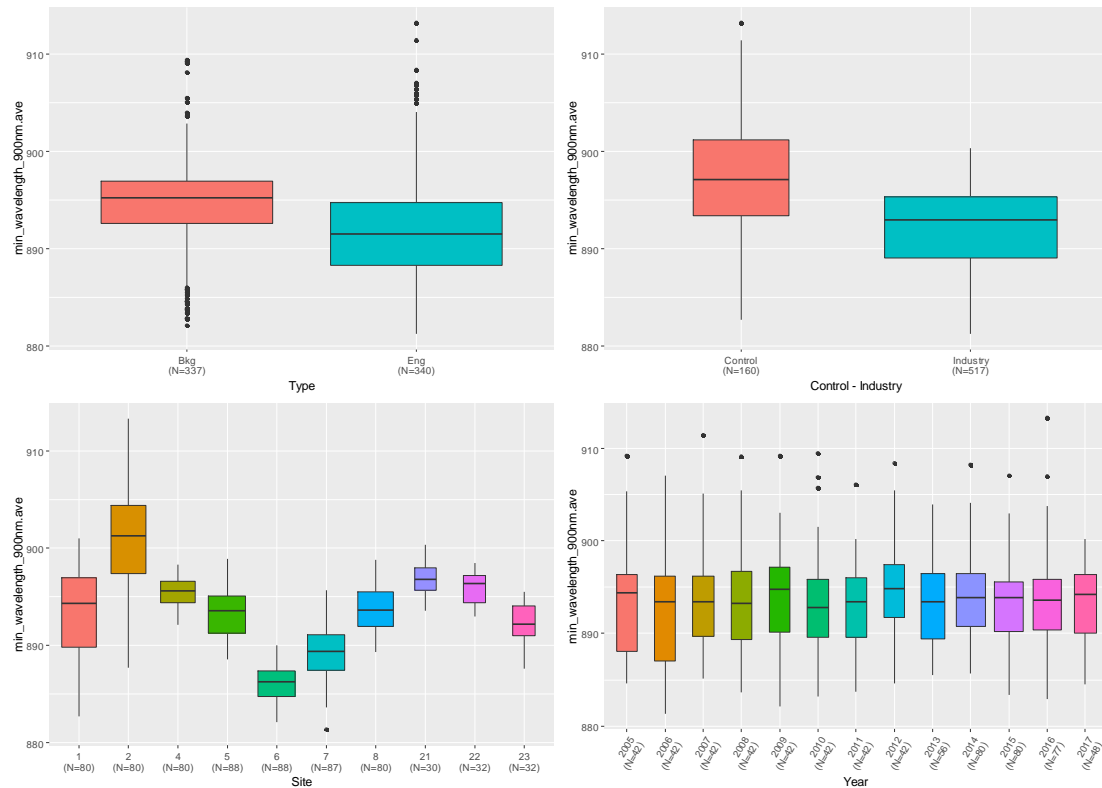


Figure 49. Distribution of minimum wavelength at 900 nm made with the ASD instrument, all sites.

D.2 Yara and Control Sites Only, Years 2005-2017

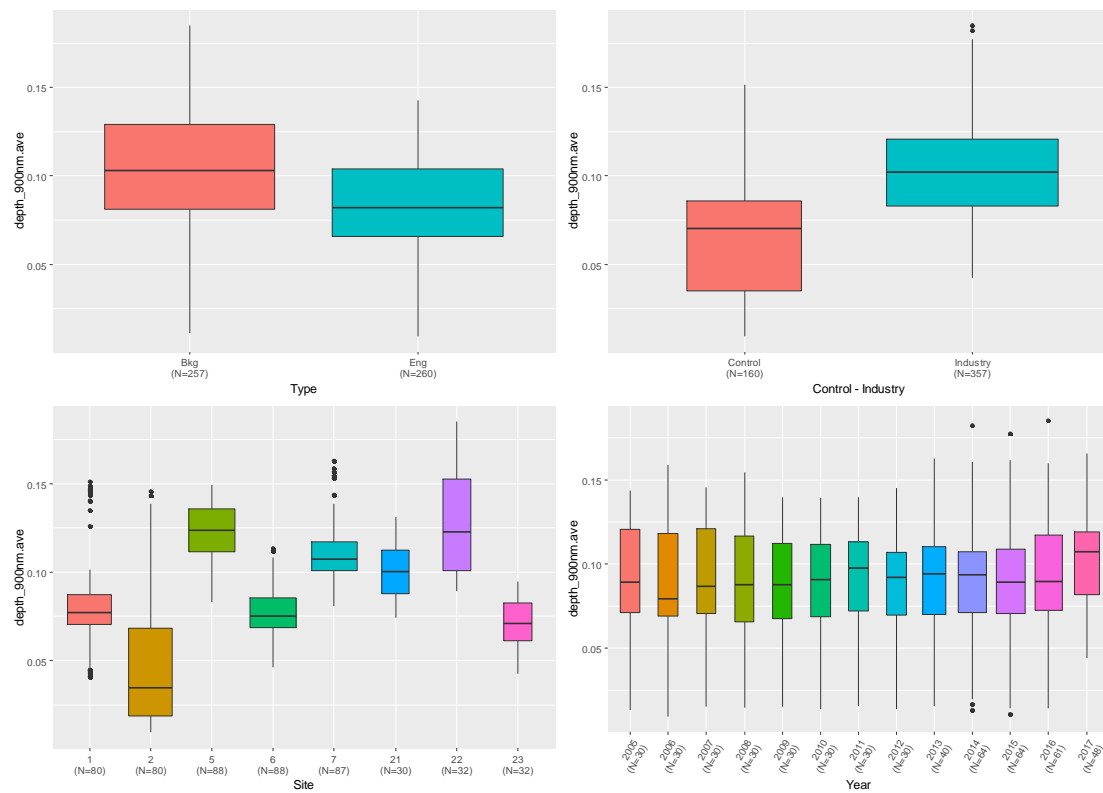


Figure 50. Distribution of depth at 900 nm made with the ASD instrument, Yara and Control sites only.

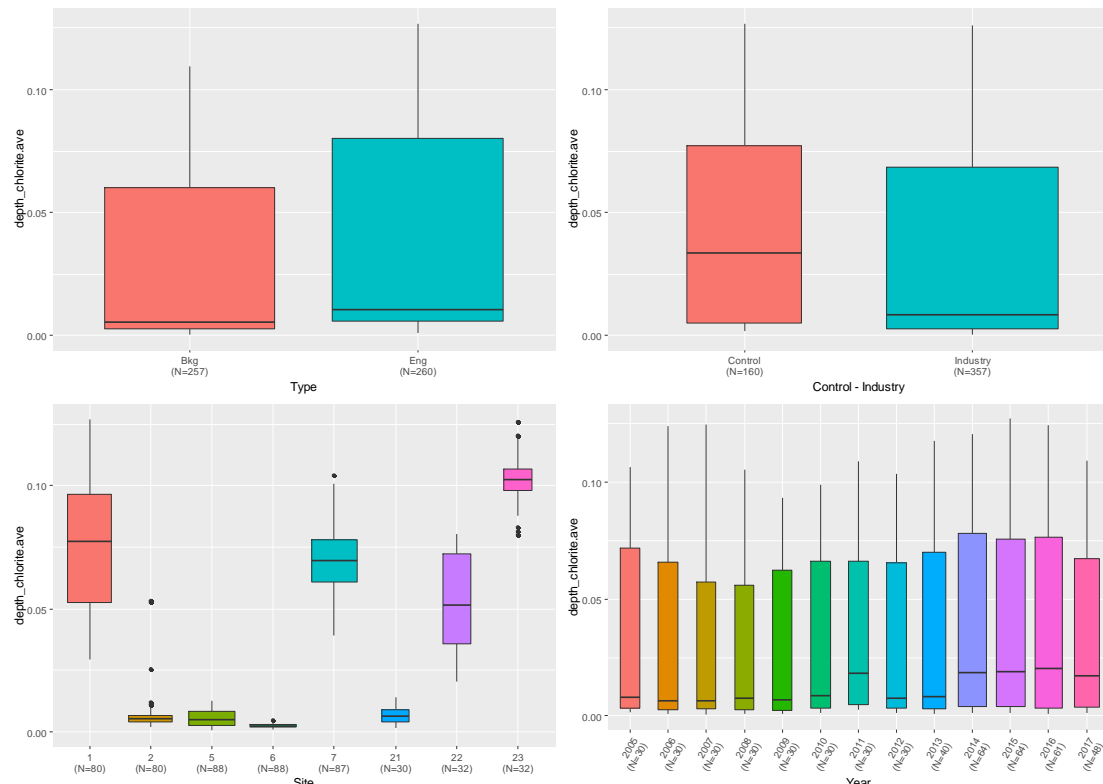


Figure 51. Distribution of depth of chlorite made with the ASD instrument, Yara and Control sites only.

DATA ANALYSIS AUSTRALIA PTY LTD

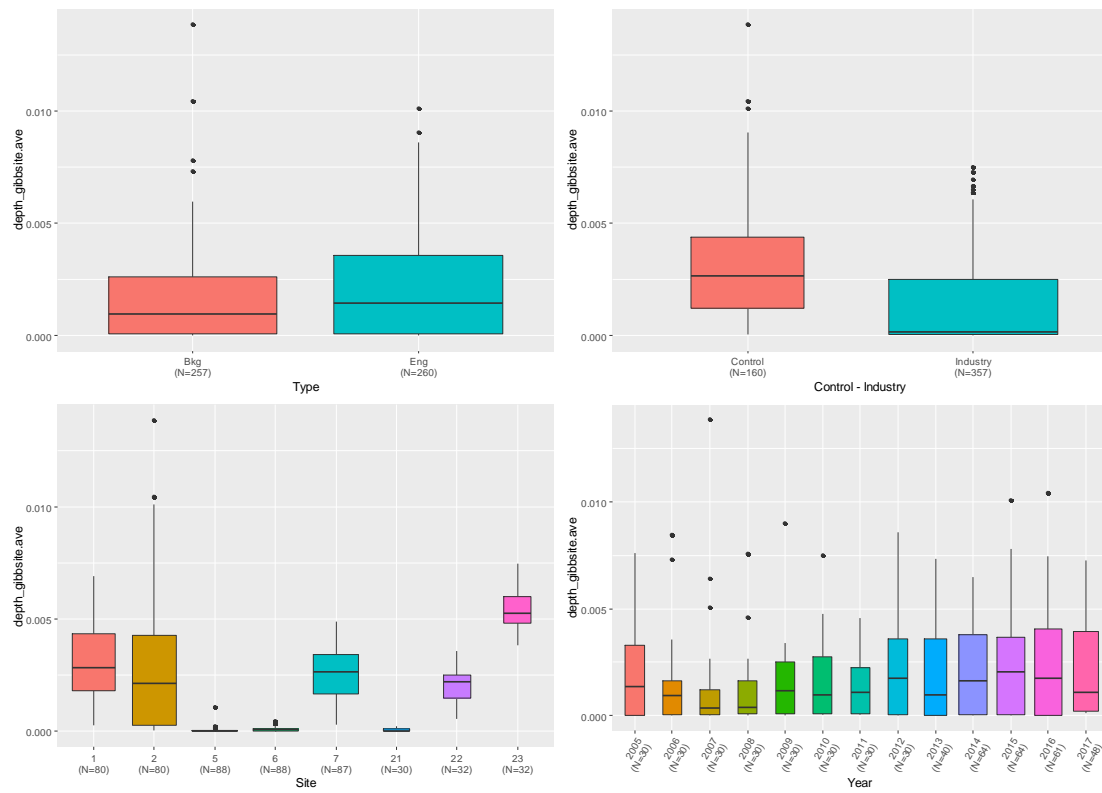


Figure 52. Distribution of depth of gibbsite made with the ASD instrument, Yara and Control sites only.

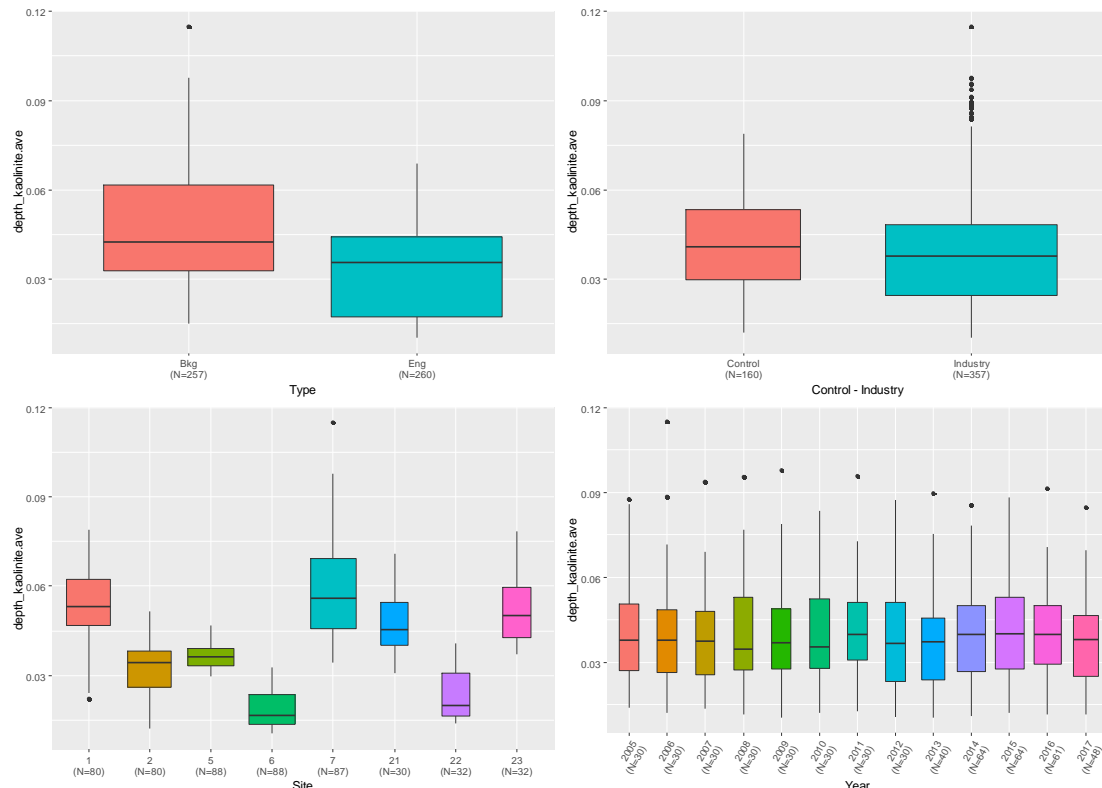


Figure 53. Distribution of depth of kaolinite made with the ASD instrument, Yara and Control sites only.

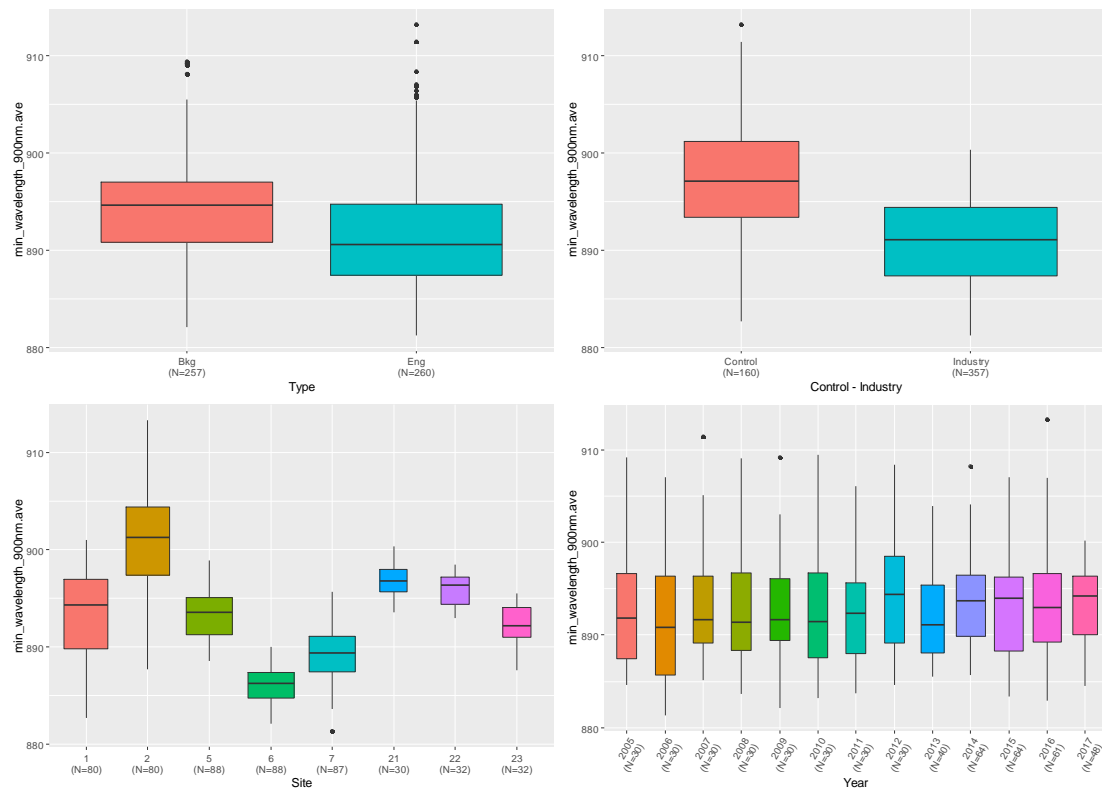


Figure 54. Distribution of minimum wavelength at 900 nm made with the ASD instrument, Yara and Control sites only.

Appendix E. Comparison between Instruments

These figures show the trends of the L*, a* and b* values in the background and engravings over the period 2004-2017, split by KM and ASD. Each figure covers one site. Note that sites 1, 2, 4, and 8 were not visited in 2017.

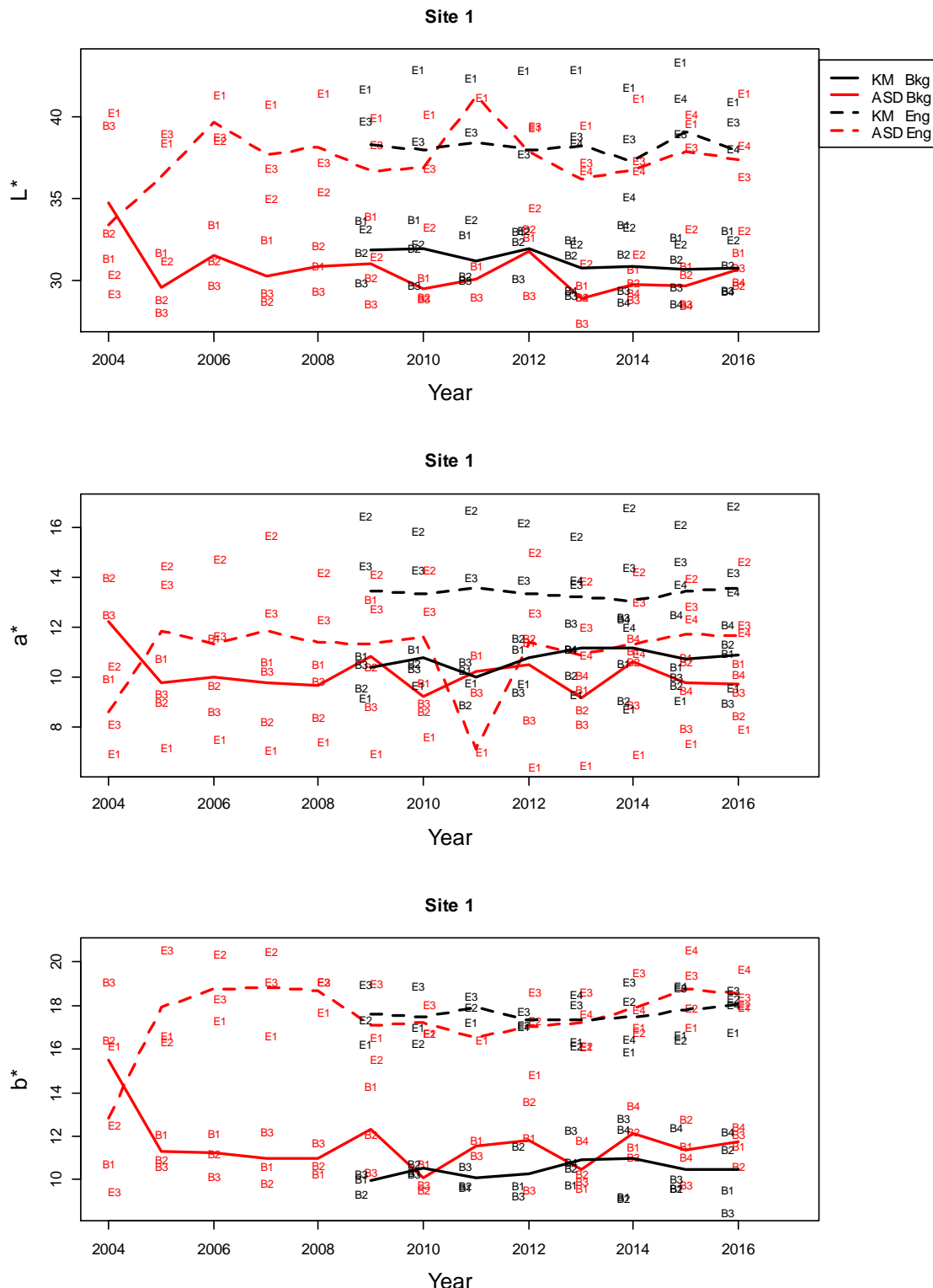


Figure 55. Individual readings and average L^* , a^* , b^* values for Site 1. Black lines and points represent the KM Spectrophotometer and red lines and points the ASD spectrometer. Engraving points are represented by the letter E (and the corresponding spot number) for individual readings and the dashed lines for their averages; and background points are represented by the letter B (and the corresponding spot number) for their individual readings and the solid lines for their averages.

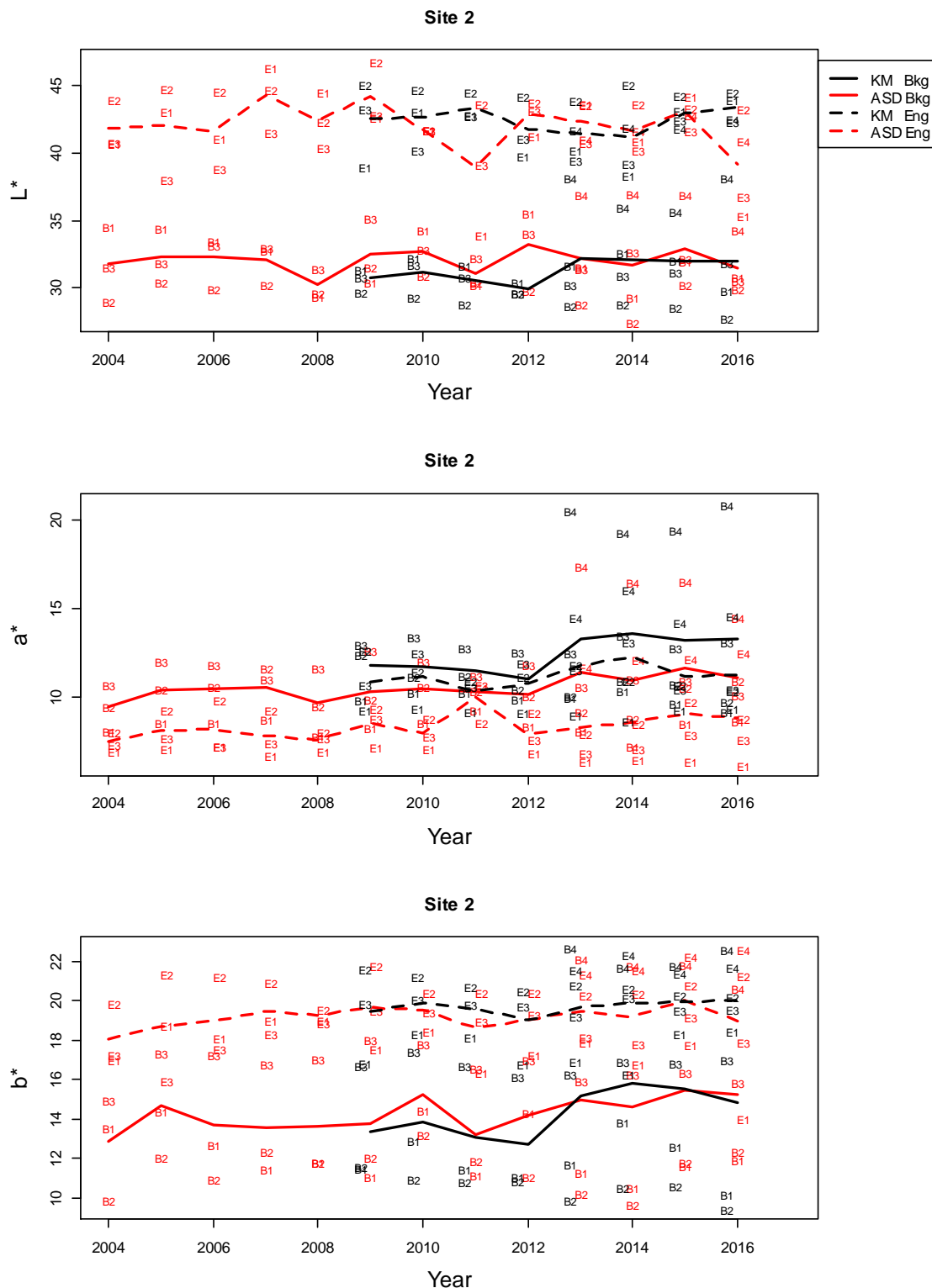


Figure 56. Individual readings and average L^* , a^* , b^* values for Site 2. Black lines and points represent the KM Spectrophotometer, and red lines and points the ASD spectrometer. Engraving points are represented by the letter E (and the corresponding spot number) for individual readings and the dashed lines for their averages; and background points are represented by the letter B (and the corresponding spot number) for their individual readings and the solid lines for their averages.

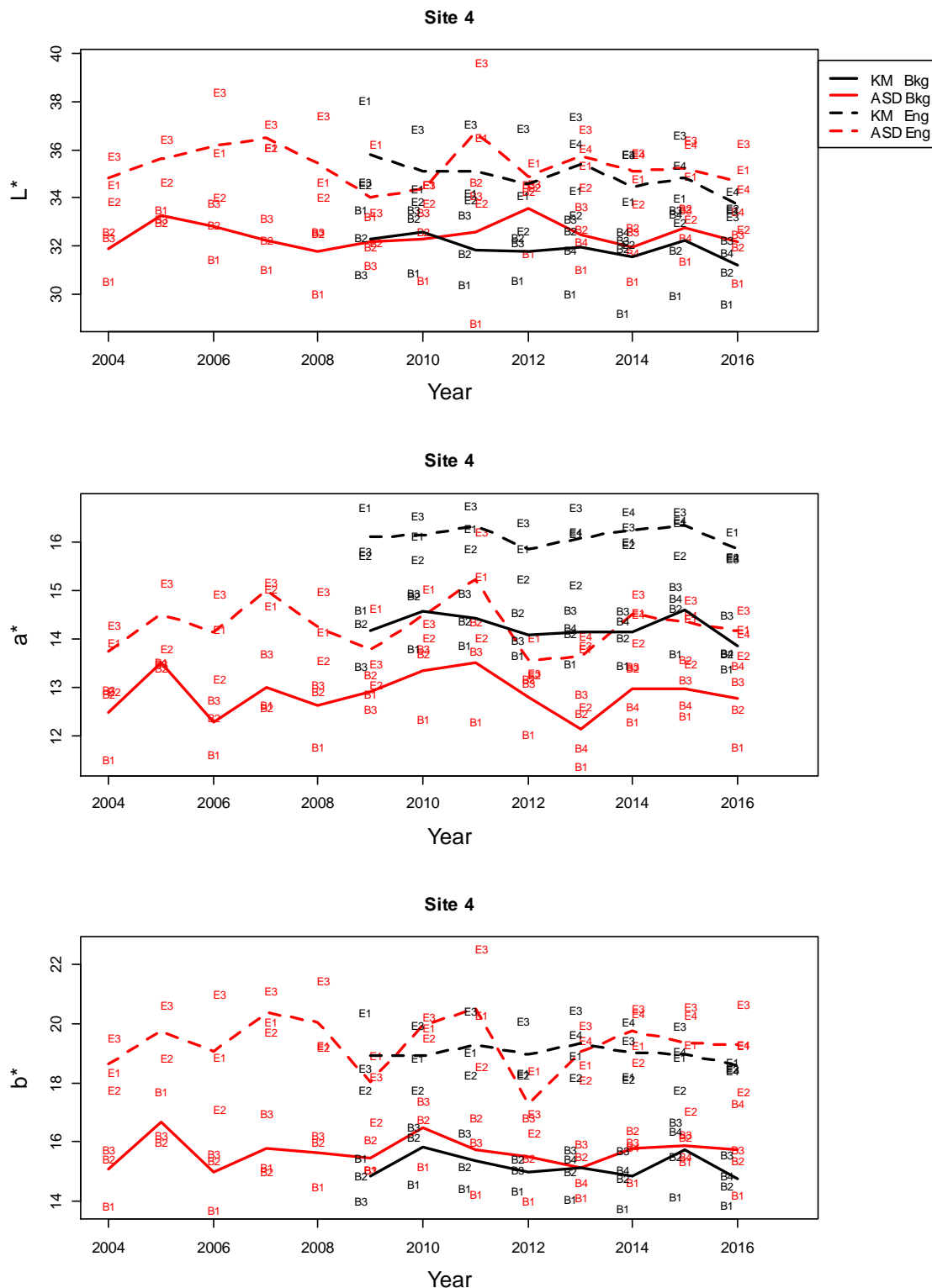


Figure 57. Individual readings and average L^* , a^* , b^* values for Site 4. Black lines and points represent the KM Spectrophotometer, and red lines and points the ASD spectrometer. Engraving points are represented by the letter E (and the corresponding spot number) for individual readings and the dashed lines for their averages; and background points are represented by the letter B (and the corresponding spot number) for their individual readings and the solid lines for their averages.

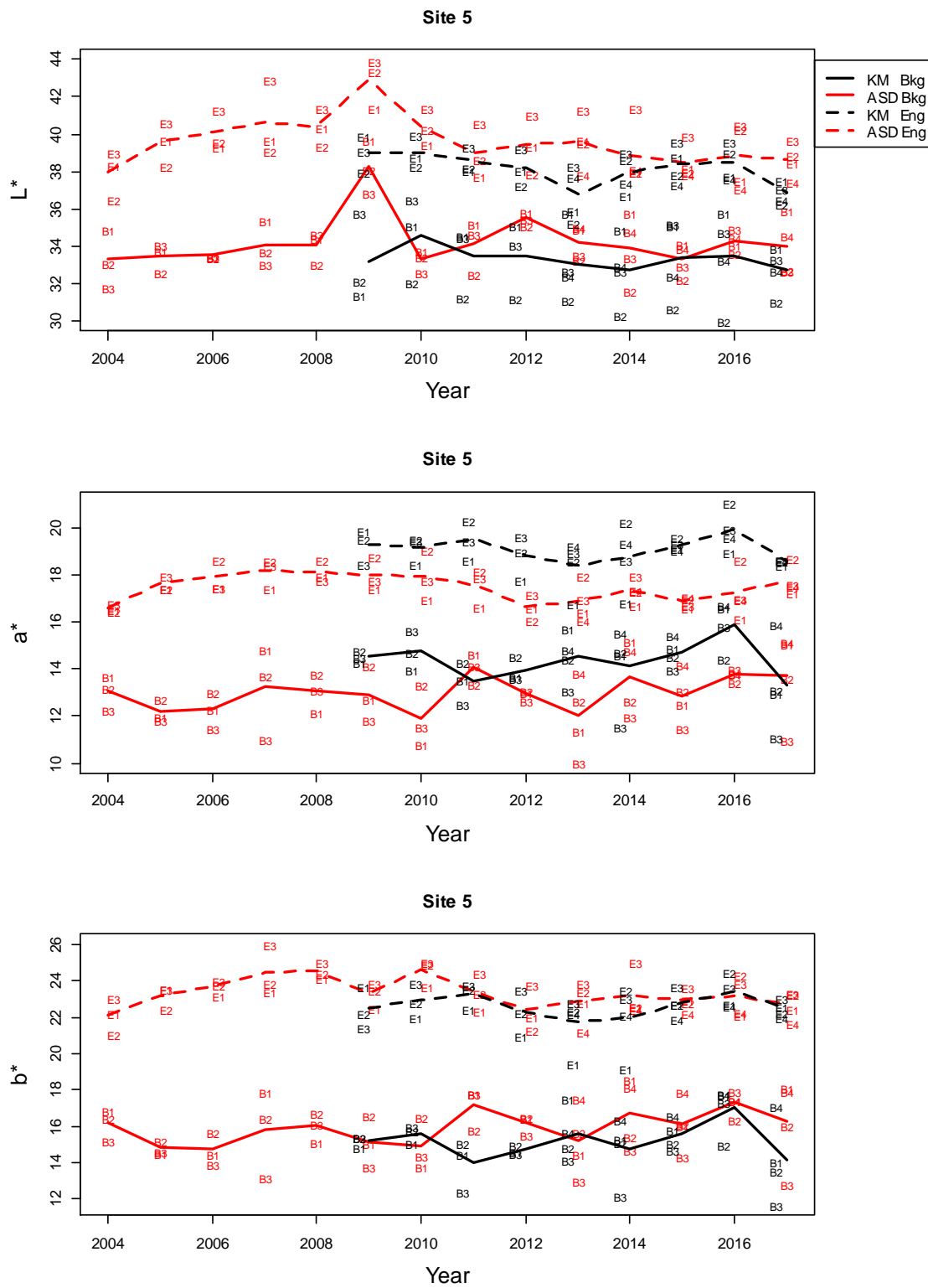


Figure 58. Individual readings and average L^* , a^* , b^* values for Site 5. Black lines and points represent the KM Spectrophotometer, and red lines and points the ASD spectrometer. Engraving points are represented by the letter E (and the corresponding spot number) for individual readings and the dashed lines for their averages; and background points are represented by the letter B (and the corresponding spot number) for their individual readings and the solid lines for their averages.

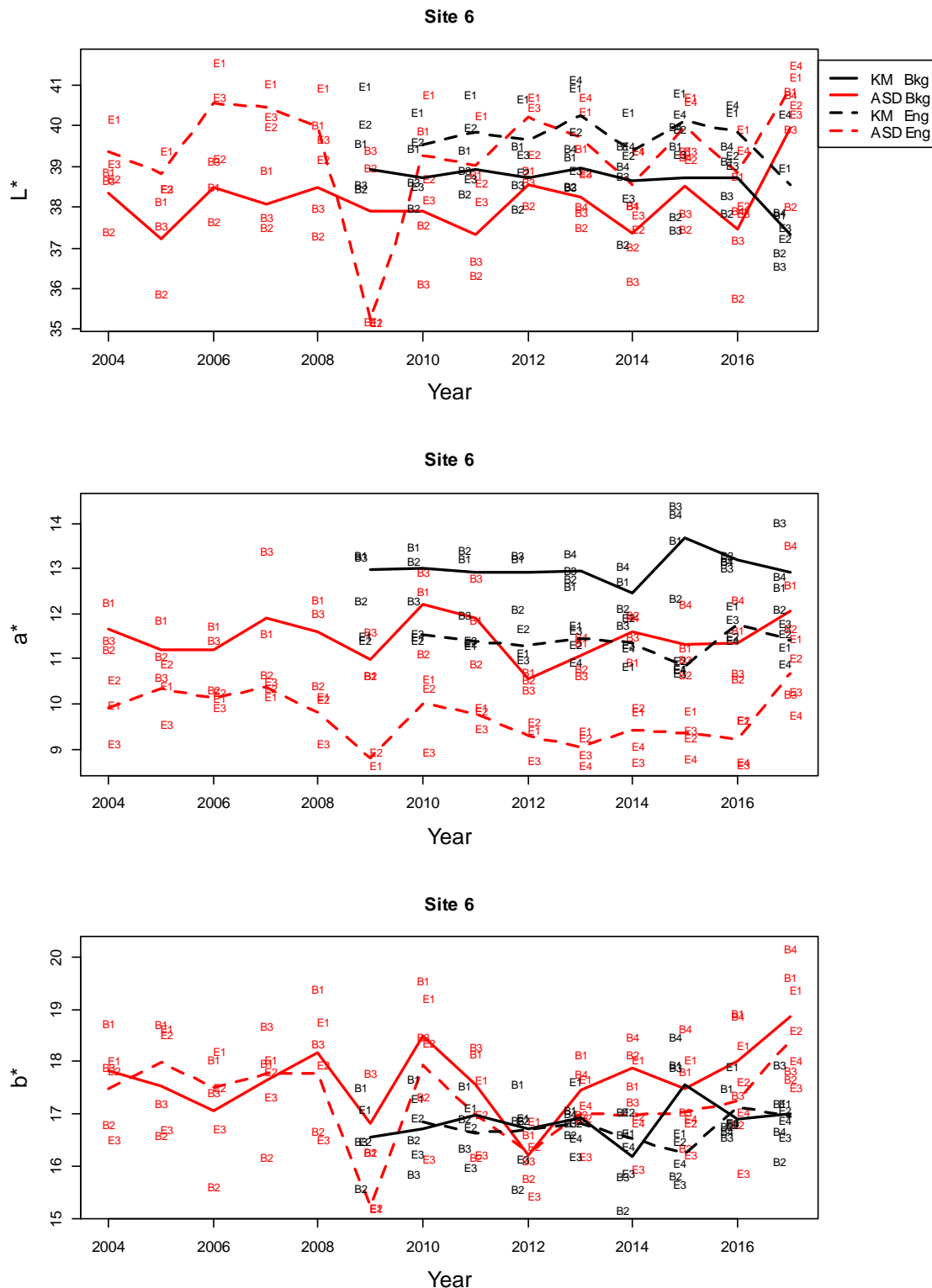


Figure 59. Individual readings and average L^* , a^* , b^* values for Site 6. Black lines and points represent the KM Spectrophotometer, and red lines and points the ASD spectrometer. Engraving points are represented by the letter E (and the corresponding spot number) for individual readings and the dashed lines for their averages; and background points are represented by the letter B (and the corresponding spot number) for their individual readings and the solid lines for their averages.

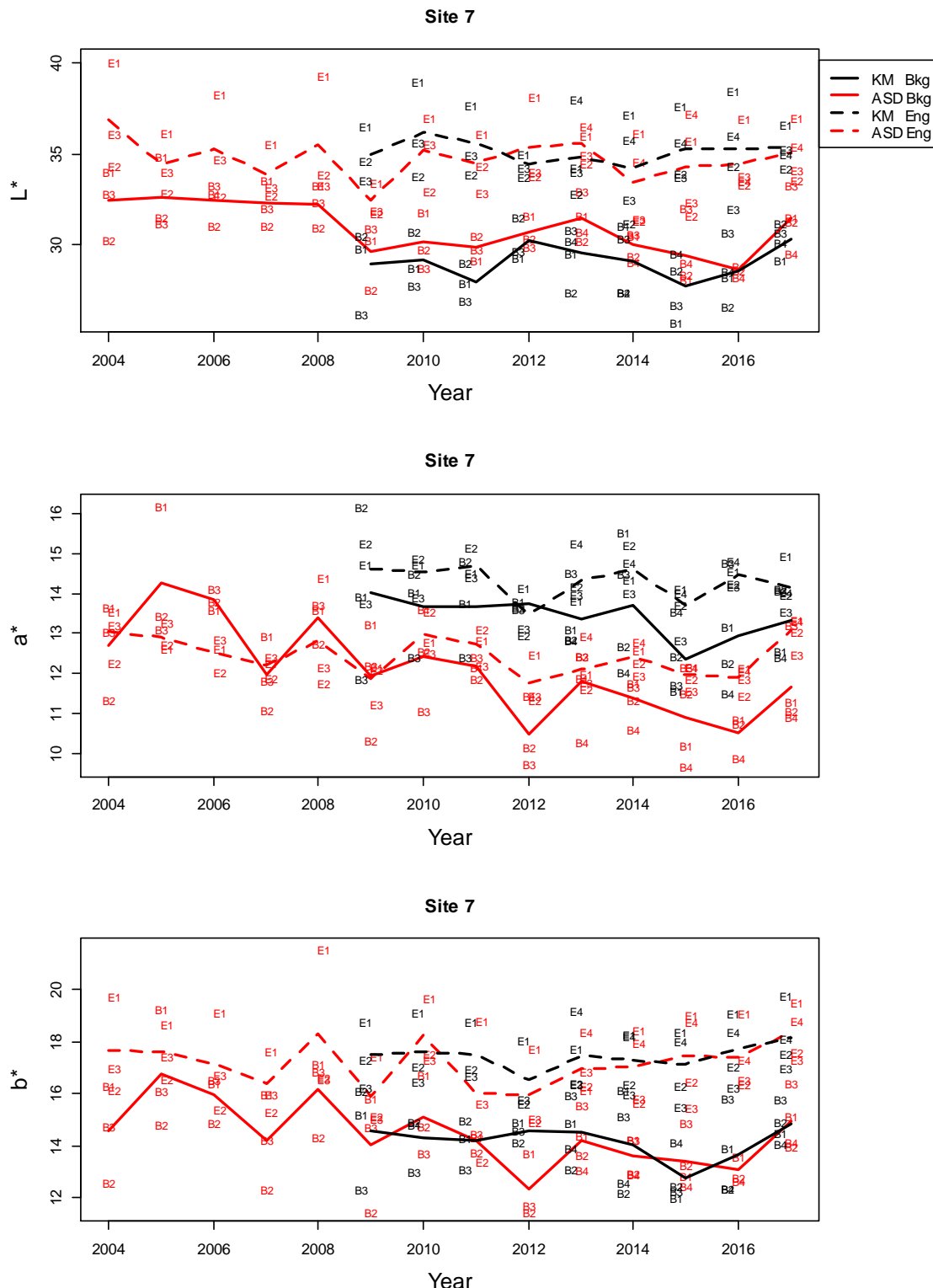


Figure 60. Individual readings and average L^* , a^* , b^* values for Site 7. Black lines and points represent the KM Spectrophotometer, and red lines and points the ASD spectrometer. Engraving points are represented by the letter E (and the corresponding spot number) for individual readings and the dashed lines for their averages; and background points are represented by the letter B (and the corresponding spot number) for their individual readings and the solid lines for their averages.

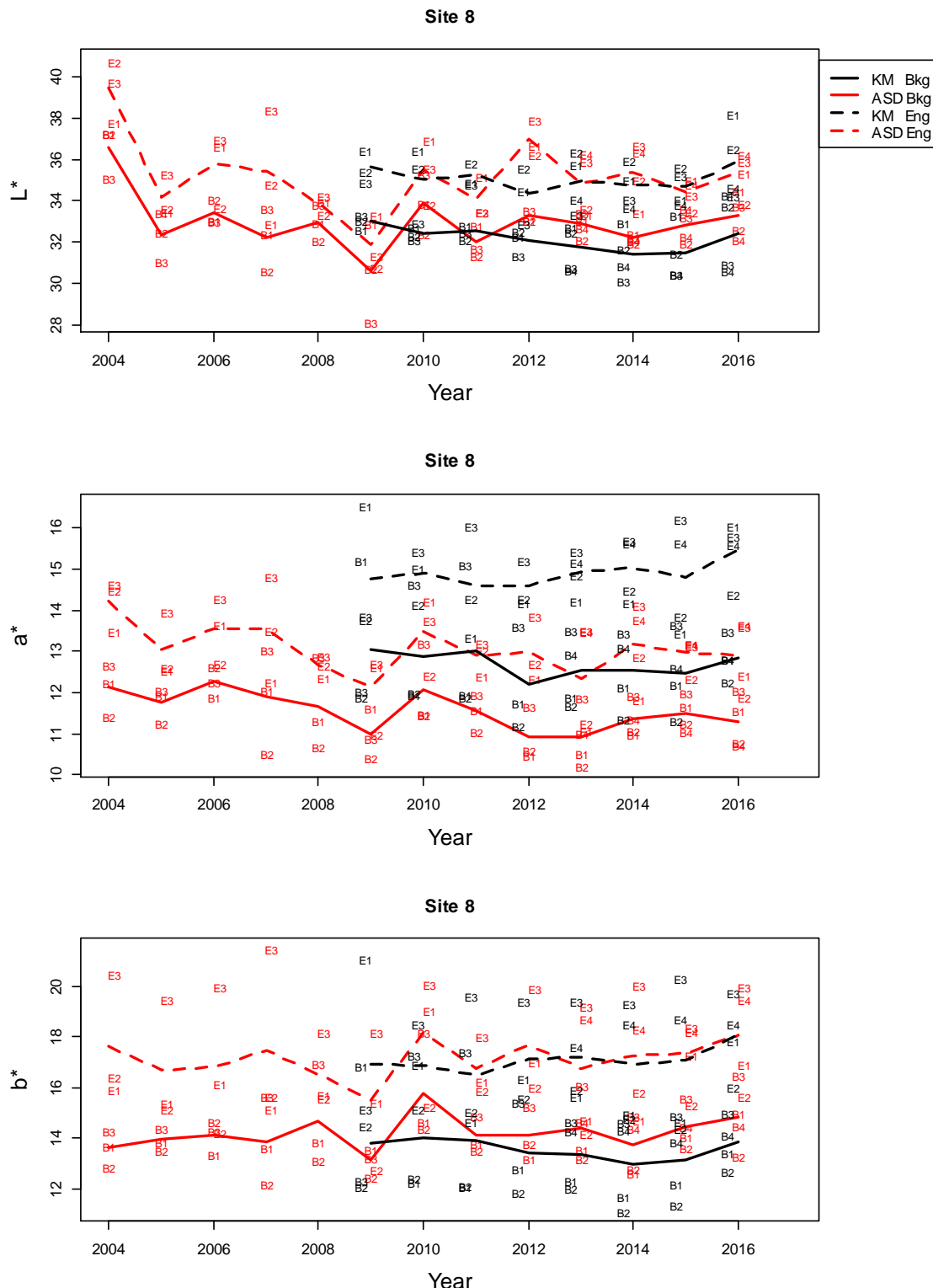


Figure 61. Individual readings and average L^* , a^* , b^* values for Site 8. Black lines and points represent the KM Spectrophotometer, and red lines and points the ASD spectrometer. Engraving points are represented by the letter E (and the corresponding spot number) for individual readings and the dashed lines for their averages; and background points are represented by the letter B (and the corresponding spot number) for their individual readings and the solid lines for their averages.

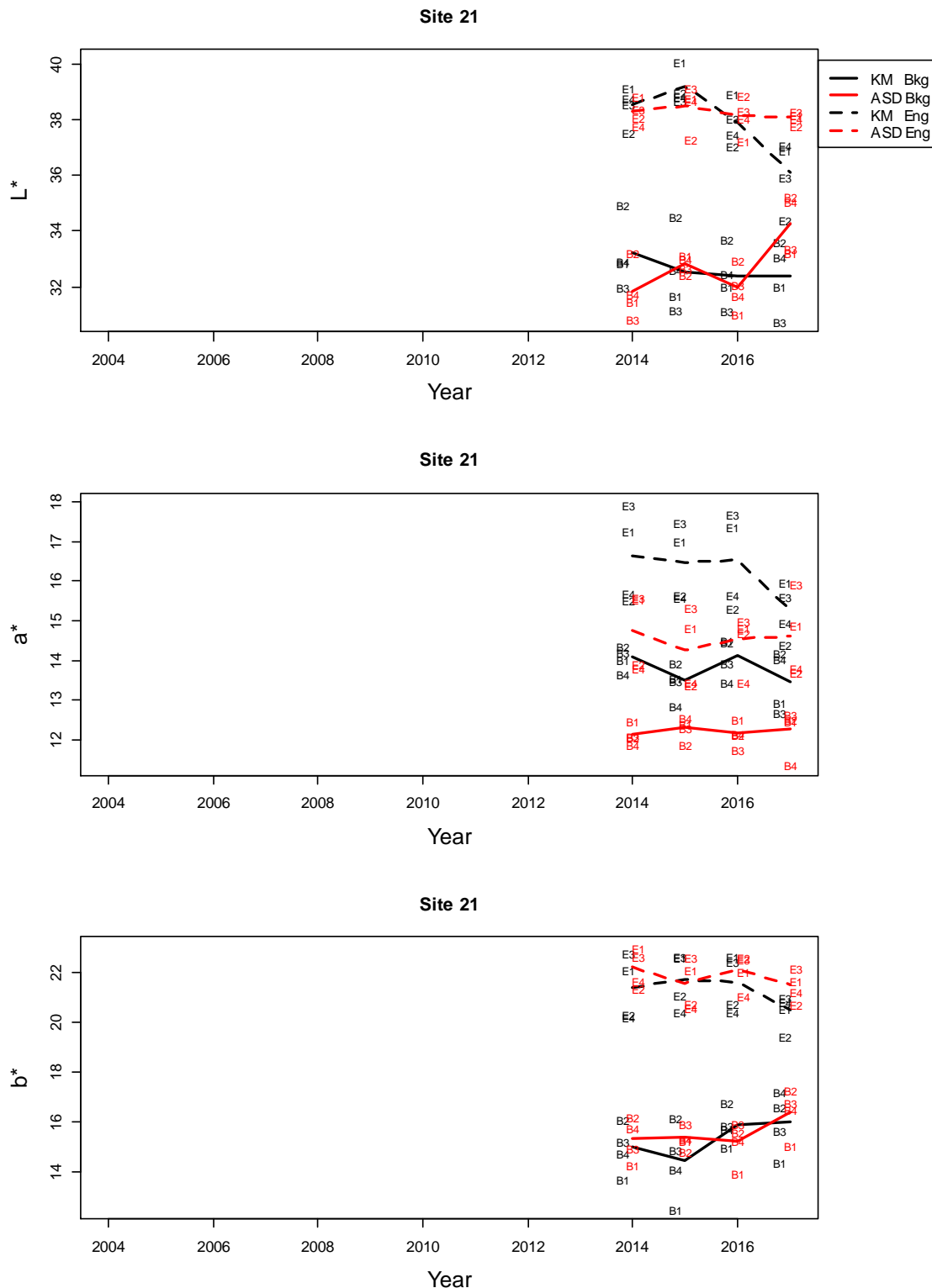
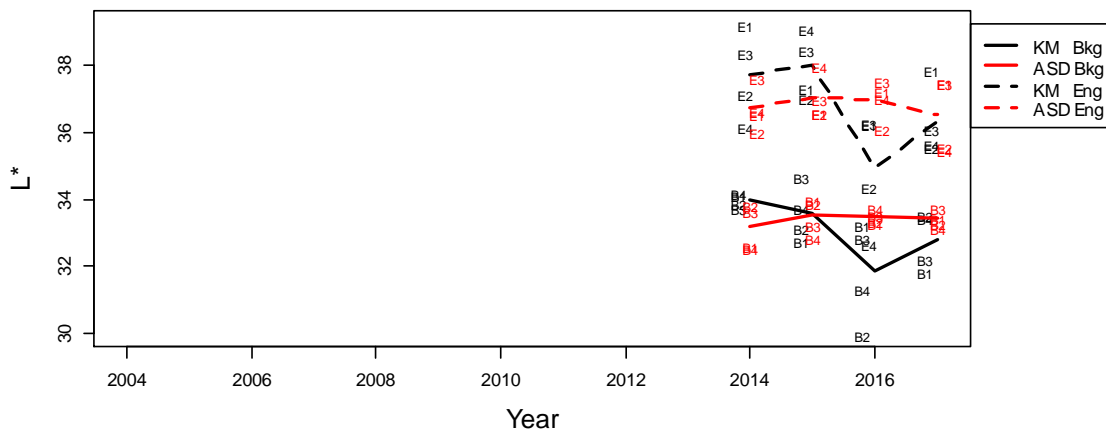
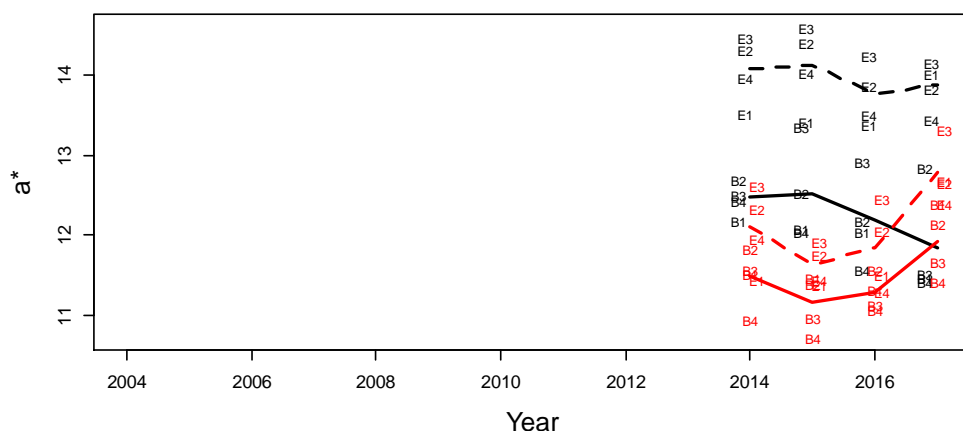


Figure 62. Individual readings and average L^* , a^* , b^* values for Site 21. Black lines and points represent the KM Spectrophotometer, and red lines and points the ASD spectrometer. Engraving points are represented by the letter E (and the corresponding spot number) for individual readings and the dashed lines for their averages; and background points are represented by the letter B (and the corresponding spot number) for their individual readings and the solid lines for their averages.

Site 22



Site 22



Site 22

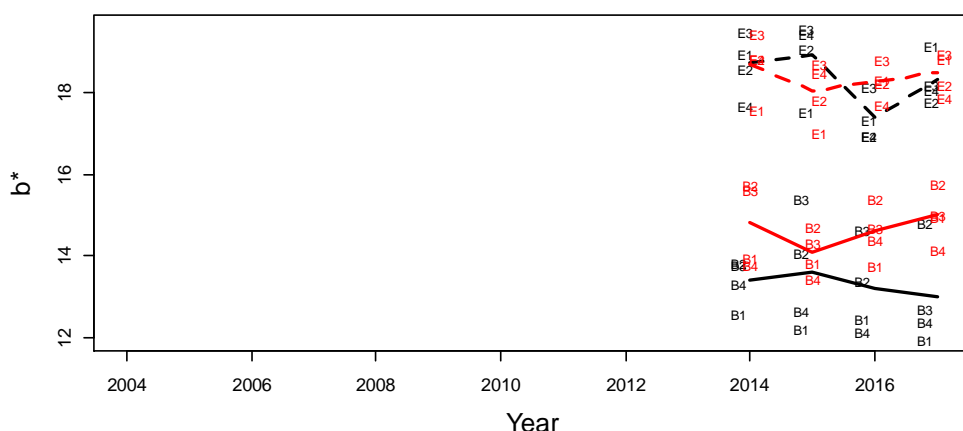


Figure 63. Individual readings and average L^* , a^* , b^* values for Site 22. Black lines and points represent the KM Spectrophotometer, and red lines and points the ASD spectrometer. Engraving points are represented by the letter E (and the corresponding spot number) for individual readings and the dashed lines for their averages; and background points are represented by the letter B (and the corresponding spot number) for their individual readings and the solid lines for their averages.

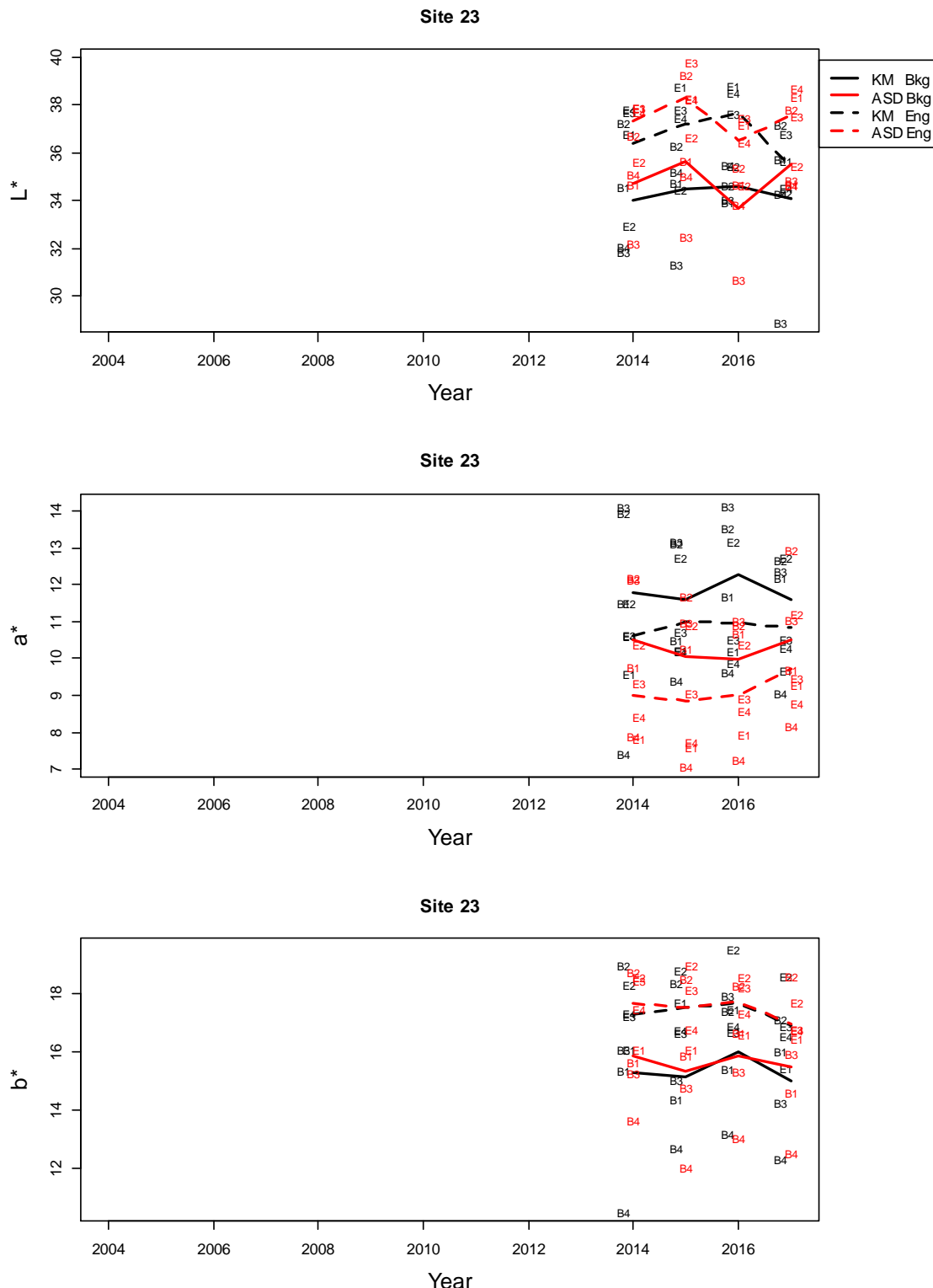
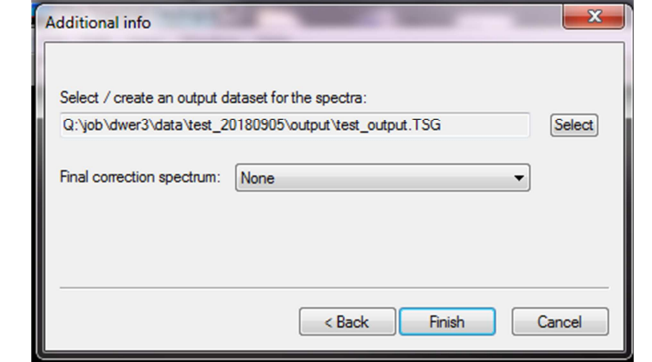
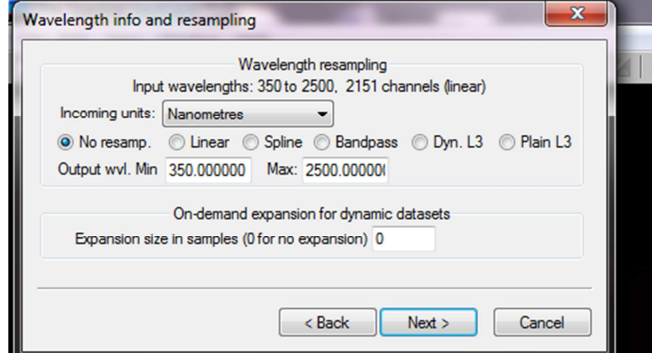
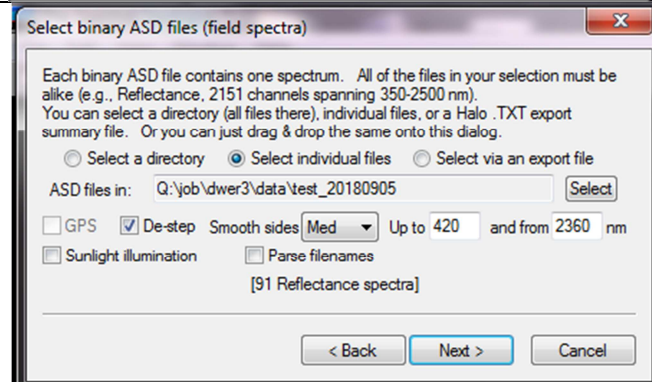
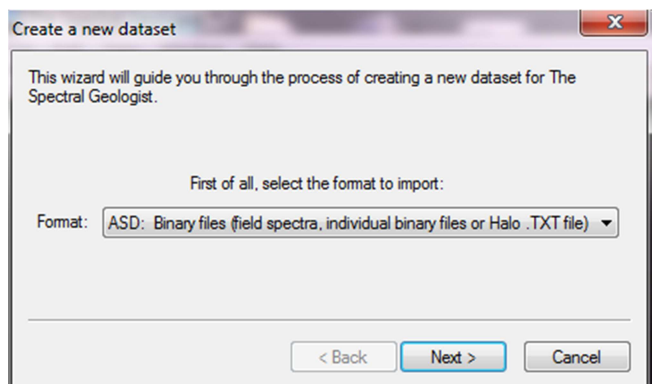


Figure 64. Individual readings and average L^* , a^* , b^* values for Site 23. Black lines and points represent the KM Spectrophotometer, and red lines and points the ASD spectrometer. Engraving points are represented by the letter E (and the corresponding spot number) for individual readings and the dashed lines for their averages; and background points are represented by the letter B (and the corresponding spot number) for their individual readings and the solid lines for their averages.

Appendix F. Conversion of ASD Data using the TSG Program

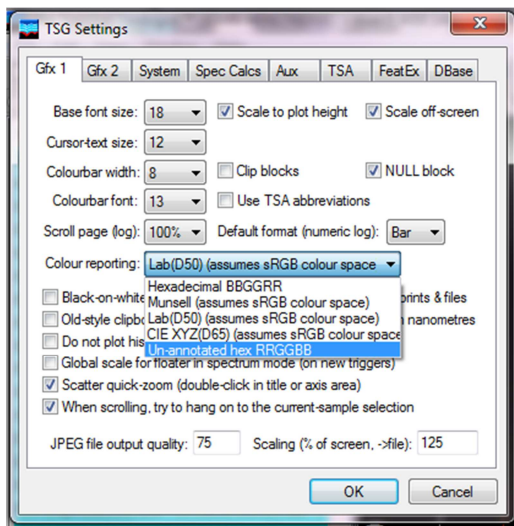
Read ASD data into TSG

1. Stick with default options

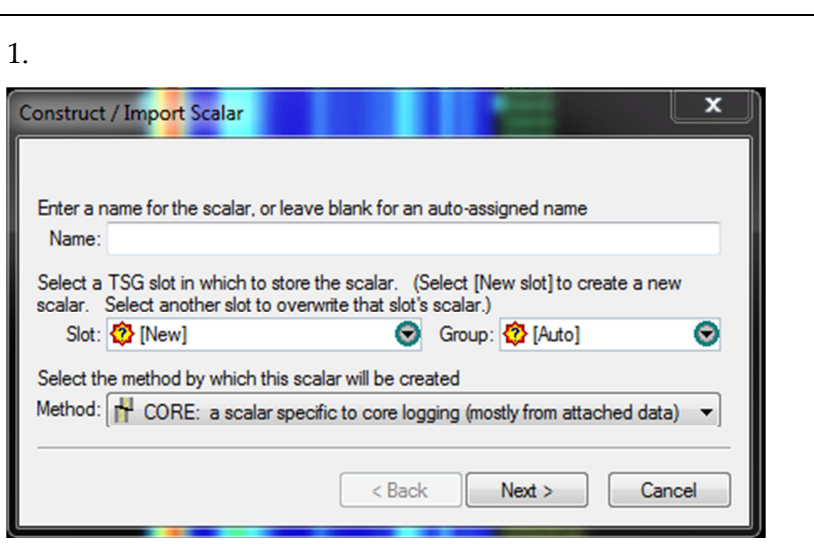


Extract LAB

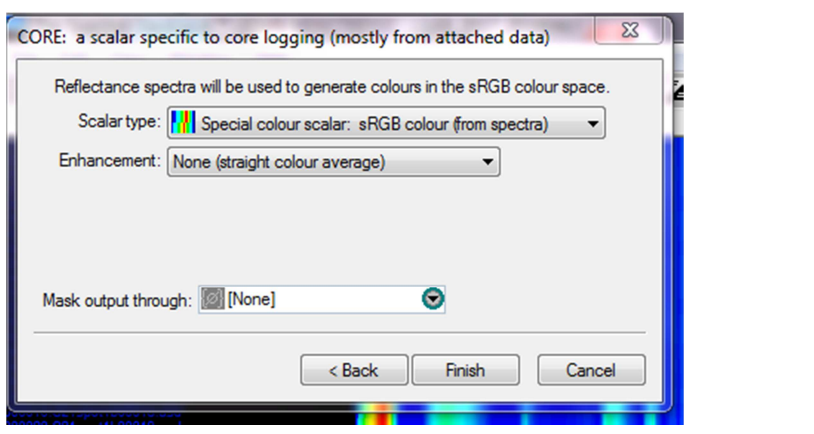
First Go to File -> Settings then Colour Reporting, and choose “Lab(D50)”



Then, Go to Edit -> New Scalar, and choose “scalar specific to core logging”



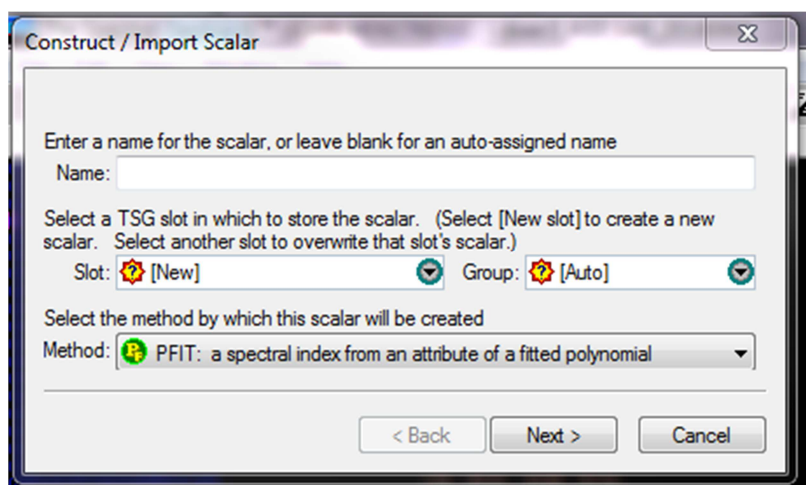
2. It is necessary to change the default to “**None (straight colour average)**”



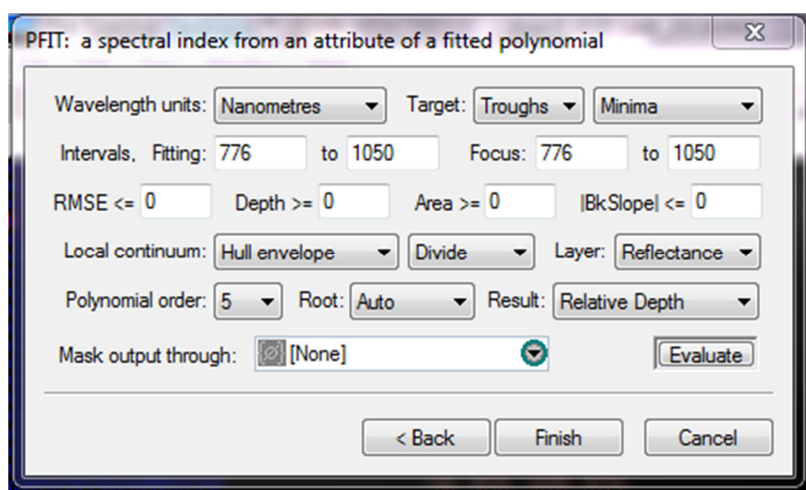
Calculation of Depth 900 nm

Go to Edit -> New Scalar, and choose "a spectral Index from an attribute of a fitted polynomial"

1.



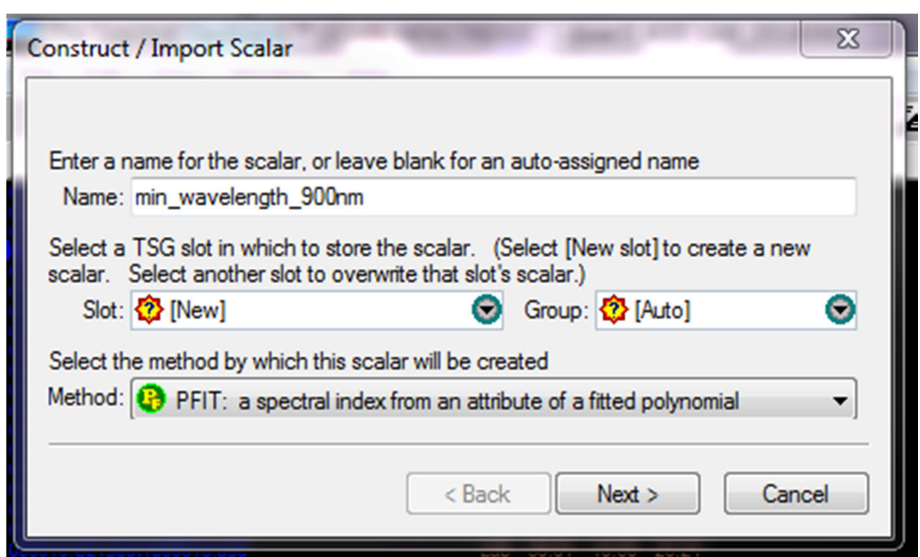
2.



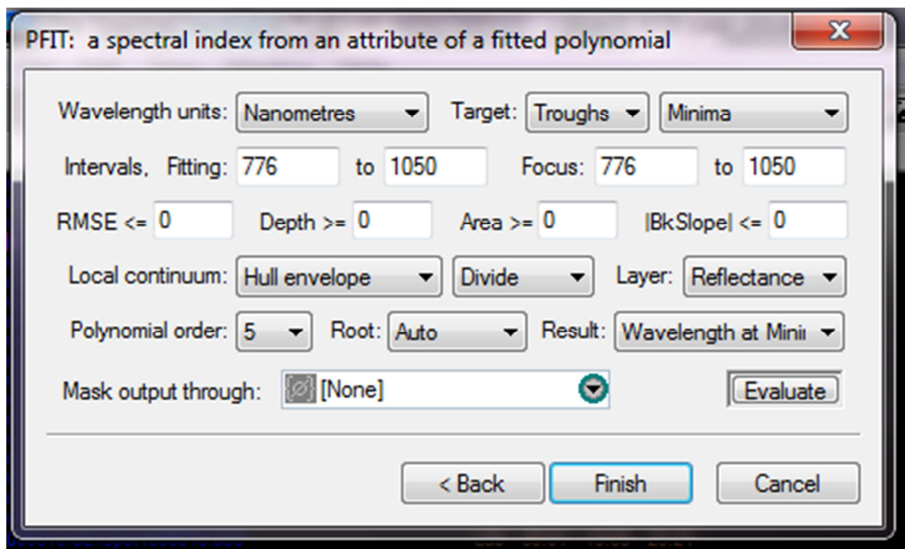
Calculation of Minimum Wavelength at 900 nm

Go to Edit -> New Scalar, and choose “a spectral Index from an attribute of a fitted polynomial”

1.



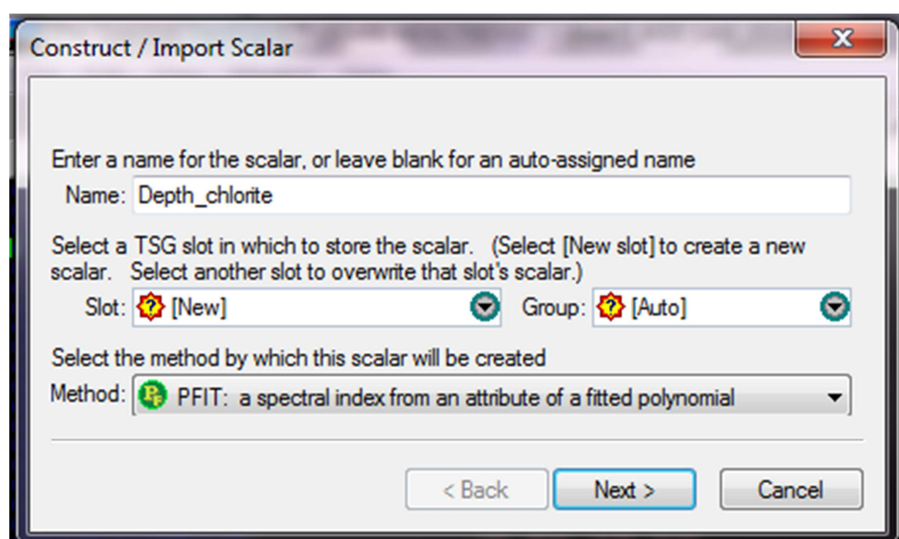
2.



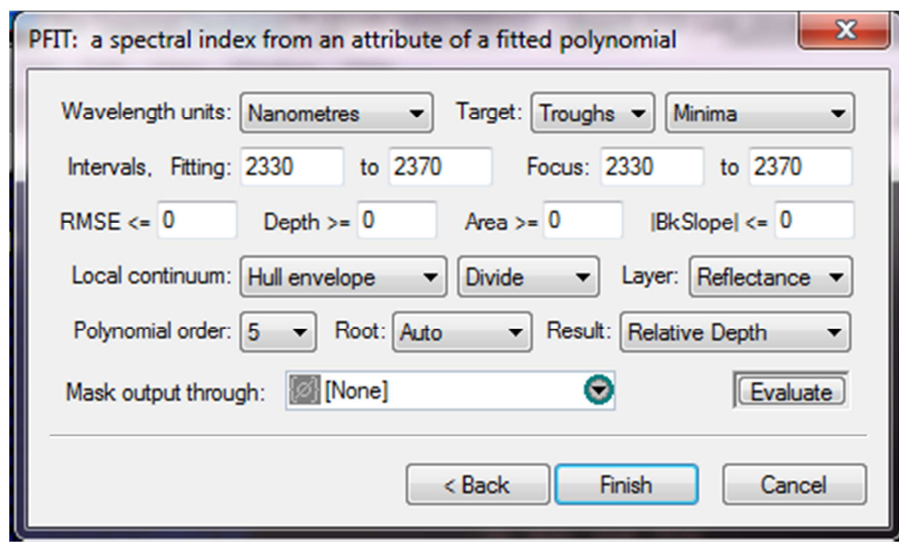
Calculation for Depth of Chlorite

Go to Edit -> New Scalar, and choose “a spectral Index from an attribute of a fitted polynomial”

1.



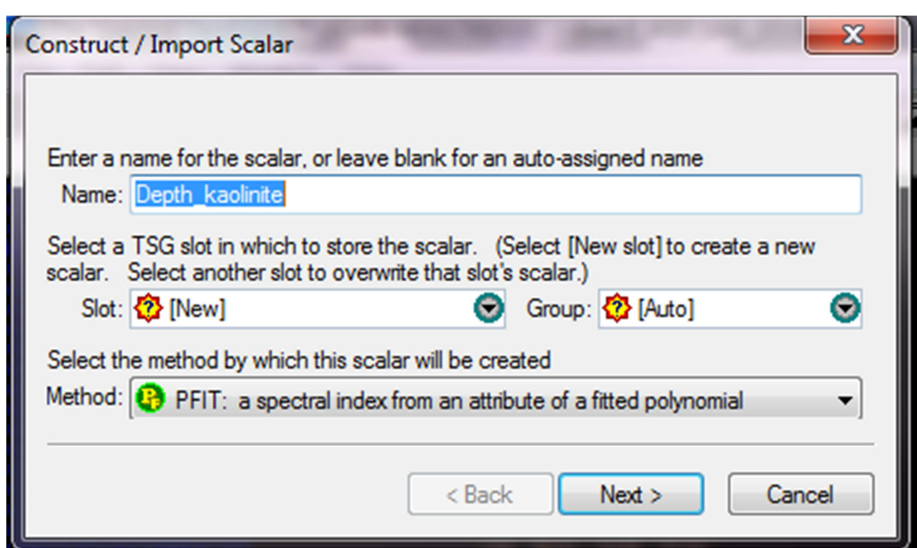
2.



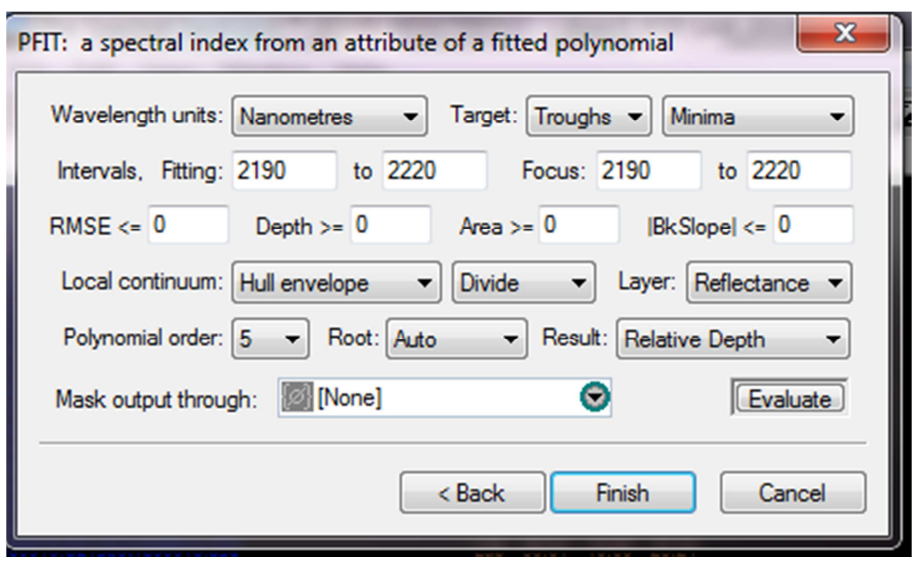
Calculation for Depth of Kaolinite

Go to Edit -> New Scalar, and choose “a spectral Index from an attribute of a fitted polynomial”

1.



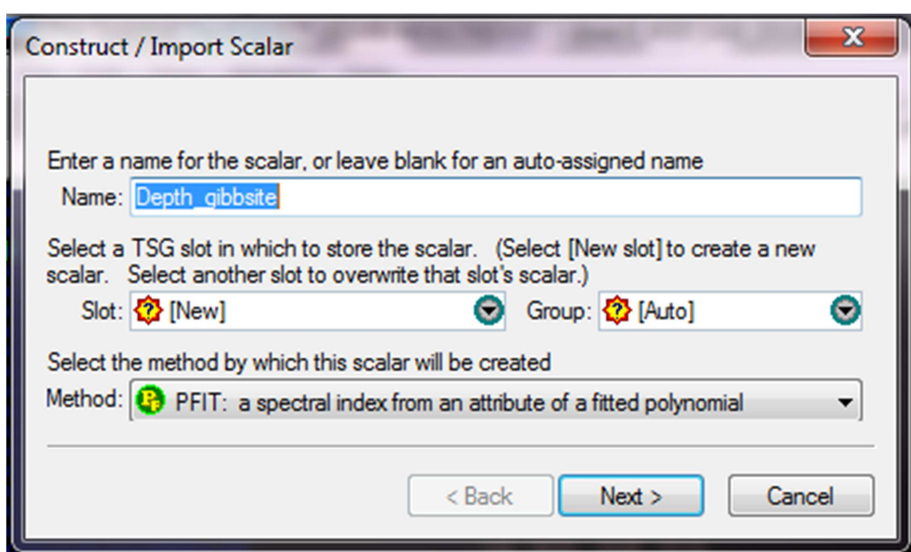
2.



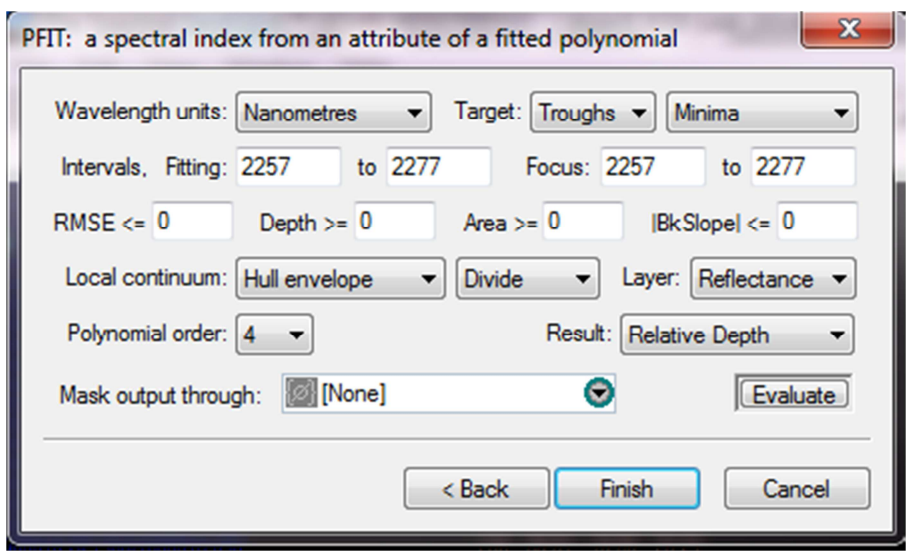
Calculation for Depth of Gibbsite

Go to Edit -> New Scalar, and choose “a spectral Index from an attribute of a fitted polynomial”

1.



2.



Appendix G. Fitted Models, Colour Data

This appendix presents the summary R output for the fitted models.

In each case, the model summaries for the full models are presented (i.e. estimates of coefficients, Standard Errors and t-values), followed by the log likelihood of the full model, the log likelihood of the reduced model and the corresponding Chi square statistic to assess the statistical significance of the key interaction terms.

G.1 KM Data, All sites

With rock type

L*

	Estimate	Std. Error	t value
(Intercept)	30.210087	1.903777	15.86849770
CIIndustry	2.971307	2.195714	1.35323028
typeEng	7.238027	1.257804	5.75449371
rockGranophyre	2.327795	2.686348	0.86652796
poly(year, 2)1	3.600033	25.246136	0.14259740
poly(year, 2)2	16.105279	23.229127	0.69332263
CIIndustry:typeEng	-4.007521	1.453805	-2.75657467
CIIndustry:rockGranophyre	-1.343889	3.024705	-0.44430417
typeEng:rockGranophyre	1.767721	1.774172	0.99636355
CIIndustry:poly(year, 2)1	-59.986837	29.042328	-2.06549687
CIIndustry:poly(year, 2)2	16.448689	25.810657	0.63728287
typeEng:poly(year, 2)1	-18.926011	30.042854	-0.62996715
typeEng:poly(year, 2)2	2.268917	27.761230	0.08172969
rockGranophyre:poly(year, 2)1	-40.962794	32.071275	-1.27724245
rockGranophyre:poly(year, 2)2	-23.969000	29.208812	-0.82060851
CIIndustry:typeEng:rockGranophyre	-1.624658	1.999735	-0.81243656
CIIndustry:typeEng:poly(year, 2)1	63.631959	36.419563	1.74719171
CIIndustry:typeEng:poly(year, 2)2	-41.838825	32.556525	-1.28511338
CIIndustry:rockGranophyre:poly(year, 2)1	107.673040	37.634711	2.86100349
CIIndustry:rockGranophyre:poly(year, 2)2	-2.486874	33.594926	-0.07402529
typeEng:rockGranophyre:poly(year, 2)1	-9.469588	40.880327	-0.23164168
typeEng:rockGranophyre:poly(year, 2)2	-26.126622	37.292509	-0.70058634
CIIndustry:typeEng:rockGranophyre:poly(year, 2)1	-58.388759	47.721543	-1.22353040
CIIndustry:typeEng:rockGranophyre:poly(year, 2)2	64.226371	42.729977	1.50307523
'log Lik.'	-10758.61	(df=37)	
'log Lik.'	-10762.69	(df=33)	
[1]	"Interaction chi square 8.15133633706137"		

a*

	Estimate	Std. Error	t value
(Intercept)	10.0043650	0.7576654	13.2042002
CIIndustry	1.3415413	0.8730021	1.5366989
typeEng	1.6542508	1.5900846	1.0403540
rockGranophyre	1.5476723	1.0666323	1.4509895
poly(year, 2)1	-3.7401946	15.8380168	-0.2361530
poly(year, 2)2	-4.2592922	14.5053069	-0.2936368
CIIndustry:typeEng	-1.7660334	1.8370905	-0.9613209
CIIndustry:rockGranophyre	-0.6049422	1.2016894	-0.5034098
typeEng:rockGranophyre	-4.1233374	2.2483225	-1.8339617

```

CIIndustry:poly(year, 2)1      -61.7822190 18.2727590 -3.3811106
CIIndustry:poly(year, 2)2      35.7208927 16.0777706  2.2217566
typeEng:poly(year, 2)1         15.9667613 17.2456970  0.9258403
typeEng:poly(year, 2)2         26.3198874 15.8290094  1.6627628
rockGranophyre:poly(year, 2)1  -14.5782767 20.5779846 -0.7084404
rockGranophyre:poly(year, 2)2   5.4932409 18.6112949  0.2951563
CIIndustry:typeEng:rockGranophyre
CIIndustry:typeEng:poly(year, 2)1  5.7586459 2.5312075  2.2750588
CIIndustry:typeEng:poly(year, 2)2  40.4013388 21.2190407  1.9040134
CIIndustry:rockGranophyre:poly(year, 2)1  -42.9499326 18.7384904 -2.2920700
CIIndustry:rockGranophyre:poly(year, 2)2  82.1513765 24.0492842  3.4159593
CIIndustry:rockGranophyre:poly(year, 2)1  -30.3795315 21.3284448 -1.4243669
typeEng:rockGranophyre:poly(year, 2)1    -7.8207594 24.0796814 -0.3247867
typeEng:rockGranophyre:poly(year, 2)2    -34.7211158 21.8610461 -1.5882641
CIIndustry:typeEng:rockGranophyre:poly(year, 2)1  -58.4789221 28.1021656 -2.0809401
CIIndustry:typeEng:rockGranophyre:poly(year, 2)2  60.6083783 25.0039979  2.4239475
'log Lik.' -6009.015 (df=37)
'log Lik.' -6017.765 (df=33)
[1] "Interaction chi square 17.5004142908001"

```

b*

	Estimate	Std. Error	t value
(Intercept)	11.5712358	0.9339839	12.38911677
CIIndustry	3.3417226	1.0777189	3.10073663
typeEng	6.6845638	1.9842471	3.36881621
rockGranophyre	3.8472030	1.3163406	2.92265012
poly(year, 2)1	11.8537637	19.8529437	0.59707839
poly(year, 2)2	9.5276317	18.1161489	0.52591927
CIIndustry:typeEng	-3.9662424	2.2919736	-1.73049223
CIIndustry:rockGranophyre	-2.7882835	1.4832128	-1.87989439
typeEng:rockGranophyre	-2.5649694	2.8042544	-0.91467072
CIIndustry:poly(year, 2)1	-62.1561040	23.5722677	-2.63683175
CIIndustry:poly(year, 2)2	34.5308748	20.7091959	1.66741746
typeEng:poly(year, 2)1	-0.2679065	24.9495381	-0.01073793
typeEng:poly(year, 2)2	37.1280690	22.9622778	1.61691577
rockGranophyre:poly(year, 2)1	-47.2864009	26.4046357	-1.79083709
rockGranophyre:poly(year, 2)2	-10.9532339	23.8461395	-0.45932944
CIIndustry:typeEng:rockGranophyre	3.6729244	3.1574465	1.16325784
CIIndustry:typeEng:poly(year, 2)1	53.0950812	30.2557578	1.75487527
CIIndustry:typeEng:poly(year, 2)2	-61.9835003	26.8273405	-2.31046012
CIIndustry:rockGranophyre:poly(year, 2)1	116.2691224	30.9022192	3.76248456
CIIndustry:rockGranophyre:poly(year, 2)2	-23.1915801	27.3506130	-0.84793639
typeEng:rockGranophyre:poly(year, 2)1	5.0208954	34.0634629	0.14739827
typeEng:rockGranophyre:poly(year, 2)2	-55.5463247	30.9795908	-1.79299736
CIIndustry:typeEng:rockGranophyre:poly(year, 2)1	-81.2213103	39.8108817	-2.04017863
CIIndustry:typeEng:rockGranophyre:poly(year, 2)2	82.3441124	35.4794625	2.32089515
'log Lik.'	-8356.477	(df=37)	
'log Lik.'	-8364.781	(df=33)	
[1]	"Interaction chi square 16.6073040223782"		

	Estimate	Std. Error	t value
(Intercept)	10.9273638100	1.0180758	10.733349952
CIIndustry	3.3697168777	1.1905079	2.830486728
typeEng	6.4733983082	1.8361331	3.525560412
rockGranophyre	4.4007618080	1.4397789	3.056553866
trend_pre	0.1049091489	0.1655128	0.633843233
trend_post	-0.1555141393	0.2074464	-0.749659555
CIIndustry:typeEng	-3.1249580605	2.1311629	-1.466315889

```

CIIndustry:rockGranophyre          -3.6483488818  1.6323778 -2.234990557
typeEng:rockGranophyre            -2.0916891757  2.5966849 -0.805522900
CIIndustry:trend_pre              -0.1676136796  0.2224523 -0.753481440
CIIndustry:trend_post             0.1210176456  0.2340930  0.516963931
typeEng:trend_pre                -0.2123671439  0.1896230 -1.119943891
typeEng:trend_post               0.3563700138  0.2378668  1.498191322
rockGranophyre:trend_pre         -0.1710686141  0.2340834 -0.730801961
rockGranophyre:trend_post        0.1086761885  0.2934036  0.370398304
CIIndustry:typeEng:rockGranophyre 2.9494725396  2.9312667  1.006210919
CIIndustry:typeEng:trend_pre     0.1820190557  0.2548933  0.714099037
CIIndustry:typeEng:trend_post    -0.2885366850  0.2684781 -1.074712153
CIIndustry:rockGranophyre:trend_pre 0.1081498705  0.2884787  0.374897264
CIIndustry:rockGranophyre:trend_post 0.0225989526  0.3226662  0.070038188
typeEng:rockGranophyre:trend_pre  0.1210799027  0.2681831  0.451482222
typeEng:rockGranophyre:trend_post -0.1924240242  0.3364019 -0.572006289
CIIndustry:typeEng:rockGranophyre:trend_pre -0.0009884714  0.3307600 -0.002988486
CIIndustry:typeEng:rockGranophyre:trend_post  0.0897705461  0.3700293  0.242603901
'log Lik.' -14447.9 (df=37)
'log Lik.' -14448.94 (df=33)
[1] "chi square 2.07420832435673"

```

G.2 ASD Colour Data, all sites

With rock type

L*

	Estimate	Std. Error	t value
(Intercept)	30.210087	1.903777	15.86849770
CIIndustry	2.971307	2.195714	1.35323028
typeEng	7.238027	1.257804	5.75449371
rockGranophyre	2.327795	2.686348	0.86652796
poly(year, 2)1	3.600033	25.246136	0.14259740
poly(year, 2)2	16.105279	23.229127	0.69332263
CIIndustry:typeEng	-4.007521	1.453805	-2.75657467
CIIndustry:rockGranophyre	-1.343889	3.024705	-0.44430417
typeEng:rockGranophyre	1.767721	1.774172	0.99636355
CIIndustry:poly(year, 2)1	-59.986837	29.042328	-2.06549687
CIIndustry:poly(year, 2)2	16.448689	25.810657	0.63728287
typeEng:poly(year, 2)1	-18.926011	30.042854	-0.62996715
typeEng:poly(year, 2)2	2.268917	27.761230	0.08172969
rockGranophyre:poly(year, 2)1	-40.962794	32.071275	-1.27724245
rockGranophyre:poly(year, 2)2	-23.969000	29.208812	-0.82060851
CIIndustry:typeEng:rockGranophyre	-1.624658	1.999735	-0.81243656
CIIndustry:typeEng:poly(year, 2)1	63.631959	36.419563	1.74719171
CIIndustry:typeEng:poly(year, 2)2	-41.838825	32.556525	-1.28511338
CIIndustry:rockGranophyre:poly(year, 2)1	107.673040	37.634711	2.86100349
CIIndustry:rockGranophyre:poly(year, 2)2	-2.486874	33.594926	-0.07402529
typeEng:rockGranophyre:poly(year, 2)1	-9.469588	40.880327	-0.23164168
typeEng:rockGranophyre:poly(year, 2)2	-26.126622	37.292509	-0.70058634
CIIndustry:typeEng:rockGranophyre:poly(year, 2)1	-58.388759	47.721543	-1.22353040
CIIndustry:typeEng:rockGranophyre:poly(year, 2)2	64.226371	42.729977	1.50307523
'log Lik.'	-10758.61 (df=37)		
'log Lik.'	-10762.69 (df=33)		
[1]	"Interaction chi square 8.15133633706137"		

a*

	Estimate	Std. Error	t value
(Intercept)	10.0043650	0.7576654	13.2042002
CIIndustry	1.3415413	0.8730021	1.5366989
typeEng	1.6542508	1.5900846	1.0403540
rockGranophyre	1.5476723	1.0666323	1.4509895
poly(year, 2)1	-3.7401946	15.8380168	-0.2361530
poly(year, 2)2	-4.2592922	14.5053069	-0.2936368
CIIndustry:typeEng	-1.7660334	1.8370905	-0.9613209
CIIndustry:rockGranophyre	-0.6049422	1.2016894	-0.5034098
typeEng:rockGranophyre	-4.1233374	2.2483225	-1.8339617
CIIndustry:poly(year, 2)1	-61.7822190	18.2727590	-3.3811106
CIIndustry:poly(year, 2)2	35.7208927	16.0777706	2.2217566
typeEng:poly(year, 2)1	15.9667613	17.2456970	0.9258403
typeEng:poly(year, 2)2	26.3198874	15.8290094	1.6627628
rockGranophyre:poly(year, 2)1	-14.5782767	20.5779846	-0.7084404
rockGranophyre:poly(year, 2)2	5.4932409	18.6112949	0.2951563
CIIndustry:typeEng:rockGranophyre	5.7586459	2.5312075	2.2750588
CIIndustry:typeEng:poly(year, 2)1	40.4013388	21.2190407	1.9040134
CIIndustry:typeEng:poly(year, 2)2	-42.9499326	18.7384904	-2.2920700
CIIndustry:rockGranophyre:poly(year, 2)1	82.1513765	24.0492842	3.4159593
CIIndustry:rockGranophyre:poly(year, 2)2	-30.3795315	21.3284448	-1.4243669
typeEng:rockGranophyre:poly(year, 2)1	-7.8207594	24.0796814	-0.3247867
typeEng:rockGranophyre:poly(year, 2)2	-34.7211158	21.8610461	-1.5882641
CIIndustry:typeEng:rockGranophyre:poly(year, 2)1	-58.4789221	28.1021656	-2.0809401
CIIndustry:typeEng:rockGranophyre:poly(year, 2)2	60.6083783	25.0039979	2.4239475
'log Lik.'	-6009.015	(df=37)	
'log Lik.'	-6017.765	(df=33)	
[1]	"Interaction chi square 17.5004142908001"		

b*

	Estimate	Std. Error	t value
(Intercept)	11.5712358	0.9339839	12.38911677
CIIndustry	3.3417226	1.0777189	3.10073663
typeEng	6.6845638	1.9842471	3.36881621
rockGranophyre	3.8472030	1.3163406	2.92265012
poly(year, 2)1	11.8537637	19.8529437	0.59707839
poly(year, 2)2	9.5276317	18.1161489	0.52591927
CIIndustry:typeEng	-3.9662424	2.2919736	-1.73049223
CIIndustry:rockGranophyre	-2.7882835	1.4832128	-1.87989439
typeEng:rockGranophyre	-2.5649694	2.8042544	-0.91467072
CIIndustry:poly(year, 2)1	-62.1561040	23.5722677	-2.63683175
CIIndustry:poly(year, 2)2	34.5308748	20.7091959	1.66741746
typeEng:poly(year, 2)1	-0.2679065	24.9495381	-0.01073793
typeEng:poly(year, 2)2	37.1280690	22.9622778	1.61691577
rockGranophyre:poly(year, 2)1	-47.2864009	26.4046357	-1.79083709
rockGranophyre:poly(year, 2)2	-10.9532339	23.8461395	-0.45932944
CIIndustry:typeEng:rockGranophyre	3.6729244	3.1574465	1.16325784
CIIndustry:typeEng:poly(year, 2)1	53.0950812	30.2557578	1.75487527
CIIndustry:typeEng:poly(year, 2)2	-61.9835003	26.8273405	-2.31046012
CIIndustry:rockGranophyre:poly(year, 2)1	116.2691224	30.9022192	3.76248456
CIIndustry:rockGranophyre:poly(year, 2)2	-23.1915801	27.3506130	-0.84793639
typeEng:rockGranophyre:poly(year, 2)1	5.0208954	34.0634629	0.14739827
typeEng:rockGranophyre:poly(year, 2)2	-55.5463247	30.9795908	-1.79299736
CIIndustry:typeEng:rockGranophyre:poly(year, 2)1	-81.2213103	39.8108817	-2.04017863
CIIndustry:typeEng:rockGranophyre:poly(year, 2)2	82.3441124	35.4794625	2.32089515

```
'log Lik.' -8356.477 (df=37)
'log Lik.' -8364.781 (df=33)
[1] "Interaction chi square 16.6073040223782"
```

G.3 ASD Spectral Data, All sites

Depth_900nm

	Estimate	Std. Error	t value
(Intercept)	0.090785921	0.02855949	3.17883571
CIIndustry	0.027081362	0.03299496	0.82077260
typeEng	-0.020263039	0.01664105	-1.21765375
rockGranophyre	-0.018688813	0.04038523	-0.46276356
poly(year, 2)1	0.044605649	0.04310631	1.03478227
poly(year, 2)2	-0.013000254	0.04073797	-0.31911887
CIIndustry:typeEng	-0.008262382	0.01927433	-0.42867294
CIIndustry:rockGranophyre	0.025691867	0.04546808	0.56505286
typeEng:rockGranophyre	-0.021137838	0.02352255	-0.89862015
CIIndustry:poly(year, 2)1	-0.147424724	0.05467947	-2.69616226
CIIndustry:poly(year, 2)2	0.040450234	0.04839107	0.83590286
typeEng:poly(year, 2)1	-0.015587134	0.06049694	-0.25765162
typeEng:poly(year, 2)2	0.009386423	0.05730493	0.16379783
rockGranophyre:poly(year, 2)1	0.112492103	0.05907888	1.90410012
rockGranophyre:poly(year, 2)2	0.156280909	0.05577867	2.80180425
CIIndustry:typeEng:rockGranophyre	0.031906098	0.02652631	1.20280949
CIIndustry:typeEng:poly(year, 2)1	0.146127675	0.07657138	1.90838507
CIIndustry:typeEng:poly(year, 2)2	-0.010432104	0.06821876	-0.15292135
CIIndustry:rockGranophyre:poly(year, 2)1	0.044196957	0.07096553	0.62279469
CIIndustry:rockGranophyre:poly(year, 2)2	-0.170171505	0.06415136	-2.65265614
typeEng:rockGranophyre:poly(year, 2)1	-0.123752270	0.08330474	-1.48553699
typeEng:rockGranophyre:poly(year, 2)2	-0.188258181	0.07885206	-2.38748584
CIIndustry:typeEng:rockGranophyre:poly(year, 2)1	-0.007059260	0.09971973	-0.07079101
CIIndustry:typeEng:rockGranophyre:poly(year, 2)2	0.204801714	0.09062587	2.25985932
'log Lik.'	2117.67	(df=34)	
'log Lik.'	2110.17	(df=30)	
[1]	"Interaction chi square 15.0012693918434"		

Min_wavelength_900nm band

	Estimate	Std. Error	t value
(Intercept)	896.356642	3.145716	284.9451900
CIIndustry	-2.621146	3.637130	-0.7206633
typeEng	-6.890060	1.101964	-6.2525248
rockGranophyre	2.604014	4.445201	0.5858033
poly(year, 2)1	-4.310642	9.292459	-0.4638860
poly(year, 2)2	4.318825	8.877108	0.4865127
CIIndustry:typeEng	4.071034	1.309043	3.1099314
CIIndustry:rockGranophyre	-2.218129	5.008828	-0.4428439
typeEng:rockGranophyre	10.395743	1.556339	6.6796145
CIIndustry:poly(year, 2)1	24.603165	11.333875	2.1707637
CIIndustry:poly(year, 2)2	-14.153542	10.177526	-1.3906663
typeEng:poly(year, 2)1	-14.450339	12.322597	-1.1726699
typeEng:poly(year, 2)2	-20.418887	11.852303	-1.7227780
rockGranophyre:poly(year, 2)1	-6.372725	12.327620	-0.5169469
rockGranophyre:poly(year, 2)2	3.987040	11.781349	0.3384196
CIIndustry:typeEng:rockGranophyre	-9.529605	1.781035	-5.3505991

```

CIIndustry:typeEng:poly(year, 2)1          3.983401  15.655265  0.2544448
CIIndustry:typeEng:poly(year, 2)2          22.395557  14.198405  1.5773291
CIIndustry:rockGranophyre:poly(year, 2)1   -13.560495  14.759853  -0.9187419
CIIndustry:rockGranophyre:poly(year, 2)2   1.714607   13.540505  0.1266280
typeEng:rockGranophyre:poly(year, 2)1      39.099496  17.303183  2.2596708
typeEng:rockGranophyre:poly(year, 2)2      44.649881  16.645125  2.6824599
CIIndustry:typeEng:rockGranophyre:poly(year, 2)1 -30.905727  20.573890  -1.5021820
CIIndustry:typeEng:rockGranophyre:poly(year, 2)2 -44.326259  19.086530  -2.3223843
'log Lik.' -1457.461 (df=34)
'log Lik.' -1461.393 (df=30)
[1] "Interaction chi square 7.86393818858051"

```

Depth kaolinite

	Estimate	Std. Error	t value
(Intercept)	0.0617437735	0.011829190	5.21961139
CIIndustry	-0.0034102481	0.013665335	-0.24955467
typeEng	-0.0177570932	0.004468359	-3.97396341
rockGranophyre	-0.0237617306	0.016725529	-1.42068636
poly(year, 2)1	-0.0393978576	0.018939379	-2.08020855
poly(year, 2)2	0.0060451380	0.017929496	0.33716162
CIIndustry:typeEng	-0.0059204797	0.005204406	-1.13758982
CIIndustry:rockGranophyre	0.0029627008	0.018830964	0.15733134
typeEng:rockGranophyre	0.0076572086	0.006319139	1.21174876
CIIndustry:poly(year, 2)1	-0.0726188022	0.023392408	-3.10437477
CIIndustry:poly(year, 2)2	-0.0085531804	0.020767115	-0.41186176
typeEng:poly(year, 2)1	0.0241856499	0.025245444	0.95802039
typeEng:poly(year, 2)2	-0.0001791123	0.023908194	-0.00749167
rockGranophyre:poly(year, 2)1	0.0634862578	0.025279288	2.51139418
rockGranophyre:poly(year, 2)2	-0.0039976900	0.023907196	-0.16721702
CIIndustry:typeEng:rockGranophyre	0.0103881874	0.007146583	1.45358792
CIIndustry:typeEng:poly(year, 2)1	0.1024721760	0.032536896	3.14941462
CIIndustry:typeEng:poly(year, 2)2	-0.0030286051	0.028799619	-0.10516129
CIIndustry:rockGranophyre:poly(year, 2)1	0.0317486965	0.030351210	1.04604385
CIIndustry:rockGranophyre:poly(year, 2)2	0.0031300867	0.027499851	0.11382195
typeEng:rockGranophyre:poly(year, 2)1	-0.0829418257	0.035693564	-2.32371937
typeEng:rockGranophyre:poly(year, 2)2	-0.0303985725	0.033802746	-0.89929298
CIIndustry:typeEng:rockGranophyre:poly(year, 2)1	-0.0489443869	0.042653930	-1.14747662
CIIndustry:typeEng:rockGranophyre:poly(year, 2)2	0.0373995894	0.038760634	0.96488590
'log Lik.'	2691.608 (df=34)		
'log Lik.'	2684.42 (df=30)		
[1]	"Interaction chi square 14.3767835114886"		

Depth chlorite

	Estimate	Std. Error	t value
(Intercept)	0.0578809423	0.021513559	2.69044009
CIIndustry	0.0110971212	0.024852523	0.44651890
typeEng	0.0421695563	0.009718044	4.33930488
poly(year, 2)1	-0.0007448925	0.024790599	-0.03004738
poly(year, 2)2	-0.0482653544	0.022472637	-2.14773883
CIIndustry:typeEng	-0.0276513501	0.011280808	-2.45118526
CIIndustry:poly(year, 2)1	-0.0543524024	0.030869451	-1.76071815
CIIndustry:poly(year, 2)2	0.0435640664	0.026695099	1.63191250
typeEng:poly(year, 2)1	0.0058092825	0.033839967	0.17166927
typeEng:poly(year, 2)2	0.0557726358	0.030831977	1.80892180
CIIndustry:typeEng:poly(year, 2)1	0.0498422540	0.042562676	1.17103198
CIIndustry:typeEng:poly(year, 2)2	-0.0714081039	0.037097863	-1.92485761

```
'log Lik.' 738.2996 (df=22)
'log Lik.' 735.0513 (df=20)
[1] "Interaction chi square 6.49650202861744"
```

Depth gibbsite (square root)

	Estimate	Std. Error	t value
(Intercept)	2.414272e-03	0.004833201	0.499518128
CIIndustry	1.278929e-04	0.005584087	0.022903098
typeEng	2.290187e-03	0.004060619	0.563999564
rockGranophyre	-5.621336e-05	0.006835179	-0.008224124
poly(year, 2)1	1.462771e-02	0.006798918	2.151476497
poly(year, 2)2	-2.213167e-04	0.006472412	-0.034193859
CIIndustry:typeEng	-1.644866e-03	0.004694527	-0.350379494
CIIndustry:rockGranophyre	1.400141e-03	0.007695221	0.181949459
typeEng:rockGranophyre	-1.864985e-03	0.005741224	-0.324841024
CIIndustry:poly(year, 2)1	1.219549e-04	0.008835933	0.013802153
CIIndustry:poly(year, 2)2	4.470926e-03	0.007805496	0.572791990
typeEng:poly(year, 2)1	1.403783e-02	0.009796862	1.432890165
typeEng:poly(year, 2)2	8.811590e-03	0.009406563	0.936749170
rockGranophyre:poly(year, 2)1	-1.100333e-02	0.009615108	-1.144378875
rockGranophyre:poly(year, 2)2	2.048741e-02	0.009153371	2.238236761
CIIndustry:typeEng:rockGranophyre	-2.069044e-03	0.006466772	-0.319950065
CIIndustry:typeEng:poly(year, 2)1	-9.308121e-03	0.012293080	-0.757183781
CIIndustry:typeEng:poly(year, 2)2	-8.291736e-03	0.011150653	-0.743609900
CIIndustry:rockGranophyre:poly(year, 2)1	-6.202244e-03	0.011549322	-0.537022388
CIIndustry:rockGranophyre:poly(year, 2)2	-2.694126e-02	0.010503280	-2.565033445
typeEng:rockGranophyre:poly(year, 2)1	-2.176132e-02	0.013460713	-1.616654537
typeEng:rockGranophyre:poly(year, 2)2	-3.370895e-02	0.012927796	-2.607478286
CIIndustry:typeEng:rockGranophyre:poly(year, 2)1	2.368537e-02	0.016063422	1.474490792
CIIndustry:typeEng:rockGranophyre:poly(year, 2)2	3.232471e-02	0.014852561	2.176372823
'log Lik.'	3384.074	(df=34)	
'log Lik.'	3380.476	(df=30)	
[1]	"Interaction chi square 7.19586731780873"		

Appendix H. Interaction Plots,

H.1 KM Colour Data

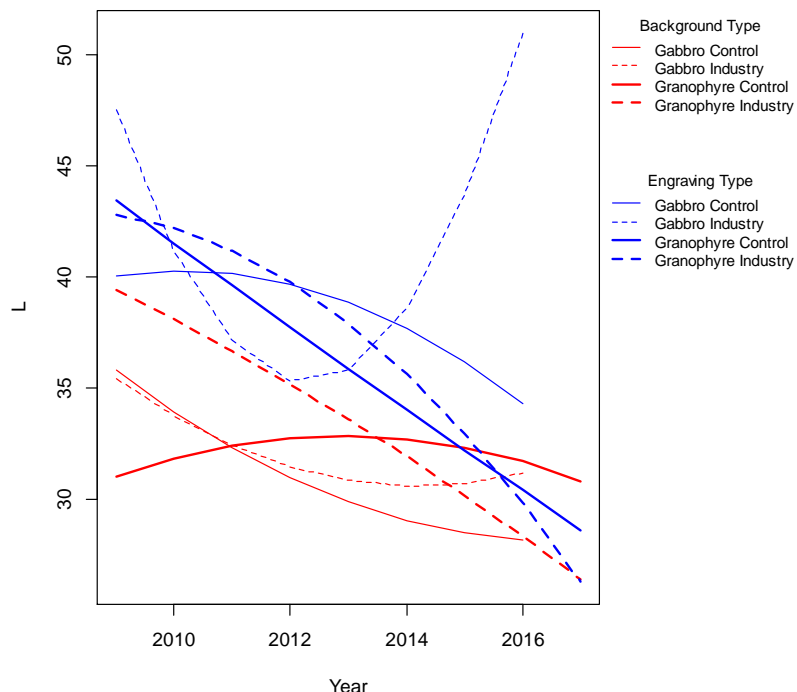


Figure 65. Interaction plot for full KM data, L^* .

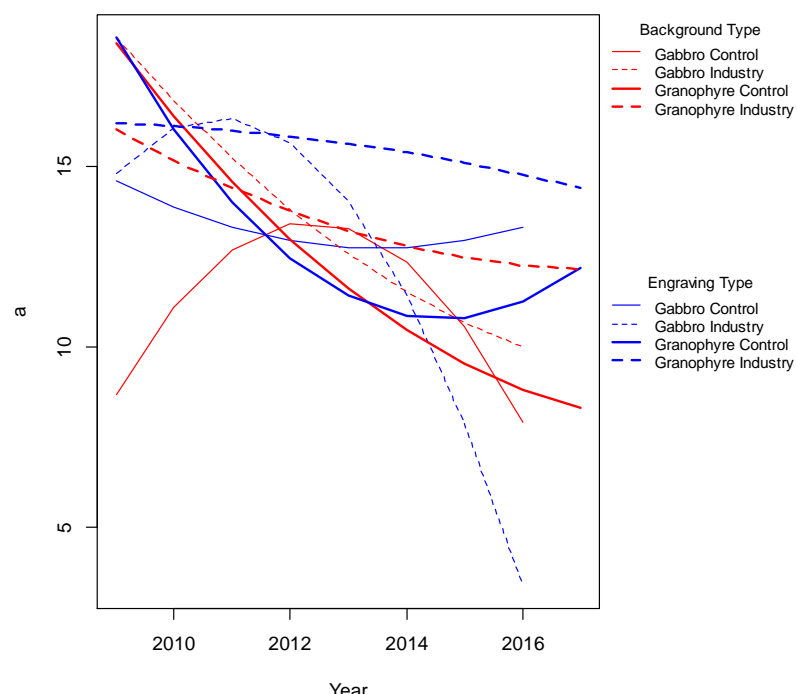


Figure 66. Interaction plot for full KM data, a^* .

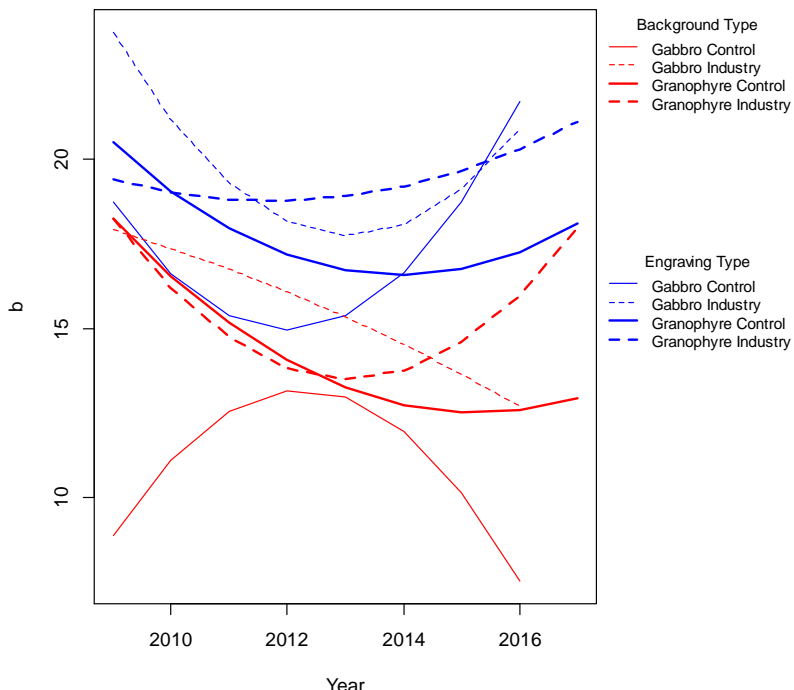


Figure 67. Interaction plot for full KM data, b^* .

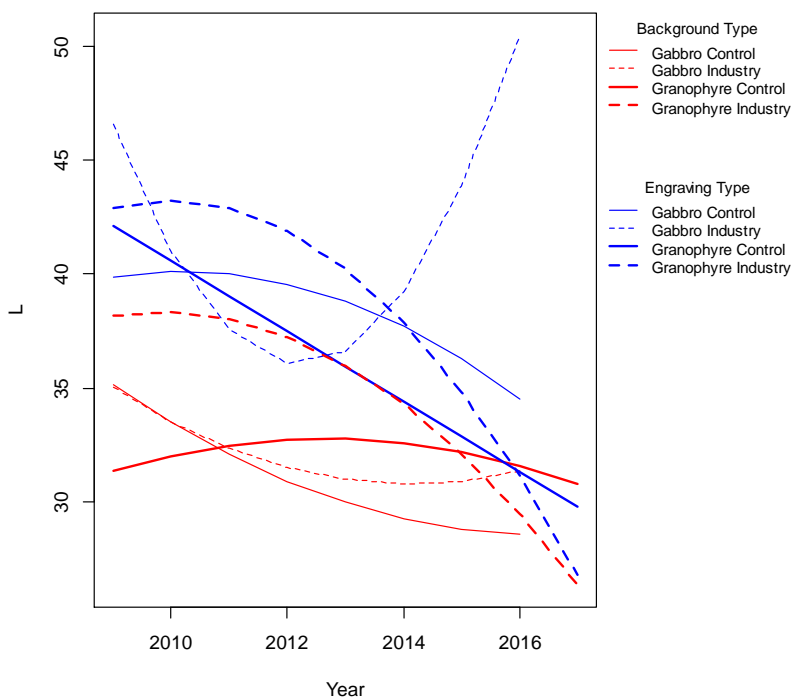


Figure 68. Interaction plot for Yara KM data, L^* .

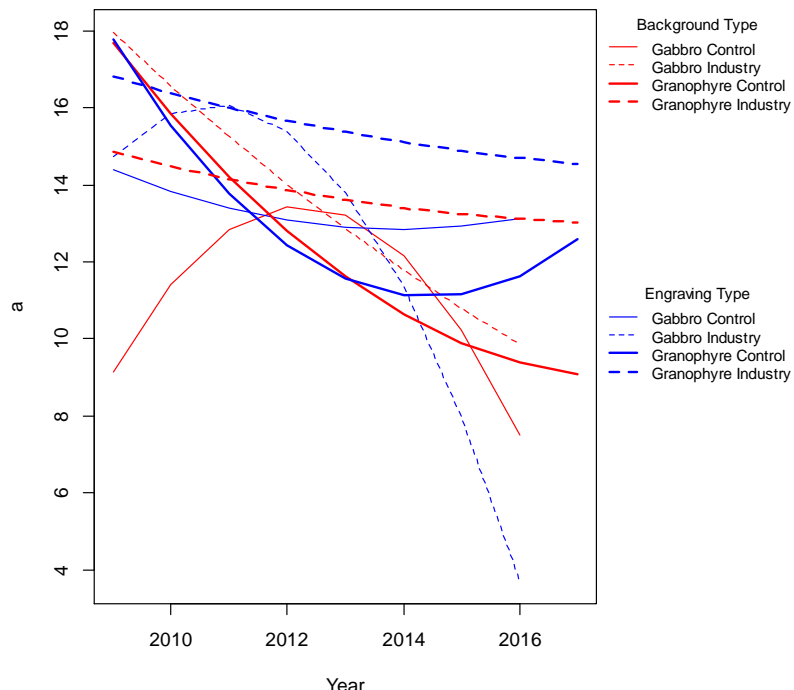


Figure 69. Interaction plot for Yara KM data, a^* .

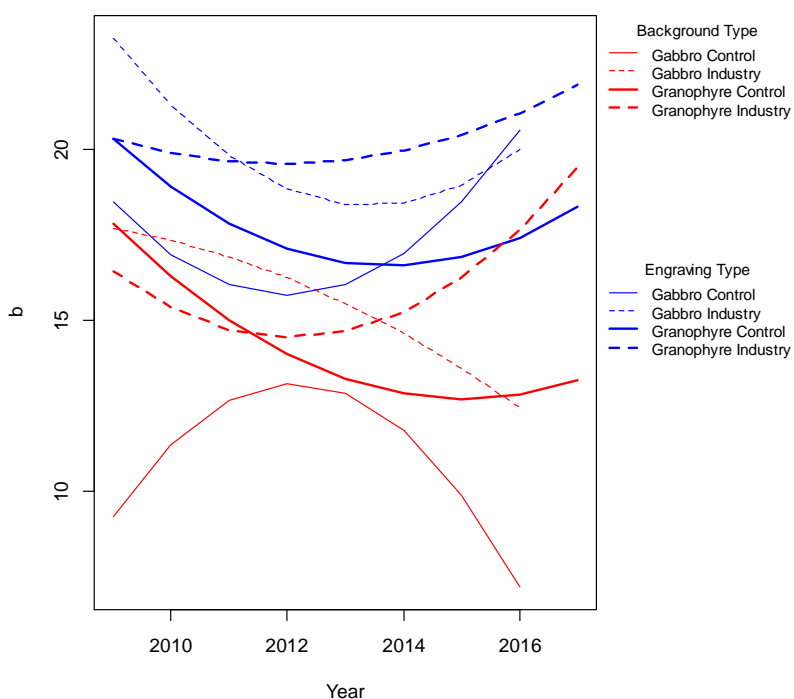


Figure 70. Interaction plot for Yara KM data, b^* .

H.2 ASD Colour Data

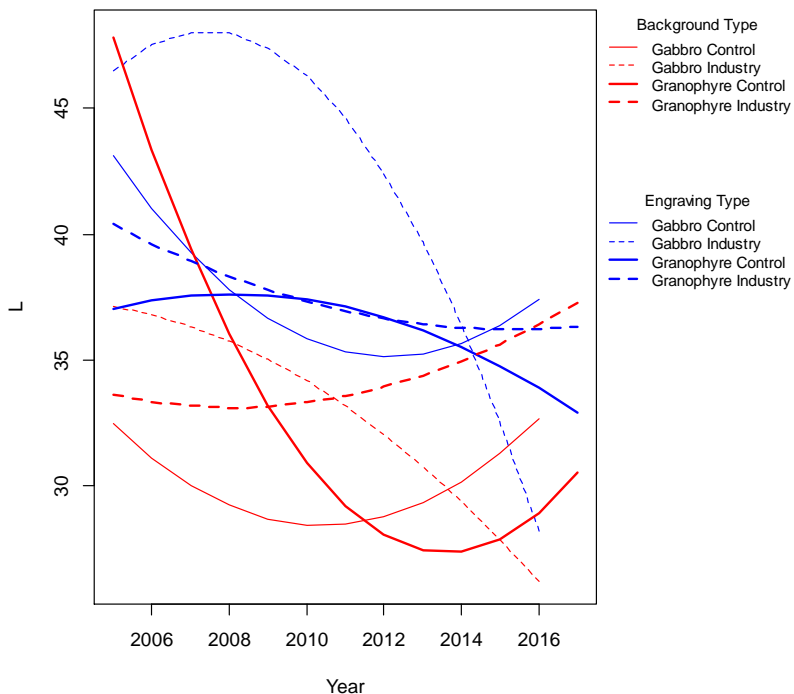


Figure 71. Interaction plot for full ASD data, L^* .

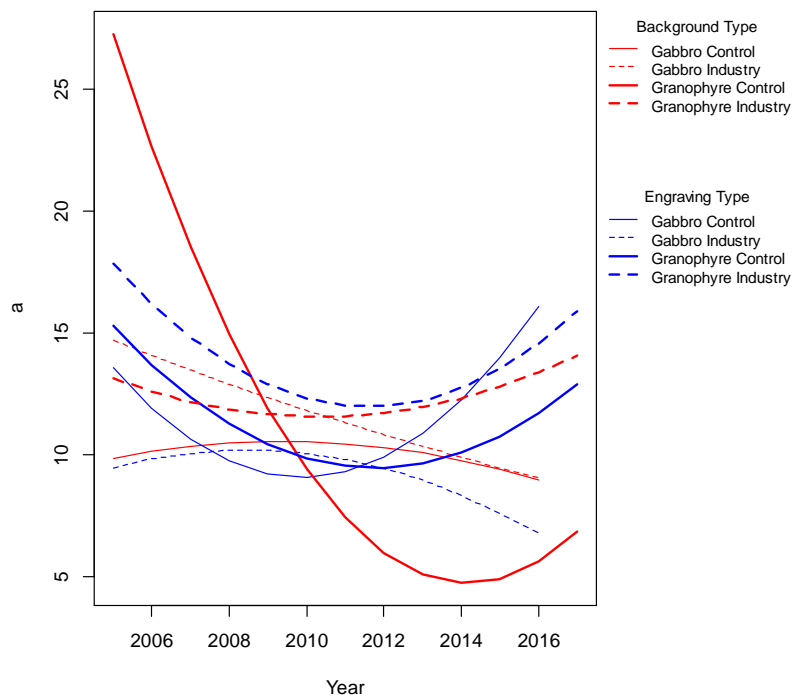


Figure 72. Interaction plot for full ASD data, a^* .

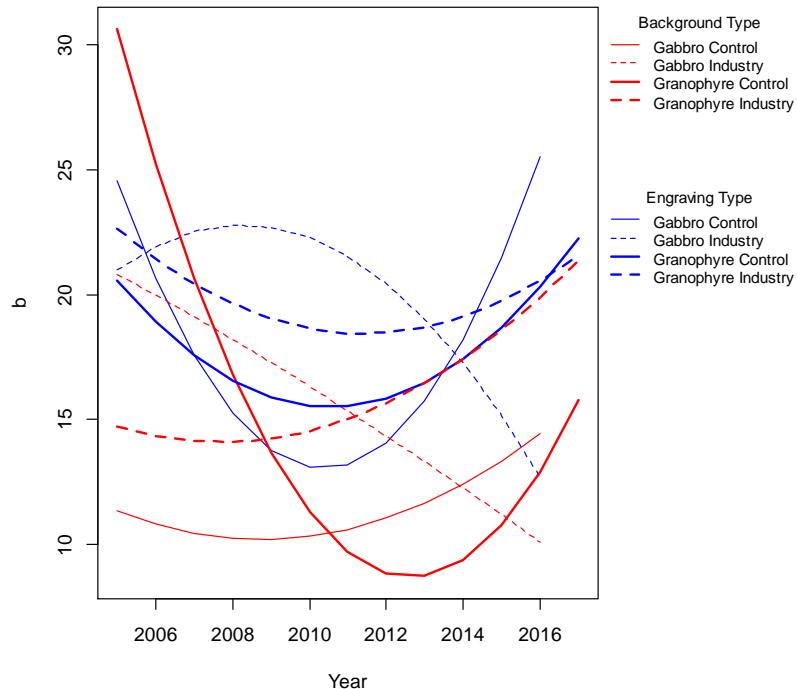


Figure 73. Interaction plot for full ASD data, b^* .

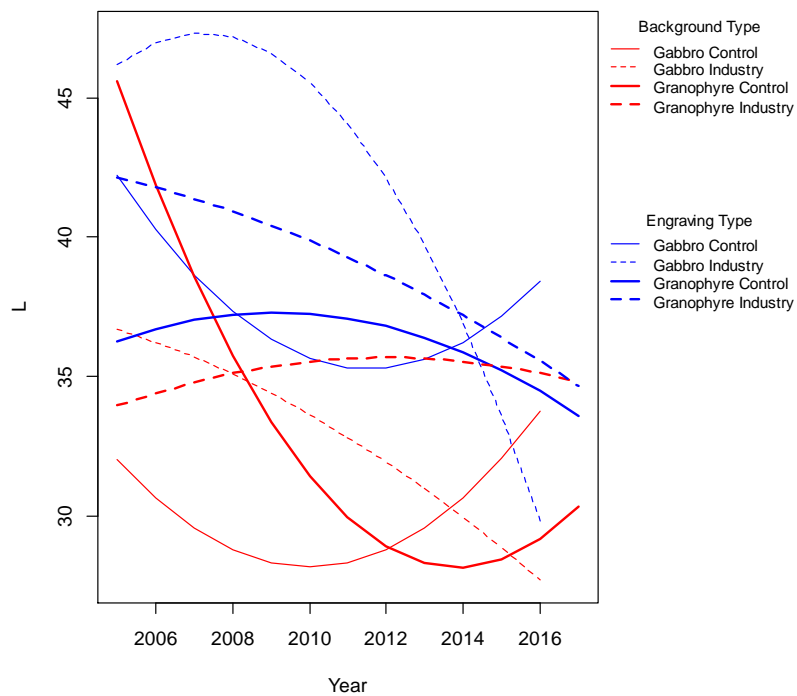


Figure 74. Interaction plot for Yara ASD data, L^* .

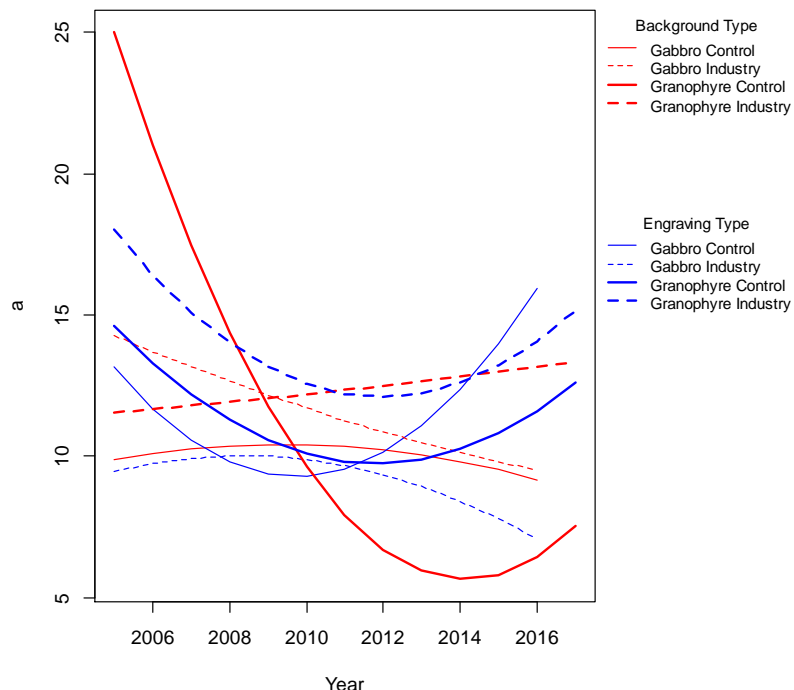


Figure 75. Interaction plot for Yara ASD data, a^* .

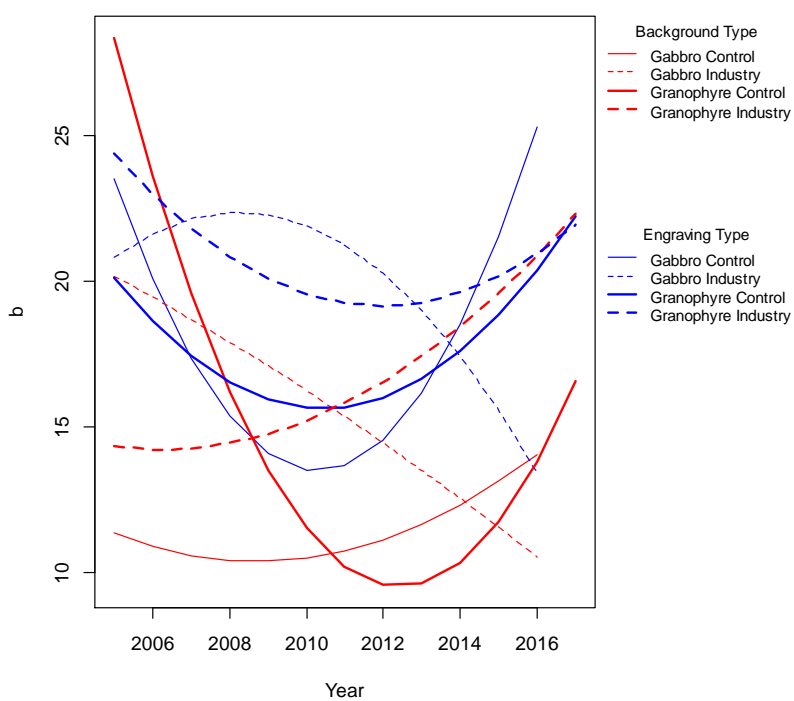


Figure 76. Interaction plot for Yara ASD data, b^* .

H.3 ASD Spectral Data

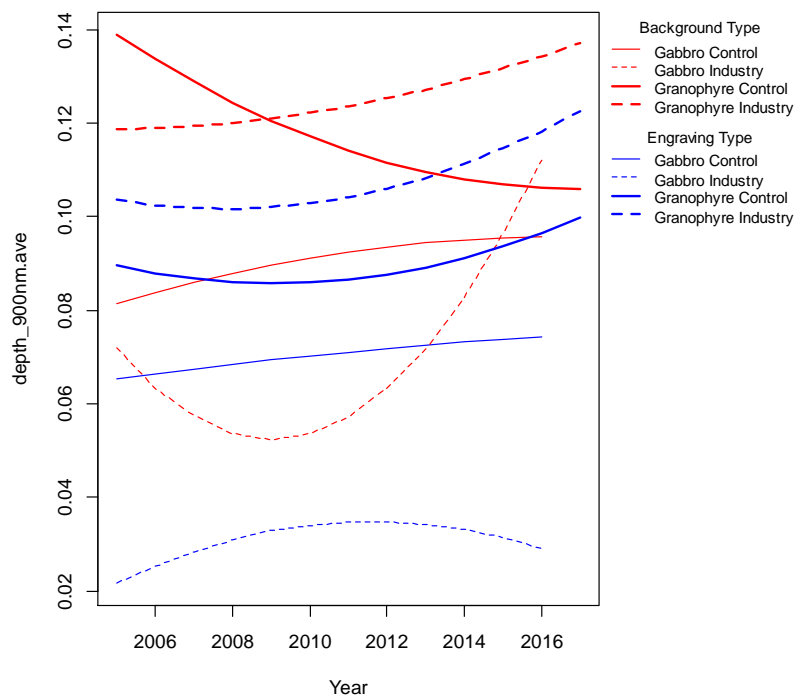


Figure 77. Interaction plot for full ASD data, depth 900nm band.

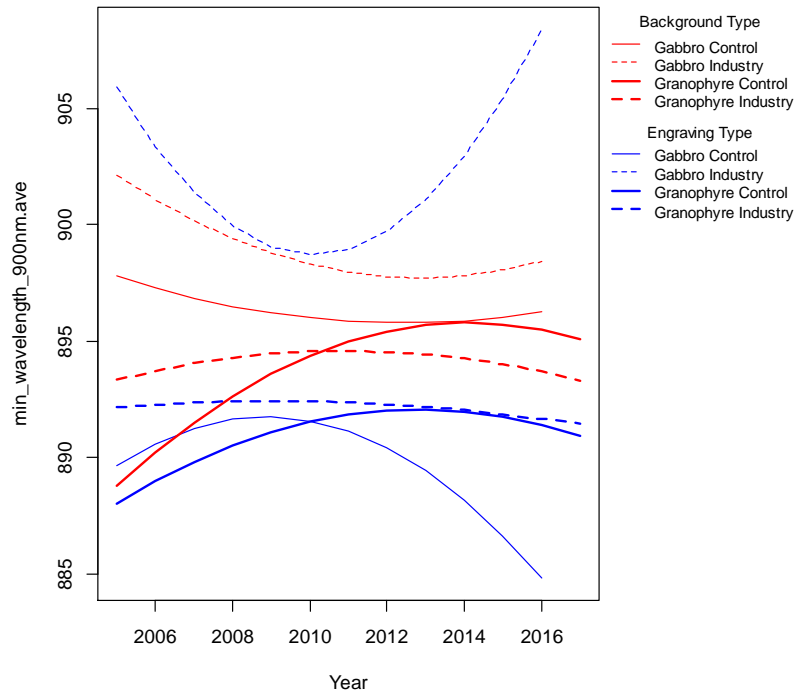


Figure 78. Interaction plot for full ASD data, minimum wavelength, 900nm band.

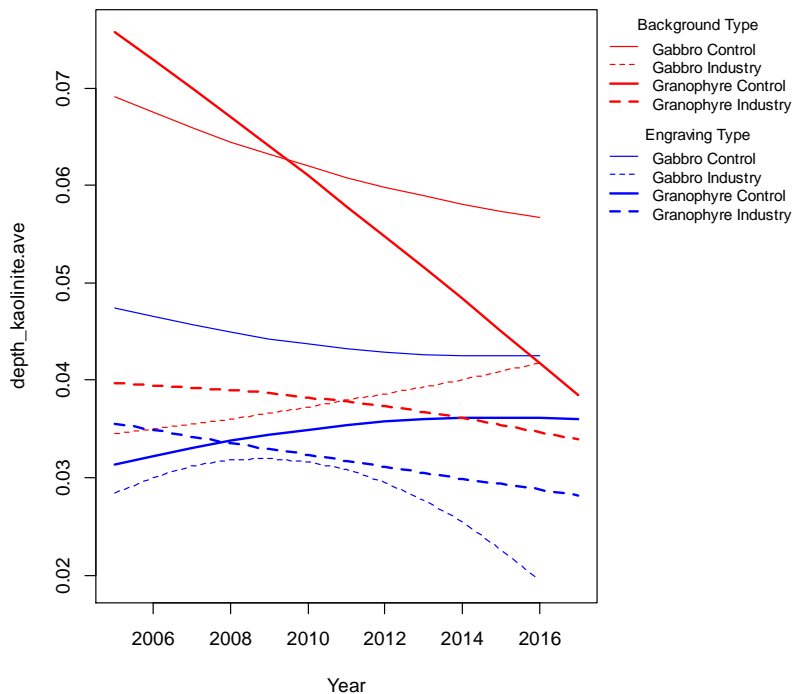


Figure 79. Interaction plot for full ASD data, depth kaolinite band.

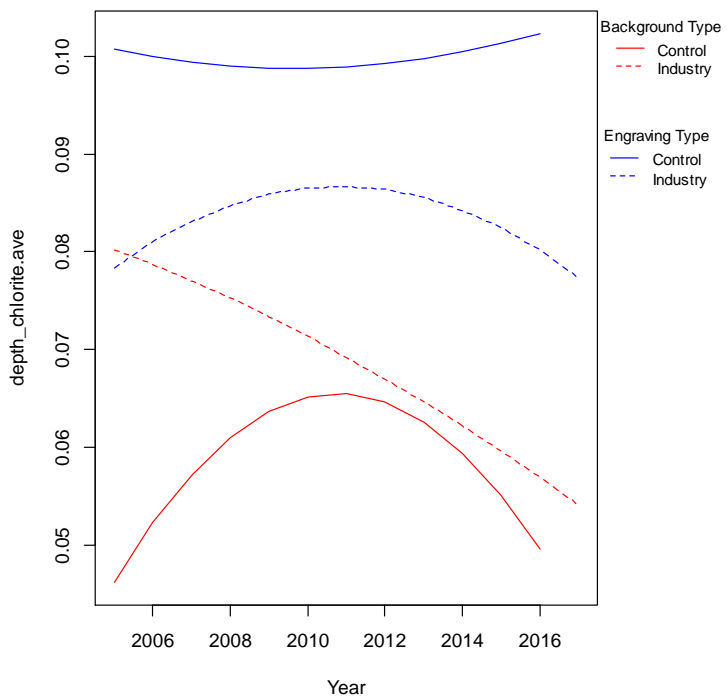


Figure 80. Interaction plot for full ASD data, depth chlorite band (gabbro sites only).

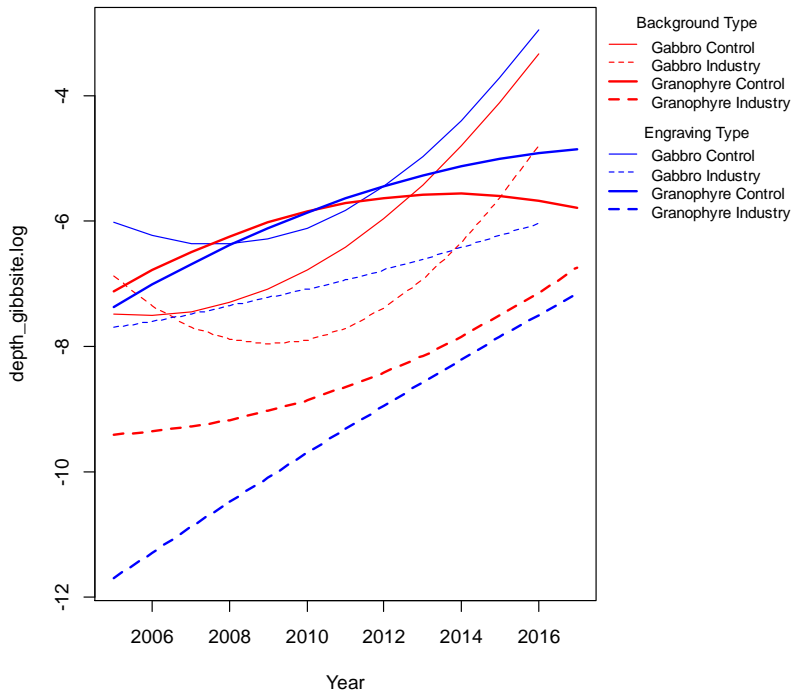


Figure 81. Interaction plot for full ASD data, depth gibbsite band (logarithm).

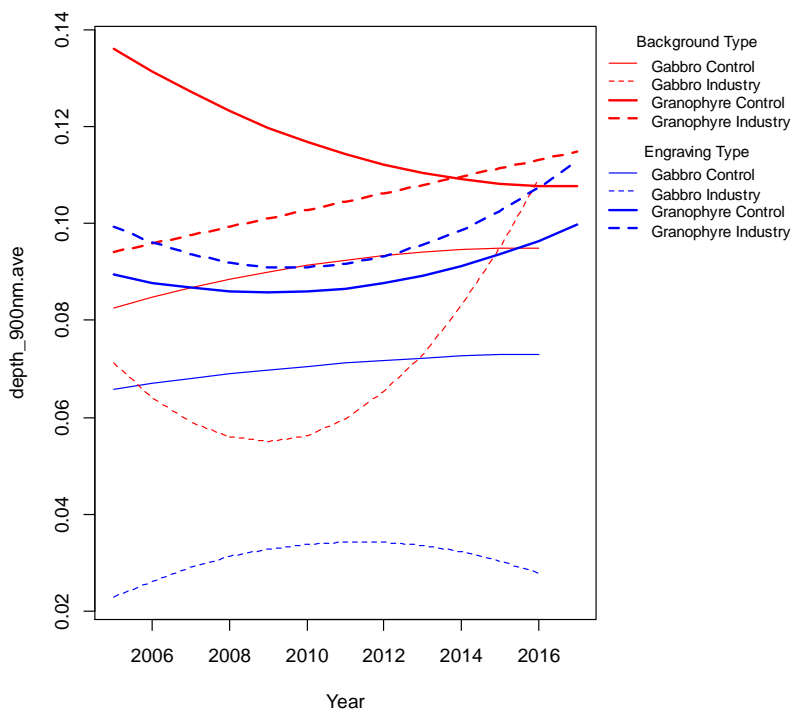


Figure 82. Interaction plot for Yara ASD data, depth 900nm band.

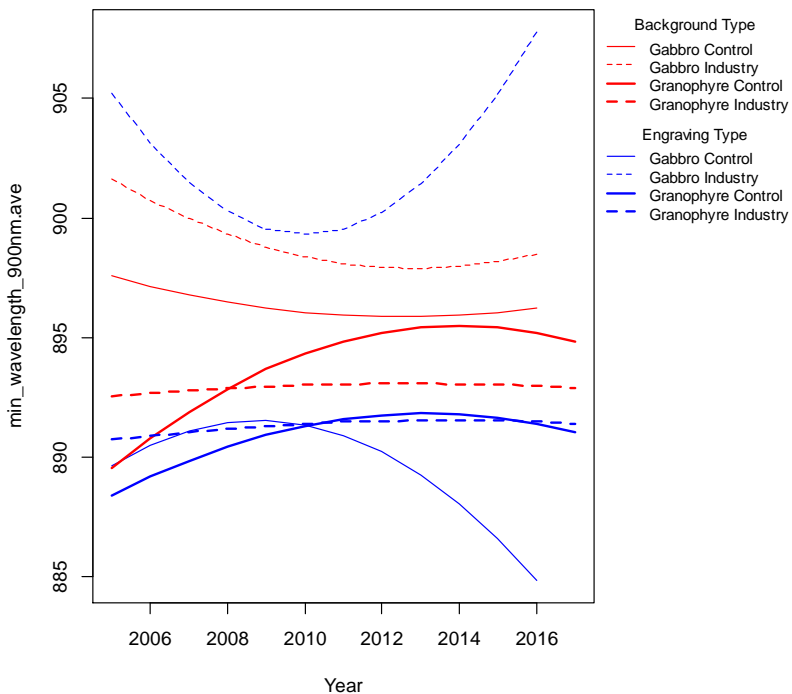


Figure 83. Interaction plot for Yara ASD data, minimum wavelength, 900nm band.

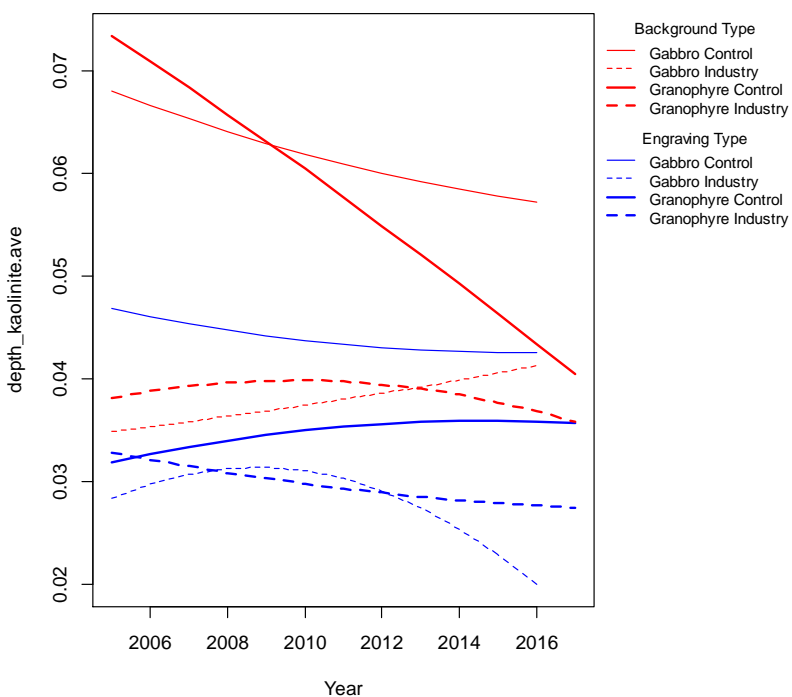


Figure 84. Interaction plot for Yara ASD data, depth kaolinite band.

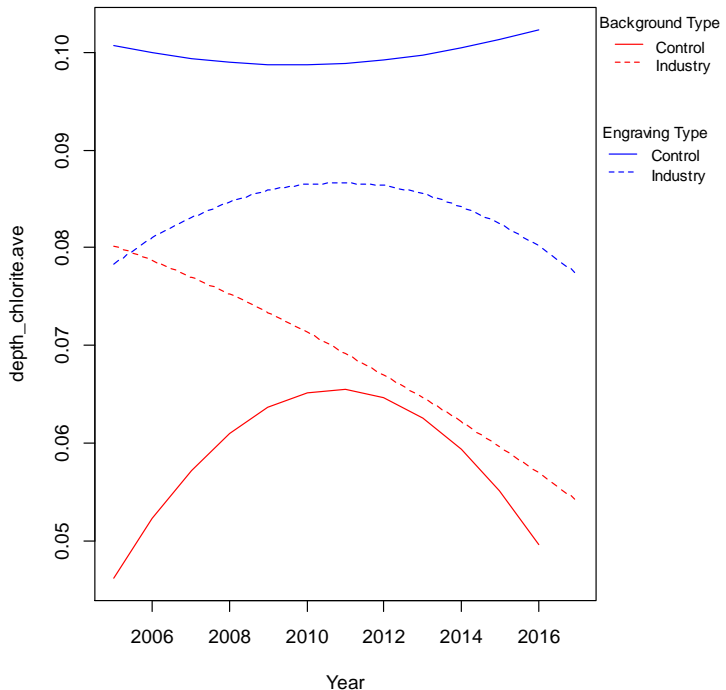


Figure 85. Interaction plot for Yara ASD data, depth chlorite band (gabbro sites only).

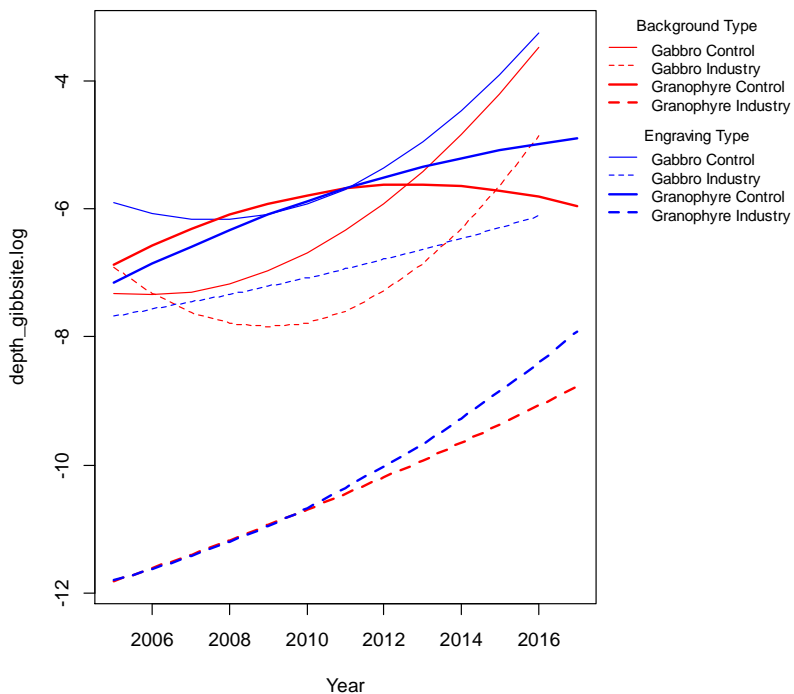


Figure 86. Interaction plot for Yara ASD data, depth gibbsite band (logarithm).